TECHNISCHE UNIVERSITÄT MÜNCHEN

Lehrstuhl für Entwicklungsgenetik

Characterization of molecular mechanisms that govern the formation of neuronal circuits in the developing vertebrate spinal sensory-motor system

Elisa Bianchi

Vollständiger Abdruck der von der Fakultät Wissenschaftszentrum Weihenstephan für Ernährung, Landnutzung und Umwelt der Technischen Universität München zur Erlangung des akademischen Grades eines

Doktors der Naturwissenschaften

genehmigten Dissertation.

Vorsitzender:	Univ.-Prof. Dr. S. Scherer
Prüfer der Dissertation:	1. Univ.-Prof. Dr. W. Wurst
	2. apl. Prof. Dr. R.A. Torres-Ruiz

Die Dissertation wurde am 20.08.2010 bei der Technischen Universität München eingereicht und durch die Fakultät Wissenschaftszentrum Weihenstephan für Ernährung, Landnutzung und Umwelt am 30.09.2010 angenommen.

Abstract

How do the millions of neurons in the vertebrate nervous system develop, grow axons over sometimes very long distances and make precise connections so that meaningful behavioral and sensational output is possible? To fulfill this complicate task, axonal pathfinding is regulated in a step-wise manner, which is controlled by attractive and repulsive guidance cues that can act over long or short distances, situated along their trajectories.

During development, motor neurons, located in the lateral motor columns (LMC), and sensory neurons, situated in the dorsal root ganglia (DRG) extend their axons along specific trajectories to reach their targets in the limb. Our understanding of the signaling pathways that govern the dorsal-ventral choice of these axons and later events like branching and target innervation is still limited.

The goal of my PhD project is to investigate the molecular mechanisms that regulate the pathfinding of motor and sensory neurons towards the dorsal or ventral limb musculature. I combined loss-of-function approaches in mouse with various cell culture paradigms and light microscopic imaging of specifically labeled neuronal subpopulations.

We employed a genome wide screening to identify novel molecules involved in the guidance of motor and sensory axons to the dorsal or ventral limb. Motor and sensory neurons were differentially labeled according to their projection patterns by injection of two fluorescently labeled dextrans into the dorsal and ventral limb musculature and separated by fluorescent activated cell sorting (FACS). Expression profiling of the differentially projecting neuronal pools using microarray analysis allowed for identification of candidate genes mediating the dorsal-ventral choice of motor and sensory axons.

We further focused our investigation on candidate genes differentially expressed in the motor neuronal population projecting to the forelimb, because microarray analysis predicted the already known differential expression of motor neuron markers in dorsally projecting, such as the LIM homeobox protein 1 (*Lim1*) and in ventrally projecting motor neurons, such

as the LIM homeodomain protein Islet-1 (*Isl1*) and Neuropilin 2 (*Npn-2*), thereby demonstrating that the screening worked successfully.

Using in situ hybridization and immunohistochemistry we validated the predicted expression of Engrailed 1 (En1), a homeodomain transcription factor in dorsally projecting motor neurons.

These methods were also applied to analyze the expression of our candidate gene at significant timepoints during embryonic development. We showed that En1 is expressed in the ventral developing limb at E11.5 when elongating axons take the dorsal-ventral decision at the base of the limb. Our mRNA expression pattern analysis of dorsal (LIM homeobox transcription factor beta (*Lmx1b*) and *Npn-2*) and ventral (Early B-cell factor 2 (*Ebf-2*)) limb markers in *En1* null embryos revealed that En1 causes ectopic ventral expression of dorsal markers and a decrease of ventral marker expression, thereby demonstrating that En1 is required for the dorsal-ventral forelimb patterning at a molecular level.

Furthermore, immunohistochemical analysis revealed the presence of En1 on motor axons projecting to the dorsal limb compartment at E11.5, when spinal projections enter the forelimb, providing further hints for its role in the guidance of motor axons elongating dorsally towards the limb.

We further characterized the role of En1 in repulsive motor axon guidance using *in vitro* cell culture assays to analyze neuronal growth under different conditions. I could show that En1 causes specific growth cone collapse of dorsally projecting motor axons in a dose-dependent manner, while it had no effect on ventrally projecting neurons.

To elucidate the role of En1 in the dorsal-ventral choice of motor axons at the base of the limb, I analyzed the development of motor axonal projections in *En1* null embryos and in mice where *En1* was specifically ablated in motor neurons by tissue-specific Cre-recombination. Retrograde tracing revealed that the complete ablation of *En1* results in dorsal-ventral miswiring of motor projections, whereas the binary decision of motor axons at the base of the limb is unaffected when *En1* was removed in motor neurons. These findings suggest that En1 expressed in the limb is responsible for the correct dorsal-ventral pathfinding of motor axons in the forelimb.

Taken together, during my PhD project I identified novel potential cues governing the dorsal-ventral choice of motor and sensory axons at the base of the limb. I unraveled and characterized En1 as a guidance cue in the motor system, demonstrating its role in the establishment of the binary choice of motor axons at the base of the limb. The results of this basic research project, therefore, contribute to our knowledge of the molecular mechanisms

governing the establishment of neuronal connectivity in the spinal sensory-motor system and may offer a starting point for the development of new treatments to re-build neuronal circuits after neurological diseases or trauma, which impair the function of the motor-spinal system.

Zusammenfassung

Wie können Millionen von Nervenzellen im Nervensystem von Wirbeltieren Fasern auswachsen, manchmal über lange Distanzen, ihre Ziele mit hoher Präzision in der Peripherie finden, und damit eine sinnvolle Verhaltenssteuerung erreichen?

Um diese komplizierte Aufgabe zu meistern, wird axonale Wegfindung schrittweise unter der Kontrolle von anziehend oder abstoßend wirkenden Wegfindungsfaktoren entlang der Wachstumsstrecke reguliert, welche ihre Wirkung über kurze oder lange Distanzen ausüben können.

Während der Entwicklung wachsen motorische Nervenfasern aus den Lateral Motor Colums (LMC) des Rückenmarks und von sensorischen Nervenzellen aus den Spinalganglien („dorsal root ganglia“, DRG) entlang spezifischer Bahnen, um ihre Ziele innerhalb der Extremitäten zu erreichen. Unser Verständnis der Signalwege, welche die Wachstumsentscheidungen jener Axone betreffen, und auch spätere Ereignisse wie Verästelung von Nerven und ziel-spezifische Innervation ist jedoch immer noch begrenzt.

Das Ziel meiner Doktorarbeit ist es, molekulare Mechanismen zu untersuchen, die die Wegfindung motorischer und sensorischer Nervenfasern zu dorsaler oder ventraler Beinmuskulatur regulieren. Dafür verwendete ich „Loss of function“ Experimente in der Maus in Kombination mit verschiedenen Zellkultur-Ansätzen und lichtmikroskopische Analyse von spezifisch markierten neuronalen Subpopulationen.

Wir setzten einen genomweiten Screen ein um neue Moleküle zu identifizieren, die in der dorso-ventralen Wegfindung von Fasern eine Rolle spielen. Motorische und sensorische Nervenzellen wurden entsprechend ihrer Projektionsmuster mit fluoreszenzgekoppelten Dextranen, die in die dorsale und ventrale Beinmuskulatur injiziert wurden, markiert und durch „Fluorescence Activated Cell Sorting“ (FACS) voneinander getrennt. Ein Expressionsprofil der unterschiedlich projizierenden Motorneuronenpools durch Microarray-Analyse erlaubte es uns, Kandidatengene für die dorso-ventrale Wachstumsentscheidung zu identifizieren.

Im weiteren Verlauf fokusierten wir unsere Untersuchung auf Kandidatengene, die von Motorneuronenpopulationen exprimiert werden, welche ihre Axone in die Vorderbeine entsenden. Die Microarray-Analyse hatte bereits die differentielle Expression bekannter Motorneuronenmarker, wie zum Beispiel des LIM homeobox proteins 1 (*Lim1*) in dorsal projizierenden Nervenzellen und des ventralen Markers LIM homeodomain protein (*Isl1*) und Neuropilin 2 (*Npn-2*) verifiziert und damit gezeigt, dass der Screen funktioniert.

Durch In Situ Hybridisierung und Immunhistochemie validierten wir die vorhergesagte Expression des Homeodomänen Transkriptionsfaktor Engrailed 1 (En1) in dorsal projizierenden Motorneuronen.

Diese Methoden wurden auch angewendet, um die Expression des Kandidatengens zu wichtigen Zeitpunkten während der Entwicklung zu analysieren. Wir konnten zeigen, dass En1 zum Zeitpunkt E11.5 in der ventralen Hälfte des sich entwickelnden Vorderbeins exprimiert ist, während die Fasern sich am dorsal-ventralen Entscheidungspunkt an der Basis des Beins befinden.

Die Analyse des mRNA Expressionsmusters dorsaler (LIM homeobox Transkriptionsfaktor beta (*Lmx1b*) und *Npn-2*) und ventraler (Early B-cell factor 2 (*Ebf-2*)) Marker für das Gewebe im Bein in *En1* null Embryonen zeigte, dass En1 ektopische ventrale Expression dorsaler Marker verursacht, sowie eine Abnahme der Expression ventraler Marker. Dies zeigt, dass En1 auf molekularer Ebene für eine korrekte dorso-ventrale Aufteilung des Vorderbeins benötigt wird.

Desweiteren zeigten immunohistochemische Analysen die Anwesenheit von En1 auf dorsal projizierenden motorische Fasern zum Zeitpunkt E11.5, wenn spinale Projektionen in das Bein einwachsen. Dies gibt weitere Hinweise auf eine Rolle von En1 bei der Führung von motorischen Axonen ins Gewebe des Vorderbeines.

Im weiteren Verlauf charakterisierten wir daher die Rolle von En1 durch Zellkultur Experimente, um neuronales Wachstum unter verschiedenen Bedingungen zu analysieren. Ich konnte zeigen, dass En1 bei dorsal projizierenden motorische Fasern zu einem dosisabhängigen Kollaps des Wachstumskegel führt, während keine Auswirkungen auf ventrale Projektionen nachzuweisen waren.

Um mehr über die Rolle von En1 während der dorsal-ventralen Entscheidungsphase der motorische Fasern herauszufinden, analysierte ich deren Projektionen in *En1* null Embryonen und in Embryonen, in denen En1 durch gewebespezifische Cre-Expression nur in Motorneuronen abgeschaltet wurde. Retrograde Markierung von Motorneuronen zeigte, dass das Fehlen von En1 im gesamten Organismus zu dorso-ventralen Fehlern bei der Wegfindung

führt, wohingegen diese Entscheidung nicht beeinträchtigt wird, wenn *En1* spezifisch in Motorneuronen fehlt. Diese Ergebnisse deuten an, dass En1, das vom Gewebe im Bein exprimiert wird, für die Projektionen beider Motorneuronenpopulationen verantwortlich ist.

Zusammengefasst habe ich während meiner Doktorarbeit neue mögliche Wegfindungsfaktoren identifiziert, die für die dorso-ventrale Entscheidung motorischer und sensorischer Fasern wichtig sind. Desweiteren konnte ich eine Rolle für En1 als Wegfindungsmolekül im motorischen System aufzeigen, und dessen Bedeutung bei der binären Entscheidung von motorischen Axonen in der Plexusregion entschlüsseln. Die Resultate dieses Grundlagenforschungs-Projekts tragen daher zum Wissen über molekulare Mechanismen bei, die die Entwicklung neuronaler Netzwerke des sensorisch-motorischen Systems steuern und bieten möglicherweise einen Ansatzpunkt für die Entwicklung neuer Behandlungsmöglichkeiten, neuronale Netzwerke nach Krankheit oder Trauma wieder herzustellen.

Contents

1 Introduction

1.1 The establishment of neuronal connectivity

During development millions of neurons in the vertebrate nervous system elongate their axons often over long distances and establish precise connections with their targets, so that meaningful behavioral and sensational output is possible.

The establishment of functional neural connectivity requires at least three sequential events: the polarized outgrowth of axons and dendrites from differentiated neurons, axon pathfinding, and the recognition of the appropriate synaptic partner. Axons find their correct targets guided by attractive and repulsive cues present along their trajectories that can act over long or short distances (Tessier-Lavigne and Goodman, 1996; Dickson, 2002)).

The expression of guidance molecules in the environment and the activation of specific receptors on growth cone, at the leading edge of the elongating axon, need to be regulated temporally and spatially to control axonal elongation, turning, or retraction. The growth cone of a developing axon undergoes continuous and stochastic extension of filopodia and lamellipodia that continuously investigate the environment. These movements are used by the axon to elongate or retract, depending on the detection of external stimuli (Smith, 1988).

The appropriate axonal steering and extending decision is achieved after the binding of the ligands to their receptors present on the growth cone surface and the subsequent activation of signal transduction pathways (reviewed in (Huber et al., 2003)) that lead to cytoskeletal reorganization (Nobes and Hall, 1995; Tapon and Hall, 1997; Giniger, 2002).

1.1.1 Guidance cues and their role in neuronal network formation

The best characterized cues that govern the formation of many different neuronal systems consist in conserved families of guidance molecules including Netrins, Slit, ephrins and Semaphorins (Tessier-Lavigne and Goodman, 1996; Song and Poo, 2001). Their discovery and functional characterization provided a key contribution to understanding the molecular mechanisms that direct axon guidance. The capacity of these cues to govern the elongation of so many different neuronal types depends on the molecular interaction they establish with the growing axons. An individual axon, indeed, may be subject to attractive and repulsive forces coming from the same axon guidance source which act on different receptors expressed on the axonal surface at specific developmental time points. In the following part I will give some examples of the mechanisms of action of these conserved guidance cues in different systems, such as the motor and visual system, where they act as short- and long distance attractive and repulsive cues, in order to highlight their multifunctional role and their fundamental contribution in the establishment of neural circuitries.

1.1.1.1 Netrins

Netrins are a family of laminin-related small (molecular weight approximately 70-80 kDa) secreted proteins that can be both attractants and repellents (Chisholm and Tessier-Lavigne, 1999), by binding to their receptors DCC and unc-5, respectively (Culotti and Kolodkin, 1996; Tessier-Lavigne and Goodman, 1996; Przyborski et al., 1998). Netrins mediate growth cone attraction during spinal cord development, attracting commissural axons over long distances to the floor plate, where they are secreted (Tessier-Lavigne et al., 1988; Colamarino and Tessier-Lavigne, 1995; Serafini et al., 1996), during the establishment of *Drosophila melanogaster* (*Drosophila*) peripheral motor axon pathfinding (Harris et al., 1996; Loomis et al., 1996; Mitchell et al., 1996) and during the formation of the visual system in mammals, acting as short-range guidance cues for retinal axons (Deiner et al., 1997). Their versatility is demonstrated by the fact that they exert a repulsive action during the development of other neural networks. In *Caenorhabditis elegans* (*C. elegans*), they repell dorsally migrating axons (Hedgecock et al., 1990) and in mammalian spinal cord, being expressed in the floor plate and in the dorsal horn, Netrins provide repulsive signals for trochlear motor axons (Colamarino and Tessier-Lavigne, 1995) and DRG sensory neurons (Watanabe et al., 2006), respectively.

1.1.1.2 Ephrins

Eph tyrosine kinase receptors and their membrane-bound ligand ephrins are an ancient and versatile system involved not only in axon guidance, but also in a variety of developmental functions such as cell migration, vascular formation and synaptic plasticity (Knoll and Drescher, 2002). They are divided into two classes: EphA (EphA1-EphA8) and EphB (EphB1-EphB6) receptors, which bind ephrin-As (ephrinA1-ephrinA5) and ephrin-Bs (ephrinB1-ephrinB6), respectively (Wilkinson, 2001). They can act as bidirectional signal transducers, since the signal can originate from the ephrin ligands as well as from the Eph receptors in the so-called "forward" and "reverse" signaling, respectively (reviewed in (Kullander and Klein, 2002)). The visual system represents the best characterized model for studying the function of the ephrin/Eph signal. During vertebrate retinotectal formation, a gradient of ephrinAs expression in the tectum provides a repulsive signal for retinal axons that express EphA receptors on their surface (Cheng et al., 1995; Drescher et al., 1995), allowing the establishment of a topographic map along the anterior-posterior axis. Mapping along the dorsal-ventral axis, in contrast, involves attractive signaling mediated by ephrinB and EphB receptors (Hindges et al., 2002; Mann et al., 2002). Ephrin/Eph signal controls axon guidance in many other systems, too, such as in the forebrain, where commissural axons are repelled from region of EphB expression (Henkemeyer et al., 1996) while they are attracted by EphA4-expressing regions (Kullander et al., 2001), in the vomeronasal system, where the EphA/ephrinA "reverse" signaling contributes to the generation of the olfactory map (Knoll et al., 2001) and in the motor system, where ephrinAs/EphA and ephrinBs/EphB mediate the dorsal-ventral axonal choice at the base of the limb (Eberhart et al., 2002; Kania and Jessell, 2003; Luria et al., 2008).

1.1.1.3 Semaphorins

Semaphorins (Sema) belong to a large family of guidance cues composed of more than twenty members divided into eight classes according to their phylogenic relationship with a common Sema domain (Yazdani and Terman, 2006). They function as repellents or inhibitors during axon pathfinding, branching, and targeting (Kolodkin et al., 1992; Luo et al., 1993). Semaphorins exert a repulsive action through receptor complexes that include the Plexins (Plx) as signal-transducing subunits (Tamagnone et al., 1999) and the Neuropilins (Npn) as ligand-binding subunits (He and Tessier-Lavigne, 1997; Kolodkin et al., 1997). Secreted Sema3A induces growth cone collapse *in vitro* of many different neuronal types, which

include DRG neurons (Luo et al., 1993; Messersmith et al., 1995), motor neurons (Shepherd et al., 1996; Varela-Echavarria et al., 1997), sympathetic neurons (Adams et al., 1997; Koppel et al., 1997) sensory neurons from the cranial nerve ganglia V and VII (Kobayashi et al., 1997), olfactory sensory neurons (Kobayashi et al., 1997; Renzi et al., 2000), cortical neurons (Bagnard et al., 1998) and hippocampal neurons (Chedotal et al., 1998). *In vivo*, Sema3A prevents DRG axons from entering the dorsal horn of the spinal cord during early development (Fitzgerald et al., 1993), while Sema3A ventral expression at later stages prevents dorsally projecting afferents from invading the ventral horn of the spinal cord (Messersmith et al., 1995; Shepherd et al., 1997). Semaphorins can also maintain axonal fasciculation, creating repulsive corridors when they are present in the environment around the elongating axons (Culotti and Kolodkin, 1996; Taniguchi et al., 1997; Cheng et al., 2001) and it was shown that Sema3A/Npn-1 signaling mediates axon guidance in cortical and hippocampal neurons as well as motor and sensory neurons (He and Tessier-Lavigne, 1997; Kolodkin et al., 1997). In addition to its role in the development of the nervous system, Npn-1 constitutes the binding receptor for the vascular endothelial growth factor (VEGF) and plays a role in angiogenesis and heart development (Gu et al., 2003).

1.1.1.4 Slits

Another class of conserved axon guidance molecules are the Slits, a family of large secreted proteins (approx. 190 kDa) that act through the Roundabout (Robo) receptors. Slits have a bifunctional role in axon guidance, on one side providing growth cone repulsion and on the other side stimulating axonal branching and elongation (Wang et al., 1999). The repulsive role of Slit-Robo signaling in axon guidance was first studied in *Drosophila*, where Slits are expressed at the ventral midline and prevents ipsilateral axons that express Robo receptors from crossing the midline and commissural axons that also express Robo from recrossing (Battye et al., 1999; Kidd et al., 1999). Slit proteins also play a role in the formation of the optic chiasm in vertebrates (Fricke et al., 2001; Plump et al., 2002). They are expressed at the chiasm and control the choice of ipsilateral or controlateral projections (Ringstedt et al., 2000; Plump et al., 2002).

1.1.1.5 Cell adhesion molecules

In addition to these classical axon guidance molecules mentioned above, axon elongation and steering are also mediated by other guidance factors that collaborate to direct neuronal projections towards their targets.

Among these cues, cell adhesion molecules (CAMs) play key roles in the formation of neuronal networks, where they are involved in different processes including growth cone guidance, axon fasciculation, and formation and stabilization of synapses. They mediate contact-dependent axonal motility maintaining adhesive interactions between the elongating axons and specific cells along their pathway (Covault and Sanes, 1986; Rutishauser and Jessell, 1988). The best characterized receptors implicated in axon guidance within the CAMs, are the cell adhesion molecule L1 (Landmesser et al., 1988), neural CAM (NCAM) (Tosney et al., 1986) and polysialic acid (PSA). They were shown to control motor axon sorting and to establish target-specific fascicles before axonal projections enter the limb (Tang et al., 1992; Tang et al., 1994). In presence of PSA, NCAM allows nerve defasciculation, while axon fascicles bundles form in absence of PSA (Tang et al., 1994).

1.1.1.6 Neurotrophins

Another class of molecules, the Neurotrophins well-known as essential regulators of neuronal survival and morphology, also play a role in the control of axonal extension, pathway selection, peripheral target innervations, and synaptic plasticity. The neurotrophin signaling system is highly complicate and requires the specific activation of particular neurotrophin family members and receptors to form complexes or to act independently, depending on the diverse neuronal functions they control. Axon growth triggered by neurotrophic factors implicates both retrograde signals that allow appropriate gene expression and local signals acting at the growth cone, where axonal response is regulated by the levels of cyclic nucleotides. It has been shown that neurotrophins regulate transcription factors implicated in axon targeting decision, such as PEA3 and ER81, which are members of the ETS family of transcription factors (Arber et al., 2000) and that the elongation of sensory and motor neurons in the limb bud is neurotrophin-dependent (Patel et al., 2000).

1.1.1.7 Morphogens

Also morphogens play multifunctional roles in many aspects of embryonic development (Lee and Jessel, 1999). They are well characterized as factors specifying cell fate and determinants of tissue patterning. More recent studies demonstrated that morphogen gradients are also implicated in axonal pathfinding during the development of the nervous system. In particular, members of three families of morphogens have been shown to play an important role in neural circuit assembly: the bone morphogenetic proteins (BMP), Wnt and Sonic hedgehog (Shh). BMPs and Shh are expressed along the dorsal-ventral axis of the vertebrate spinal cord where they collaborate with Netrin-1 to control axonal pathfinding of commissural neurons from the dorsal spinal cord to the ventral midline (Charron et al., 2003; Bourikas et al., 2005). Multiple Wnt family proteins guide commissural and cortical motor axons along the anterior-posterior axis (Dickson, 2005; Liu et al., 2005) and the medio-lateral graded distribution of Wnt in the optic tectum provides guidance information for retinal axons (Schmitt et al., 2006; Zou and Lyuksyutova, 2007).

1.2 The spinal sensory-motor system

Among the diverse models and systems used by researchers to investigate the molecular mechanisms regulating axonal pathfinding, one very commonly used is the mouse developing spinal sensory-motor system. This system is suited for the study of axon guidance because it is anatomically relatively simple and accessible for *in vivo* experiment manipulations. Many guidance events are necessary during the elongation of motor and sensory axons from their cell bodies, localized in the spinal cord and DRG, respectively, to their targets in the periphery.

1.2.1 Motor and sensory neuron differentiation

Motor neurons differentiate from progenitor cells in the ventral half of the neural tube in response to the inductive actions of Sonic hedgehog, which is secreted by the notochord (Marti et al., 1995; Roelink et al., 1995; Ericson et al., 1997). After motor neurons have left the cell cycle, they acquire columnar subtype identities and can be distinguished in four motor neuron populations on the basis of cell body position, axonal projections, and gene expression (Jessell, 2000). The medial compartment of the medial motor column (MMCm) and the lateral division of the medial motor column (MMCl) innervate axial muscles throughout the body

and body wall muscles at thoracic level, respectively (Figure 1.1). The preganglionic motor column (PMC) neurons are only present at thoracic level and innervate the sympathetic ganglia, whereas the lateral motor column (LMC) neurons are present only at limb levels and extend their axons towards limb muscles (Figure 1.1). LMC motor neurons are organized in a topographic manner that displays their targets in the distal limb (Jessell, 2000; Landmesser, 2001; Sharma and Belmonte, 2001). Motor neurons that extend their axons to the dorsal part of the limb are situated in the lateral LMC (LMCl), while motor neurons projecting their axons to the ventral limb musculature are located in the medial LMC (LMCm).

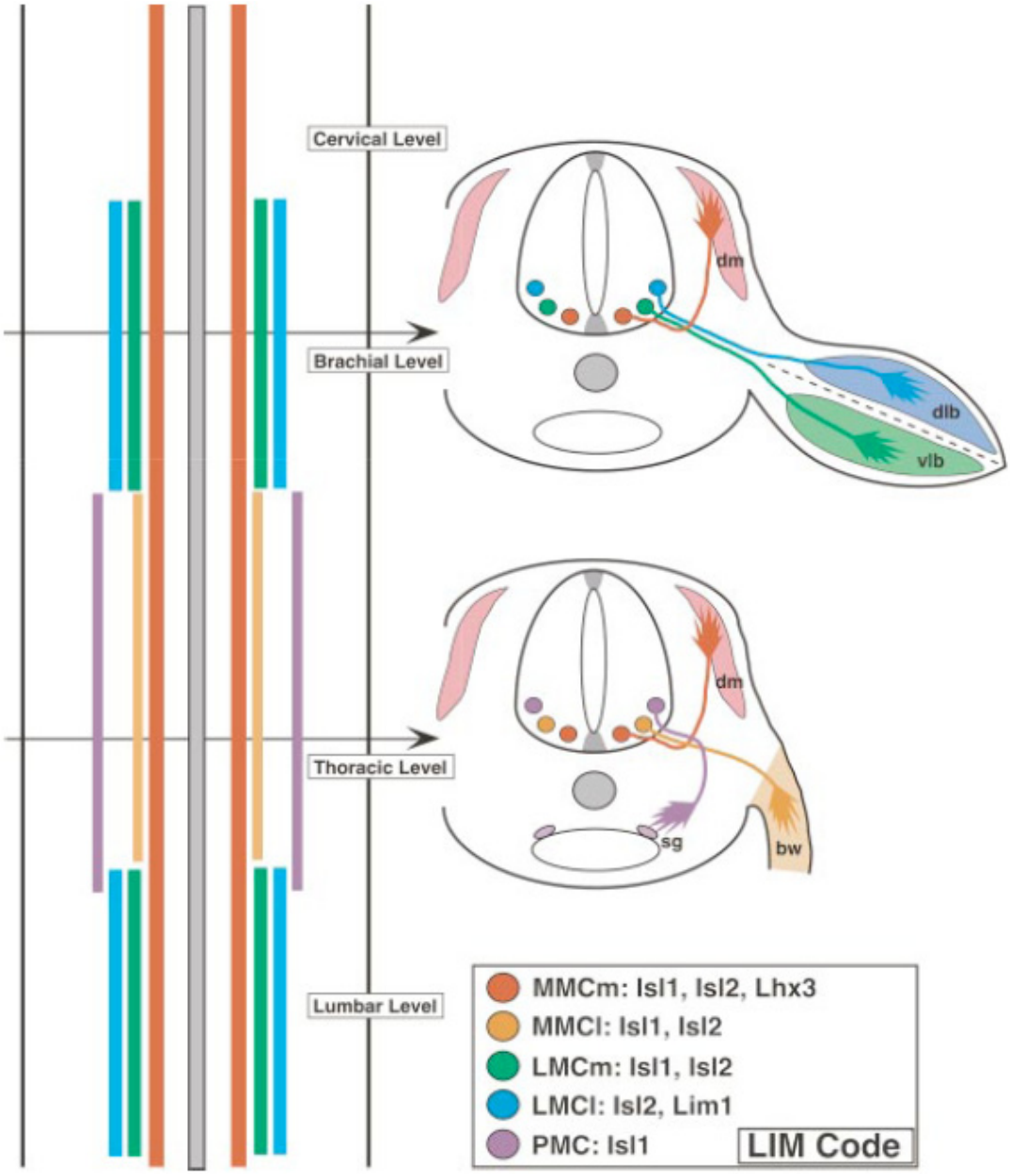

Figure 1.1. Motor neuron organization in the developing spinal cord, on the basis of cell body position, axonal projections and gene expression. Spinal cord motor neurons are

organized in longitudinal columns. After motor neurons have left the cell cycle, they acquire columnar subtype identities. The median motor column (MMC) can be divided into a medial (m) group, which is found at all rostrocaudal levels and projects to axial muscles, and a lateral (l) group, found only at thoracic levels and projecting to body wall muscles. Preganglionic motor column (PMC) are present only at thoracic level. Lateral motor column (LMC) neurons are generated only at limb levels and send axons into the limb mesenchyme and are divided in two divisions: LMCl neurons project to the dorsal limb and LMCm neurons extend their projections to the ventral part of the limb. (Picture taken from (Shirasaki and Pfaff, 2002)).

The two LMC divisions are specified by the expression of two LIM-homeodomain transcription factors, *Isl1* and *Lim1* (Figure 1.2). *Isl1* is initially expressed by all LMC neurons and its expression is then downregulated in LMCl neurons starting around E11.5, when the expression of *Lim1* in this specific neuronal population begins (Tsuchida et al., 1994; Riddle et al., 1995; Vogel et al., 1995; Kania et al., 2000; Kania and Jessell, 2003).

The other key-players in the sensory-motor system are the sensory neurons. They derive from neural crest cells that delaminate from the dorsal neural tube and migrate ventrally, invade the anterior sclerotome and form the DRG. Sensory neurons send out two projections, to a peripheral target, such as the skin or skeletal muscle in the limb, and to motor neuron cell bodies in the spinal cord, thereby a neural circuit is generated (Figure 1.2). Sensory neurons synapse directly with motor neurons in the spinal cord, creating a reflex arch that allows actions to occur very quickly. DRG sensory neurons can be distinguished into different subtypes delineated by the expression of different receptor tyrosine kinases (Trks) (Kaplan et al., 1991; Klein et al., 1991). Trks serve as receptors for the neurotrophic factors nerve growth factor (NGF), brain-derived neurotrophic factor (BDNF) and neurotrophin-3 (NT-3). TrkA is expressed by many nociceptive and thermoceptive afferents, TrkB is expressed by a subpopulation of cutaneous mechanoreceptive neurons and TrkC is expressed by proprioceptive neurons (Bibel and Barde, 2000; Huang and Reichardt, 2001).

1.2.2 Guidance motor and sensory axons towards the limb

Axonal extension towards the limb requires intricate coordination of cell surface and secreted molecules expressed by cells in the intermediate environment or in the final target regions which are recognized by their corresponding receptors and the intracellular effectors expressed in the elongating projections (Okamoto and Kuwada, 1991; Hamburger, 1993; Jessell, 2000). LMC motor axons exit the spinal cord through the ventral roots, are then joined by sensory axons emerging from the DRG, and proceed together until they arrive at the plexus

region at the base of the limb. Here, they defasciculate and form new bundles which are target-specific and, starting around embryonic day 11.0 (E11.0) in the mouse forelimb, LMCl motor and DRG sensory axons elongate towards the dorsal limb, whereas LMCm motor and DRG sensory axons extend their trajectories towards the ventral part of the limb (Tosney and Landmesser, 1985).

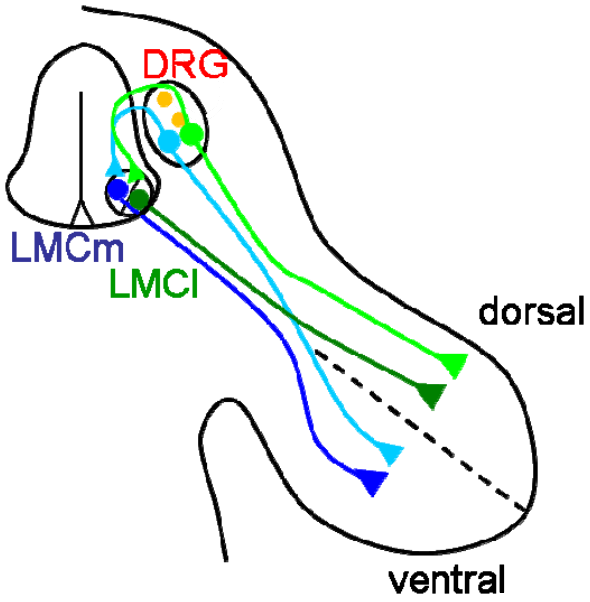

Figure 1.2. Schematic representation of the sensory-motor circuit. Motor neurons projecting to the dorsal limb musculature are situated in the lateral LMC (LMCl, dark green) and motor neurons projecting ventrally are located in the medial LMC (LMCm, dark blue). Proprioceptive sensory neurons are located in the DRG and project their axons towards the spinal cord to innervate motor neurons and towards their peripheral muscle targets (light green and light blue).

A strategy that elongating axons use to reach their targets during development is the extension along trajectories that consist of other axons or blood vessels growing in the same direction.

Classical data in chick indicate that motor axons lead DRG sensory axons to their muscular targets towards periphery. It was shown that sensory neurons are unable to find their correct pathway in the absence of motor neurons and, following cutaneous elongating axons, they project to inappropriate target areas (Landmesser and Honig, 1986), but the molecular mechanism regulating these processes still need to be unrevealed. More recent data showed that in the absence of Npn-1/Sema3A signaling, motor axons and sensory axons outgrowth precociously in the limb and are defasciculated (Huber et al., 2005). It was also demonstrated that the fasciculation of motor and sensory axons elongating towards the limb is controlled by

axo-axonal interactions of the Npn-1 receptor which is expressed on both axonal projections extending towards the periphery (Huettl et al., submitted).

Interestingly, the nervous and the circulatory system during their establishment use common regulatory cues and signaling pathways. It has been shown that interactions between molecules expressed by axons and blood vessels extending along the same direction are required for appropriate pathfinding. For example, the binding of the vascular-derived endothelin family member Edn3, expressed on extending sympathetic axonal projections, to the endothelin EdnrA receptor, present on the surface of internal carotid arteries, provides an essential signal for newborn sympathetic neurons to choose the correct trajectory to innervate their targets (Makita et al., 2008).

1.2.3 Signaling pathways that regulate the dorsal-ventral choice of motor axons at the base of the limb

In the past years, ligand-receptor pairs have been identified that regulate the dorsal-ventral axon pathfinding (Kania and Jessell, 2003; Huber et al., 2005).

Several studies in mouse and chick reported the role of the ephrinAs/EphA4 signaling in the guidance of LMCl axons into the dorsal limb compartment. Indeed, ephrinA2/A5 present in the ventral limb mesenchyme repels LMCl axons expressing EphA4 on their surface, directing them to the dorsal limb (Helmbacher et al., 2000; Kania and Jessell, 2003). It has been shown that the ablation of *EphA4* causes LMCl axon to misproject into the ventral limb, and the ectopic expression of EphA4 on LMCm axons causes dorsally rerouting of ventrally projecting neurons (Eberhart et al., 2002).

Another ligand-receptor pair that contributes to the establishment of the correct motor axon binary choice at the base of the limb is composed of the glial-cell-derived neurotrophic factor (GDNF) and its receptor Ret. The GDNF/Ret cooperates with the ephrinA/EphA4 signaling to guide LMCl axons towards the dorsal limb musculature. Indeed, in *GDNF* or *Ret* mutant mice, LMCl axons fail to project dorsally and aberrantly innervate the ventral part of the limb and it has been shown that this phenotype is enhanced in *EphA4* and *Ret* double knock out mice (Kramer et al., 2006).

While ephrinA/EphA4 signaling is required for the dorsal-ventral choice of LMCl motor axons, the ephrinB2/EphB1 signaling directs the LMCm axons to innervate the ventral limb, revealing a symmetrical molecular mechanism used by motor axons in the selection of dorsal or ventral trajectories. The presence of ephrinB2 in the dorsal limb mesenchyme,

indeed, provides repulsive signaling for LMCm axons that express the EphB1 receptors on their surface, directing them to the ventral limb compartment (Luria et al., 2008).

A previously identified signaling cue that instructs a ventral trajectory of LMCm axons is Sema3F that binds to Npn-2. The expression of Npn-2 on LMCm motor axons confers responsiveness to the chemorepulsive cue Sema3F present in the dorsal part of the limb, guiding LMCm axons to their target muscles in the ventral limb (Huber et al., 2005). It was also shown that the timing of motor axon fasciculation and ingrowth into the limb is regulated by the Sema3A/Npn-1 signaling, showing that these two class 3 Semaphorins control different aspects of limb innervation (Huber et al., 2005).

1.2.4 Transcription factors contribute to the establishment of the dorsal-ventral choice of motor axons at the base of the limb

Transcription factors play a fundamental role in the regulation of axonal pathfinding. In the spinal cord they influence the expression of specific cell-surface receptors on the elongating axons, whereas transcription factors in the limb control the expression of guidance cues in the target area, thereby coordinating the response of neurons to the guidance molecules.

LIM-homeodomain transcription factors are expressed in the spinal cord by subsets of LMC neurons. The expression of *Lim1* and *Isl1* in the lateral and medial aspect of the LMC, respectively, contributes to the generation of motor neuron diversity (Lance-Jones et al., 2001) and confers to motor neurons the ability to select specific axonal pathways to innervate muscular targets (Shirasaki and Pfaff, 2002; Dalla Torre di Sanguinetto et al., 2008). *Lim1* in the lateral division of the LMC regulates the expression of EphA4 receptors on LMCl axons, partially contributing to the guidance of LMCl axons into the dorsal part of the limb. In fact, the absence of *Lim1* in LMCl neurons causes a random dorsal-ventral choice of the axons at the limb bifurcation point (Kania et al., 2000; Kania and Jessell, 2003). In the medial LMC, *Isl1* controls the expression of EphB1 receptors on the surface of LMCm axons, enabling them to project correctly towards the ventral limb compartment (Tsuchida et al., 1994; Kania and Jessell, 2003). The role of the LIM-homeodomain proteins in the control of motor axons trajectories is conserved, since studies in *Drosophila* and *C. elegans* showed that motor neurons which synapse with specific muscles express particular combinations of LIM-homeodomain proteins (Hobert et al., 1998; Thor et al., 1999).

Transcription factors expressed in the axonal target area play an instructive role in the dorsal-ventral choice of motor axons, too. *Lmx1b* LIM-homeodomain transcription factor in the dorsal mesenchyme of the developing limb controls the expression of ephrinAs, promoting a dorsal trajectory for LMCl axons (Chen et al., 1998; Helmbacher et al., 2000; Kania and Jessell, 2003).

Taken together, the work of the past 15 years enormously contributed to our knowledge of neural circuit formation, unravelling the mechanisms and the molecular mediators that regulate axon guidance in the spinal sensory-motor system.

Previous studies, however, principally focused on the guidance of motor axons and now we know many molecular factors and signalling pathways that guide motor axons from the spinal cord to the limb, molecules that control their dorsal-ventral decision at the base of the limb and we also possess markers to distinguish the motor neuronal populations on the base of their peripheral projection patterns. The scenario is different for the sensory neuron population where both axon guidance cues mediating the dorsal-ventral binary decision and markers to distinguish them with regard to the limb compartment they innervate still need to be identified.

Further investigation is needed on one side to identify novel guidance cues regulating motor and sensory axon guidance and, on the other side, to understand the molecular mechanisms implicated in the dorsal-ventral binary decision at the base of the limb.

This PhD thesis, therefore, contributes to take a step further in understanding the molecular mechanisms governing axon guidance that lead to the establishment of neuronal connectivity in the spinal sensory-motor system, on one hand by investigating novel guidance cues governing the dorsal-ventral choice of motor and sensory neurons and, on the other hand, by unravelling and functionally characterizing Engrailed 1 as a guidance cue that contributes to the establishment of motor axonal binary decision at the base of the limb.

1.3 Aim of the study

1.3.1 Unbiased screening approach for novel cues involved in the dorsal-ventral axon guidance decision

As described above, a number of adhesion molecules and guidance cues have been identified in the past 15 years that are involved in mediating the dorsal-ventral guidance decision of motor axons. However, single or combined deletion of these cues or their receptors, while leading to significant guidance errors, could not abolish the fidelity of this choice altogether. Surprisingly, nothing is known about the molecular cues that regulate dorsal-ventral guidance for sensory neurons. To date, there are no markers available to distinguish sensory neurons based on their dorsal-ventral projecting pattern.

These data prompted us to look for new axon guidance cues that still await discovery. We therefore set out to identify novel factors that govern the dorsal-ventral binary decision of motor and sensory axons at the base of the limb. We employed a cDNA microarray screen to identify genes differentially expressed in dorsally and ventrally projecting motor or sensory neurons. Retrograde fluorescent labeling based on the projection patterns (Figure 1.3) combined with fluorescence activated cell sorting (FACS) allowed for generation of highly enriched samples of neuronal subpopulation.

Genome-wide expression profiling resulted in four lists of candidate genes differentially expressed either in motor or sensory neurons projecting either to the dorsal or ventral fore- or hindlimb. The predicted expression patterns of promising candidates were validated using in situ hybridization (ISH) at significant developmental timepoints in combination with markers for medial or lateral LMC neurons.

The most promising candidate, Engrailed 1 (En1), was functionally characterized *in vitro* using primary cultured motor neurons. The role of En1 in establishing axon projections was further analyzed *in vivo* using genetic loss of function approaches to delete *En1* either in all cells or cell-type-specific in motor neurons.

The genome-wide screening we employed allowed to successfully assessing differential regulated genes in motor and sensory neuronal populations innervating the dorsal and ventral limb. Indeed, microarray analysis predicted the already known differential expression of some motor neuron markers in dorsally projecting, such as the LIM homeobox protein 1 (*Lim1*) and ventrally projecting motor neurons, such as the LIM homeodomain

protein Islet-1 (*Isl1*) and Neuropilin 2 (*Npn-2*), thereby demonstrating the reliability of the screens.

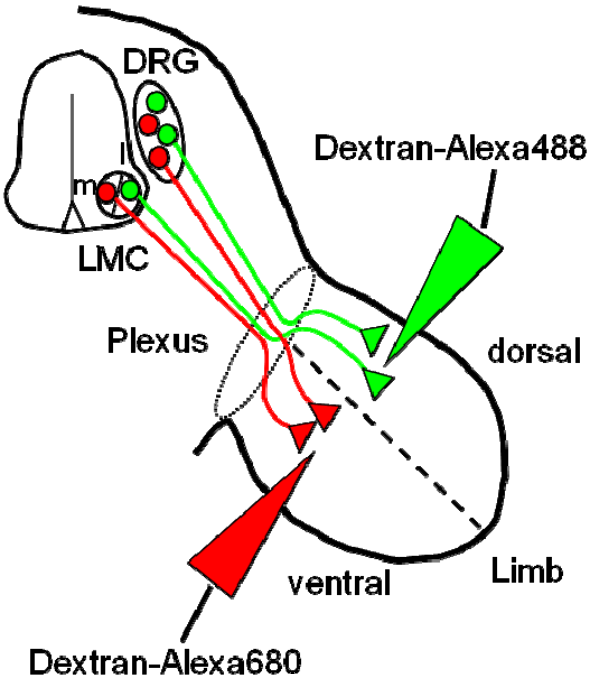

Figure 1.3. Schematic representation of the retrograde labeling technique. Sensory and motor neurons are differentially labeled according to their projection patterns by injection of two fluorescent dextrans into the dorsal and ventral limb musculature of an E12.5 mouse embryo. The fluorescent dyes are retrogradely transported to the cell bodies.

1.3.1.1 Engrailed 1 is a repulsive cue for motor axons

Among the candidate genes predicted to be differentially expressed in neurons either projecting dorsally or ventrally to the limb, we found membrane and extracellular proteins, components of signal transduction pathways, and transcription factors.

A particularly interesting candidate was En1, with a validated higher mRNA expression level in the LMCl compared to LMCm motor neurons at E12.5. We chose to focus our investigation on En1 first because it is a transcription factor and second also because of recent reports that En can directly repel retinal and tectal axons (Brunet et al., 2005; Wizenmann et al., 2009).

En1 is a member of the homeodomain transcription factor family which shares a highly conserved sequence of 60 amino acids, the homeodomain (HD), composed of three α-helices (Figure 1.4). The third α-helix is also called the recognition helix since it represents the DNA-binding domain (Desplan et al., 1985; Gehring, 1985; Gehring et al., 1994).

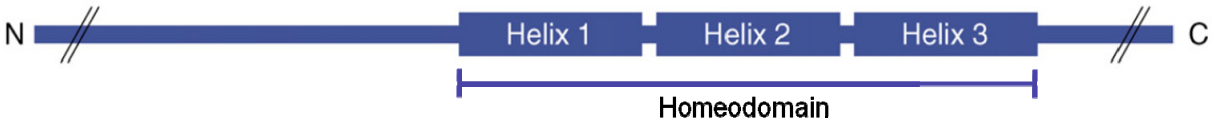

Figure 1.4. Structure of the Engrailed 1 protein. En1 is characterized by the presence of the homeodomain, a 60 amino acids sequence, consisting of 3 α-helices, which shares high homology sequence within the members of the homeobox transcription factor family (picture modified from (Brunet et al., 2007)).

Engrailed was first identified in *Drosophila*, where it has a role in the segmentation and polarity of the body and in the development of the nervous system (Kornberg, 1981; Lawrence and Struhl, 1982).

Studies of En expression patterns among a wide range of metazoans suggested an evolutionary conserved role (Patel et al., 1989). Homologues of En are present in numerous species including annelids (Wedeen and Weisblat, 1991), mollusks (Wanninger and Haszprunar, 2001), echinoderms (Lowe and Wray, 1997), chordates (Holland et al., 1997), and vertebrates (Joyner et al., 1985). The two En proteins (En1 and En2) present in mouse and chick were identified based on their homology to the *Drosophila En* gene (Joyner et al., 1985; Joyner and Martin, 1987).

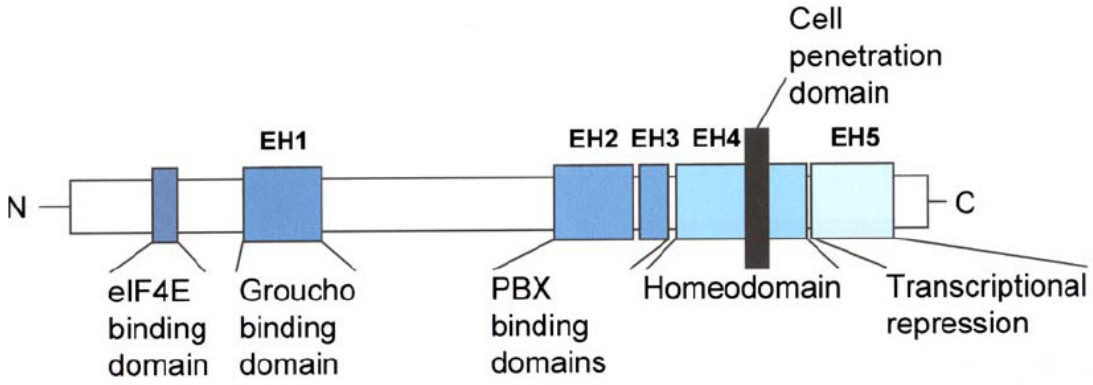

Figure 1.5. Functional domains of Engrailed. EH: En homology region. The transcription activity of En is determined by the phosphorilation of a region between EH1 and EH2. EH5 is responsible for transcriptional repression. The secretion and internalization sequences are located within the Homeodomain (picture taken from (Morgan, 2006)).

Although En homologues share a high functional similarity, they have a relatively small degree of sequence conservation. Comparing sequences among different phyla, revealed five regions of similarity, called En homology regions (EHs) and designated as EH 1-5 with the highest level of conservation (90%) within the homeodomain (EH4) (Logan et al., 1992)

(Figure 1.5). EH1 and EH5 mediate transcriptional repression, with EH1 by recruiting the co-repressor Groucho (Tolkunova et al., 1998), while EH2 and EH3 bind PBX, a homeodomain transcription factor that modulates the binding affinity and specificity of En to DNA (van Dijk and Murre, 1994; Peltenburg and Murre, 1997).

En proteins, in addition to their localization in the nucleus, which corresponds to their well-known role as transcriptional regulators, were also detected in the cytoplasm and in membrane fractions (Joliot et al., 1997; Zhong et al., 2010). It was shown that En proteins can be secreted and internalized from cells (Cosgaya et al., 1998; Joliot et al., 1998) and might thus be involved in non-cell-autonomous signaling (Prochiantz and Joliot, 2003). Recent studies show that the secretion of En protein takes place without the presence of a signal peptide and that this process requires the nuclear translocation of the protein suggesting that nuclear factors may be important for the export of En from the cell. After En is synthesized in the cytoplasm, the nuclear localization signal (NLS) mediates its translocation into the nucleus. En is then exported into the cytoplasm through the nuclear export signal (NES), located between helices 2 and 3 of the homeodomain (Figure 1.6). Prior to secretion, En associates with membrane fractions enriched in cholesterol and glycosphingolipids, caveolae-like vescicles or microdomains (Joliot et al., 1997), suggesting the presence of an axonal transport mechanism, since microdomains are primarily, although not exclusively, located to the axons (Dotti and Simons, 1990; Dotti et al., 1991). The exact mechanism regulating En secretion is unknown, although it is clear that it depends upon a conserved 11 amino acids sequence called Δ1, which is a part of the nuclear export signal (NES, (Joliot et al., 1998), Figure 1.6). It was also shown that the phosphorylation status of the En C-terminal end represents an important mechanism controlling intercellular homeoprotein secretion (Maizel et al., 2002).

En can be internalized and have a direct access to the cell cytoplasm and nucleus, without the requirement of the classical endocytosis. This process requires the presence of a 16 amino acids sequence within the homeodomain called Penetratin which is necessary and sufficient for the internalization of En by neighboring cells (Figure 1.6) (Derossi et al., 1994; Chatelin et al., 1996).

Another important property characteristic of En is its ability to directly bind the eukaryotic translation initiation factor 4E (eIF4E), through a sequence located on the N-terminal side ((Nedelec et al., 2004), Figure 1.5), thereby activating local translation of new proteins in growth cones that allow for axon turning (Brunet et al., 2005).

Thus, En is a transcription factor with multifaceted and complex functions, as it not only modulates transcription, but also translation with different mechanisms involving secretion and internalization.

Vertebrates have two En proteins, En1 and En2, which have very similar functions during brain development (Hanks et al., 1995; Hanks et al., 1998). They control the patterning of the mid-hindbrain junction, a region which gives rise to the cerebellum, where they start to be expressed in a broad band at 1-somite-stage and 5-somites-stage, respectively and continue to be expressed in this region throughout development (Wurst et al., 1994; Joyner, 1996; Darnell and Schoenwolf, 1997). In the adult, expression of both genes is limited to the same set of neurons in the ventral tegmental area and in the substantia nigra, where they play a role in the survival of adult mid-brain dopaminergic neurons (Sonnier et al., 2007).

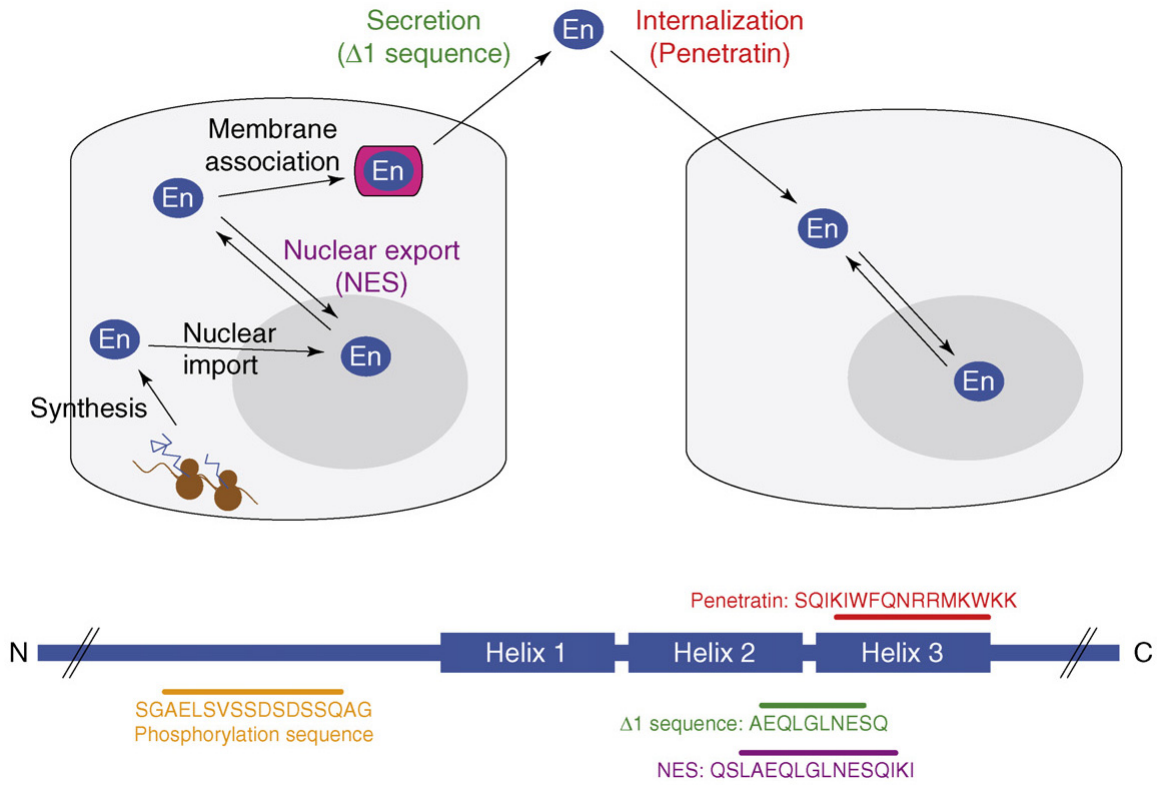

Figure 1.6. Mechanisms of secretion and internalization of the En protein. En1 protein secretion does not require a signal peptide. After En protein is synthesized, it enters the nucleus (Nuclear import sequence) and exits from the nucleus using the Nuclear export sequence (NES). En associates with membranes and the Δ1 sequence mediates its secretion. Internalization of the En protein is also unconventional and requires a sequence of 16 amino acids called Penetratin (picture taken from (Brunet et al., 2007)).

At E9.5, En1 starts to be expressed also in a rostral-to-caudal progression in two lateral stripes along the hindbrain, in the spinal cord and DRG (Davidson et al., 1988; Davis and Joyner, 1988) of mouse, chick, zebrafish, and *Xenopus laevis* (*Xenopus*) (Davidson et al., 1988; Gardner et al., 1988; Davis et al., 1991), suggesting an important role during early spinal cord development. In the mouse spinal cord En1 marks a class of interneurons (V1) (Burrill et al., 1997; Saueressig et al., 1999; Moran-Rivard et al., 2001) located at the margins of the spinal cord at approximarely E10.5, that later migrate more ventrally and settle in the vicinity of motor neurons around E12.5 (Matise and Joyner, 1997; Pierani et al., 2001).

Interestingly, rather than been required for the survival, migration or expression of other transcription factors in the developing spinal cord (Matise and Joyner, 1997), En1 protein seems to be involved in axonal pathfinding (Saueressig et al., 1999). Studies in mouse reveal that En1 is expressed specifically by interneurons that extend their axons towards the motor column, suggesting that they synapse with motor neurons. *En1* mutant mice show interneuron axon defasciculation and axonal disorganized trajectories, revealing that En1 controls fasciculation and axon pathfinding of interneurons projecting to motor neurons (Saueressig et al., 1999). It was also shown in chick that En1-expressing interneurons exhibit a direct synaptic connection with motor neurons that is likely to be GABAergic (Wenner et al., 2000).

En1 homozygous mutant mice die shortly after birth because of developmental defects: cerebellum and colliculi are missing and the third and fourth cranial nerves are absent (Wurst et al., 1994). *En1* null mice also show sternum and ribs disorganization and limb patterning defects at morphological and structural levels (Wurst et al., 1994). Indeed, it was shown that En1, starting at E9.5 to be expressed in the ventral ectoderm of the developing limb bud, represses the dorsalizing action of Wnt7a, a secreted factor present in the dorsal ectoderm, thereby collaborating to pattern the limb (Wurst et al., 1994; Loomis et al., 1996). En1 is also expressed in other structures, including the sympathetic ganglia, the cranial mesenchyme, the mandibular arches (Davis et al., 1991), the vagus nerve, the somites, the heart and the cloaca (Zhong et al., 2010).

Differently from the phenotypes observed in $En1^{-/-}$ mice, the ablation of *En2* causes milder defects. *En2* mutant mice ($En2^{-/-}$) are viable and exhibit only light patterning errors in the adult cerebellum (Joyner et al., 1991; Millen et al., 1994). The replacement of the *En1* coding sequence with the *En2* sequence in $En1^{2ki/2ki}$ mutant mice completely rescues all *En1* mutant phenotypes (Hanks et al., 1995), demonstrating that the function En1 and En2 is partially redundant in the midbrain.

In addition to the DNA-binding domain regulating the well-known role of En as transcription factor, the presence of amino acid domains involved in nuclear export, secretion and internalization (Prochiantz and Joliot, 2003), prompted researchers to investigate the possibility that En may have a direct role in intercellular communication. Interestingly, studies in *Xenopus* and chick visual systems revealed that En can also act as a direct axon guidance cue, repelling retinal and tectal axons (Brunet et al., 2005; Wizenmann et al., 2009). *In vitro* experiments in *Xenopus* demonstrated that soluble En protein is presented in an external gradient, is internalized by retinal axons, and triggers the local translation of proteins that elicit axonal turning (Brunet et al., 2005). More recent data in chick demonstrated that extracellular En, expressed in a posterior to anterior gradient in the tectum, regulates the pathfinding of temporal retina axons, thereby contributing to the formation of the retinotectal map (Wizenmann et al., 2009).

These findings prompted us to investigate whether En1 plays a similar role in the spinal sensory-motor system. Our data show that En1 causes specific growth cone collapse of dorsally projecting motor axons *in vitro* and that the dorsal-ventral motor axonal choice at the base of the limb is impaired in *En1* mutant mice. Therefore, En1 represents an interesting candidate to mediate forelimb motor axon guidance, contributing to the formation of the vertebral sensory-motor system.

The results of this PhD thesis reveal novel guidance cues that govern the dorsal-ventral choice of motor and sensory axons, thereby providing potential molecules and markers regulating the trajectory of the axons at the base of the limb. This work, therefore, opens many possibilities to further characterize the newly identified molecules, to investigate the molecular mechanisms they use to regulate axon guidance and also to verify whether they play a role in the establishment of other systems. Furthermore, this work unravels and characterizes En1 as an axon guidance molecule in the motor system. Our data show that it repells lateral LMC axons and it contributes to regulate the establishment of the binary choice of motor axons at the base limb. Further investigation is required to understand the mechanism how En1 specificity is achieved, by investigating if En1 is specifically internalized by the LMCl neurons, which mechanism allows its internalization and which downstream cellular signalling systems are triggered in En1-mediated axon guidance.

2 Materials and Methods

2.1 Mouse embryo manipulation

2.1.1 Mutant mice

The following mouse lines were used: *En-1*^{Lki} (*LacZ* knock-in) (Hanks et al., 1995), *En-1*^{cond} (Sgaier et al., 2007), *Hb9-GFP* (Wichterle et al., 2002), *Hb9-Cre* (Arber et al., 1999).

2.1.2 Genotyping

Tail clips were used for the preparation of DNA samples for genotyping. Adult tissue was incubated over night at 56°C in a shaker in 200µl Fast Prep Buffer (50mM KCl, 10mM Tris-HCl, 2.5mM $MgCl_2$-$6H_2O$, 0.1mg/ml Gelatin, 0.45% Nonidet P40, 0.45% Tween 20) containing 100µg/ml Proteinase K (Invitrogen). Embryonal tissue was digested for 2 hours at 56°C in 50µl of Fast Prep Buffer containing 30µg/ml Proteinase K. This DNA-solution was used directly as template for polymerase chain reaction (PCR). The genotype analysis was performed by PCR using Taq DNA polymerase (Quiagen, Invitrogen) in a thermocycler (SensoQuest Labcycler and Eppendorf).

En-1^{Lki} homozygous and heterozygous mutant mice were identified with the primer pair L-LacZ: CGC CAT TTG ACC ACT ACC and U-LacZ: GGT GGC GCT GGA TGG TAA (Metabion) with the following cycling parameters: 5 minutes preheating to 95°C, 38 cycles of denaturation of the DNA at 95°C for 35 seconds, annealing of the primers at 59°C for 40 seconds and polymerization at 72°C for 40 seconds. Polymerisation was finished at 72°C for 10 minutes and then put on hold at 12°C until analysis on a 2% agarose gel (BioSell

Universal Agarose in 1x TAE buffer, 150µg/ml Ethidiumbromid). *En-1*^{Lki} wild type and heterozygous mice were identified with the primer pair En1_3E7 fwd geno: AGC CGG AGC CTA AAA GTC AG and En-1R: CAC GCT GTC TCC ATC GCT (Metabion) with the following cycling parameters: 2 minutes preheating to 94°C, 35 cycles of denaturation of the DNA at 94°C for 30 seconds, annealing of the primers at 55°C for 30 seconds and polymerization at 72°C for 30 seconds. Polymerisation was finished at 72°C for 10 minutes and then put on hold at 12°C until analysis on a 2% agarose gel. To determine the presence of the *loxP* site in the *En-1*^{cond} mice the primer pair En1CKO-1a: GCC AAA CTG CTT ACG ACC G and En1CKO-2a: TGG GTG GGT AGA GAA GAG GC (Metabion) was used with the following cycling parameters: 3 minutes preheating to 95°C, 35 cycles of denaturation of the DNA at 95°C for 1 minute, annealing of the primers at 57°C for 30 seconds and polymerization at 72°C for 1 minute. Polymerisation was finished at 72°C for 10 minutes and then put on hold at 12°C until analysis on a 2% agarose gel.

The presence of the *Cre* allele was determined using the primers Forward: GTC TCC AAT TTA CTG ACC GTA CAG and Reverse: GAC GAT GAA GCA TGT TTA GCT GG (Metabion) with the following cycling parameters: 5 minutes preheating to 95°C, 30 cycles of denaturation of the DNA for 1 minute at 95°C, 1 minute annealing of the primers at 59.5°C and 30 seconds polymerization at 72°C. Polymerization was finished at 72°C for 15 minutes and then put on hold until analysis on a 2% agarose gel.

Mice were analyzed for presence of the *GFP* allele with the primer pair 872: AAG TTC ATC TGC ACC ACC G and 1416: TCC TTG AAG AAG ATG GTG CG with the following cycling parameters: 3 minutes of preheating to 95°C, 35 cycles of denaturation of the DNA at 95°C for 30 seconds, annealing of the primers for 1 minute at 60°C and polymerization for 1 minute at 72 °C. Polymerization was finished at 72°C for 15 minutes and then put on hold at 12°C until analysis on a 2% agarose gel.

2.1.3 Mouse embryo preparation for dye injections

Embryos were dissected at embryonic day 12.5 (E12.5) and prepared in DMEM/F-12 medium (Gibco). Head and tail were removed for genotyping. The embryo was cut at the level of the liver to allow for separated backfill of motor neurons projecting to the fore- or hindlimbs. The two parts of the embryo were pinned onto sylgard-plates (Dow Corning) using insect pins (Fine Science Tools). For cell sorting of motor or sensory neurons, between 20 and 30 embryos were pooled.

2.1.4 Retrograde labeling of neurons

For the retrograde tracing of motor and DRG neurons and subsequent use for fluorescence activated cell sorting (FACS) dextran-conjugated Alexa488 (3000MW, Molecular Probes) and dextran-conjugated Alexa680 (3000MW, Molecular Probes) were injected into the dorsal and ventral limb musculature, respectively, using glass needles (TW100-4, World Precision Instruments).

After injection, the medium was changed. Embryos were incubated for 3 or 5 hours for DRG and motor neurons, respectively, in aerated medium: a bubble stone connected to 5% CO_2 in 95% O_2 gas (Linde) was added to the plate.

To investigate the dorsal or ventral choice of sensory and motor axons histologically, dextran-conjugated Alexa680 was replaced by dextran-conjugated Rhodamine (3000MW, Molecular Probes).

After 3 to 5 hours of incubation in aerated medium, backfilled embryos were fixed in 4% paraformaldehyde (PFA) in PBS for 1 hour, rinsed in PBS and cryoprotected over night in 30% sucrose in PBS. On the following day embryos were washed twice in PBS, frozen in tissue tek O.C.T. embedding medium (Sakura) and kept at -80°C until further analysis.

2.1.5 Preparation of motor and DRG neurons

For motor neuron preparation, spinal cords were extracted and the ventral part, containing the motor neurons, was separated from the dorsal part with a small cutter and then cut in 5 to 6 pieces of the same dimension with a scalpel in a Petri dish. The cervical part of the spinal cord was eliminated. The spinal cord pieces were collected in 1 ml DMEM/F-12 medium and allowed to settle. 10µg/ml trypsin (2.5%, Gibco) was added and the sample was incubated for 12 minutes at 37°C, agitating every 2 minutes by tipping the tube. 100µl heat inactivated fetal calf serum was added, the cells were triturated with a fire-polished Pasteur pipette and kept on ice until cell sorting.

For the preparation of sensory neurons, DRGs were collected in a 15 ml Falcon tube (BD Bioscience) containing 14ml DMEM/F-12 medium and pelleted by centrifugation for 5 minutes at 0.3 rpm (Centrifuge 5702, Eppendorf). 400µl trypsin were added and samples were further treated with the same procedure used for motor neurons.

2.1.6 Fluorescent activated cell sorting

Backfilled neurons were sorted using a FACStar machine (BD Bioscience), based on the presence of dextran-conjugated Alexa488 (in the dorsally projecting cells) or to Alexa680 (in the ventrally projecting cells) in their cell bodies. The two neuronal populations were separately collected and kept on ice. Samples containing approximately 3000 cells positive for Alexa488 or Alexa680 were further used for RNA preparation (at least 3 biological replicates for each cell population [brachial and lumbar MN and DRG]).

2.1.7 RNA isolation and microarray analysis

2.1.7.1 Brachial motor neurons microarray hybridization

The RNeasy Micro Kit (Qiagen) was used for RNA extraction from motor neurons projecting to the forelimb. Because of the small cell number, the Lysis buffer RTL (provided in the RNeasy kit) was supplemented with a ExpressArt Pico RNA Care reagents, N- and P-carriers (Artus), (1µl carriers per 100 ml RLT buffer) and the purification was then performed according to Qiagen's protocol. Briefly, samples were lysed and homogenized. Ethanol was added to the lysates that then were loaded onto the spin column and finally RNA was eluted in water. RNA quality was examined using an Agilent Bioanalyzer (RNA 6000 Pico Chip, Agilent 2100). The RNA amplification was performed with MessageAmp II aRNA amplification kit and Illumina TotalPrep RNA amplification kit (Ambion), according to manufacturer's protocol. Briefly, RNA was firstly reverse-transcripted in cDNA that then underwent second-strand synthesis and cleanup to become a template for *in vitro* transcription. A double-round amplification was used to synthesize biotin-labeled cRNA that was then hybridized to a Sentrix Mouse-6 BeadChip (Illumina) according to standard protocols provided by Illumina.

2.1.7.2 DRG neurons and lumbar motor neurons microarray hybridization

For RNA isolation and microarray hybridization (Agilent Whole Genome 4x44K format, One-Color) from DRG neurons projecting to the forelimb and from motor and DRG

neurons targeting the hindlimb, samples were handled by the Miltenyi Biotec Company, according to the SuperAmp preparation Kit protocol.

After FACS, samples were treated according to Miltenyi's protocol: cells were collected in a SuperAmp Tube (provided by the company) and pelleted by centrifuging at 100 rcf for 5 minutes at 4°C. The supernatant was then carefully aspirated, leaving the cells in approximately 1µl. Cells were resuspended in 6.4 µl of Lysis Buffer (Miltenyi). After 10 minutes incubation at 45°C, cells were frozen at -20°C and sent to Miltenyi on dry ice.

2.1.8 Microarray data analysis

The R-environment (http://www.r.project.org) and the specific open source software Bioconductor, based on R and intended for analysing and interpreting genetic data (http://www.bioconductor.org) were used for microarray data analysis. Because of some differences in the design and the structure of raw data from Illumina and Agilent microarray analysis, data pre-processing and data normalization had to be performed in a different way.

Data pre-processing for the raw Agilent microarrays data is based on the background correction procedure and on the analysis of 10 technical replicates for a subset of genes. This unspecific filtering procedure passes only expression values significantly different from background and exceeding some limit with sufficient low standard deviation in the analysis of technical replicates. No specific within-array normalization was performed but a quantile normalization between all arrays was implemented. After normalization all arrays were analysed jointly. The calculation of inter-array correlation and a principal component analysis with the normalized data led to the identification and exclusion of possible outlier samples (bad quality arrays) from the data set.

For Illumina microarrays intensity values come with a p-value for the difference to the background. The first unspecific filtering procedure is based on different limits for this p-value. Based on the pairwise dependencies for this data within-array normalization are performed. As a prerequisite of the normalisation step, "MA-plots" were created for all pairs. Then normalization was based on a fit of the relationship between M and A, estimating a polynomial surface with local polynomial fitting (R-function loess with parameter span=0.75). Then the same procedure as before was used to detect bad quality arrays.

In a following step, for normalized Agilent and Illumina data, statistical methods were used to rank genes in order of evidence for differential expression and to select subgroups based on statistical characteristics. To this end, a two step method was applied. First, a mixed-

effect model was employed to allow for the analysis of grouped data (grouped with respect to embryo pools). Then, an empirical Bayes method was used to shrink the probe-wise sample variances toward a common value (R-function ebayes in package limma). A table listing the top-ranked genes with fold change estimator and the estimated false discovery rates (fdr) was obtained (R-function topTable in package limma) and finally genes selected with fdr < 0.10 and log fold change > 1.

2.1.9 Synthesis of digoxigenin-labeled RNA probe

Antisense and sense riboprobes were generated by *in vitro* transcription from linearized DNA templates (Table 2.1).

The RNA synthesis was performed in 20µl volume containing 1–2µg of linearized DNA template using T3, T7, or Sp6 RNA polymerases (Fermentas) and the labeling was obtained by digoxigenin incorporation using the DIG RNA-Labeling mix (Roche). After 2 hours of incubation at 37°C, transcription was terminated on ice and RNA was precipitated by adding 0.1x Volume LiCl (Sigma) and 2.5x Volumes 100% Ethanol (Merck). The mix was kept for 30 minutes at –80°C and the precipitated RNA was washed in 70% ethanol and then dissolved in 20µl diethylpyrocarbonate (DEPC) treated water.

Name	Vector	Source and Reference	Linearization		Polymerase	
			AS	S	AS	S
Dcn	pSPORT1	ImaGenes	PstI	HindIII	SP6	T7
Dock6	pYX-Asc	ImaGenes	EcoRI	NotI	T3	T7
Ebf-2	pBluescript II KS	Wurst Lab – (Guimera et al., 2006)	BamHI	HindIII	T3	T7
Ednrb	pBluescript KS	Ginty Lab – (Makita et al., 2008)	NotI	XhoI	T3	T7
Elk3	pSPORT1	ImaGenes	NotI	SalI	SP6	T7
En1	pBluescript II KS	Wurst Lab – (Davis and Joyner, 1988)	HindIII	BamHI	T7	T3
EphA8	pT7T3D-PacI	ImaGenes	EcoRI	NotI	T3	T7
Eto	pSPORT1	ImaGenes	PstI	HindIII	SP6	T7
G-protein γ3	pCMV-SPORT6	ImaGenes	EcoRI	HindIII	T7	SP6
Gad1	pBluescript II KS	Wurst Lab – (Guimera et al., 2006)	BamHI	PstI	T3	T7
IGF2	pYX-Asc	ImaGenes	SalI	NotI	T3	T7

IGFBP5	pCMV-SPORT6	ImaGenes	EcoRI	XhoI	T7	SP6
Lmx1b	pSPORT1	Wurst Lab – (Cygan et al., 1997)	XhoI	EcoRI	SP6	T7
MDK	pBluescript LION	ImaGenes	XhoI	AscI	T7	T3
Msih2	pSPORT1	ImaGenes	EcoRI	NotI	T3	T7
Npn-2	pBluescript from λ ZAP	Kolodkin Lab – (Kolodkin et al., 1997)	EcoRI	XhoI	T7	T3
RhoJ	pT7T3D	Fort Lab –(Vignal et al., 2000)	XhoI	HindIII	T3	T7
VTN	pCMV-SPORT6	ImaGenes	SalI	NotI	T7	SP6

Table 2.1. List of plasmids and corresponding RNA probes used for in situ hybridization. AS: antisense; S: sense.

2.1.10 In situ hybridization

E12.5 CD1 mouse embryos were sectioned in 12µm transverse sections at -24°C using the cryostat CM 1950 (Leica) and mounted on superfrost microscope glass slides (Menzel). Sections were air dried at room temperature for 30 minutes and kept at –80°C until use. Slides from fresh frozen tissue were thawed for 30 minutes, fixed 12 minutes in 4% Paraformaldehyde in PBS and washed three times for 5 minutes in PBS before 10 minutes acetylation in 0.25% acetic anhydride in 1% triethanolamin (TEA [AppliChem]). This was followed by two washing steps for 5 minutes in PBS and 1 washing step for 5 minutes in 2x standard saline citrate (2x SSC). Slides were pre-hybridized for 3 hours in a humified chamber in hybridization solution (50% formamide [Sigma], 5x Denhardt's solution, 205ng/ml baker yeast tRNA and 5x SSC) at room temperature. DIG-labeled cRNA probes were dehybridized in hybridization solution for 5 minutes at 90°C and then incubated for 5 minutes on ice before applying the mix to the slides, covering them with Nescofilm (Alfresca Pharma Corporation), and hybridizing the slides in a humified chamber at 60°C over night. Fixed tissue sections, after 30 minutes thawing, were fixed on the slides for 12 minutes in 4% Paraformaldehyde in PBS, rinsed in PBS and incubated for 7 minutes in PBS containing 5µg/ml Proteinase K and 0.1% Triton X-100 (Sigma). After that the sections were treated following the same protocol as for slides from fresh frozen tissue. After overnight hybridization, sections from fresh frozen and fixed tissue were washed for 5 minutes in 5x SSC, 1 minute in 2x SSC, and 30 minutes in 50% formamide containing 0.2x SSC at 60°C followed by a washing step of 5 minutes in 0.2x SSC at room temperature. Slides were then washed for 5 minutes in Buffer 1 (100mM Tris, 150mM NaCl) before blocking for 1 hour in

1% blocking reagent (Roche) in Buffer 1. This was followed by 1–3 hours of antibody incubation with anti-DIG-Fab-fragments (Roche) in blocking solution (1:5000) in a humified chamber. Sections were washed two times for 15 minutes in Buffer 1 and one time for 5 minutes in Buffer 2 (100mM Tris, 10mM NaCl, 5mM MgCl2), followed by the light sensitive color reaction at room temperature (340mg/ml nitrobluetetrazolium [NBT, Roche] and 175 mg/ml 5-bromo-4-chloro –3 indolylphosphate [BCIP, Roche] in Buffer 2) in a humified chamber in the dark. The color reaction was stopped by washing the slides for 10 minutes in 1x TE (100mM Tris, 10mM EDTA) and sections were coverslipped with Mowiol mouting medium (Calbiochem).

Investigation of the slides was performed on a Zeiss LSM 510 Meta confocal microscope with the objectives N PLAN 10x dry and N PLAN L 20x dry.

2.1.11 Fluorescent immunohistochemistry

Frozen fixed embryo sections were dried for 30 minutes at room temperature before immunohistochemistry was performed. Slides were washed for 10 minutes in PBS and blocked for 30 minutes in PBS-T (PBS + 0.1% TritonX-100) containing 10% horse serum. Slides were incubated with primary antibodies (Table 2.2) in PBS-T containing 10% serum over night in a humified chamber at 4°C. On the second day sections were washed three times for 5 minutes in PBS-T before incubation with the secondary antibodies (Table 2.3) for one hour at room temperature in the dark. After three final wash steps for 5 minutes in PBS in the dark, sections were mounted with Mowiol mounting medium and kept in the dark until further investigation.

Microscopy was carried out as described for in situ hybridisation.

Host	Against	Dilution	Source
Mouse	Isl1/2 (39.4D5)	1:50	Developmental Studies Hybridoma Bank
Rabbit	Lim1	1:10.000	Jessell Lab
Mouse	Neurofilament (2H3)	1:50	Developmental Studies Hybridoma Bank
Rabbit	En1 (68/8)	1:7000	Prochiantz Lab
Mouse	En1 (4G11)	1:100	Developmental Studies Hybridoma Bank
Chick	GFP	1:500	Aves labs, inc.
Rabbit	GAP43 (ab11136)	1:500	AbCam

Table 2.2. Primary antibodies used for immonohistochemistry.

Host	Against	Conjugate	Dilution	Source

Donkey	mouse	alexa 488	1:250	Invitrogen
Goat	rabbit	cy2	1:250	Jackson IR
Goat	mouse	cy3	1.250	Jackson IR
goat	rabbit	cy3	1:250	Jackson IR
Donkey	chick	FITC	1:500	Jackson IR

Table 2.3. Secondary antibodies used for immonohistochemistry.

2.1.12 Evaluation of mRNA signal on embryo sections (validation of the candidates)

ISH and IHC pictures were analyzed using Photoshop (Adobe Systems). Digital images were imported to Photoshop, merged and processed for brightness and contrast.

The ventral horn of the spinal cord was outlined on the ISH image. By overlaying the ISH and the IHC pictures, the lateral motor column (LMC) was identified and outlined with a white dashed line. Then, the nuclei of the cells within the LMC region, which showed the mRNA signal in the cytoplasm, were highlighted in yellow. Overlay with the IHC picture allowed the identification of neurons both positive for ISH and IHC signals.

Lateral LMC neurons were distinguished from medial LMC neurons by Lim1 and Isl1 staining, respectively, allowing to determine whether the ISH signal was present either in the dorsally or in the ventrally projecting motor neurons. To compare the percentage of cells expressing the candidate gene located in the two investigated cell pools, cell positive for in situ hybridization (labeled yellow) and positive for either Lim1 or Isl1 were counted and compared with the microarray predictions.

2.2 Molecular biology

2.2.1 Transformation of bacteria with plasmid-DNA (BioRad protocol)

Frozen (-80°C) competent cells were thawed on ice. 50µl of cells were transferred to a cold 1.5ml tube, mixed with 1µl of DNA and let stand on ice. The Gene Pulser Xcell (BioRad) was set to 25mF, 200ohms and 1.8kV for the 0.1cm cuvettes (BioRad). The mixture of cells and DNA was transferred to the bottom of the cold electroporation cuvette and the

cuvette was pushed into contacts at the base of the chamber. After pulsing once, the parameters were checked (constant between 4-5msec). The cuvette was then removed from the chamber and the cells were quickly resuspended with 250µl S.O.C. medium (Invitrogen). After 1 hour incubation by shaking at 37°C, cells were plated on Luria Bertani (LB) agar selective Petri dishes and further incubated at 37°C over night.

2.2.2 Midi preparations for plasmid DNA isolation from bacteria

For preparations of purified plasmid DNA, bacterial colonies were picked from Petri dishes, transferred to 2ml LB selective medium and incubated for 8-9 hours at 37°C on a bacterial shaker. Cells were then transferred to 50ml LB selective medium and further incubated over night at 37°C. The following day, bacterial cultures were transferred into 50ml Falcon tubes and pelleted by centrifugation at 4000 rcf for 30 minutes at 4°C. Isolation of plasmids from bacterial cultures was performed using the Plasmid Midi Kit (Qiagen) according to the manufacturer's protocol.

2.2.3 Plasmid DNA linearization (restriction digest)

The linearization of 5-10µg DNA template plasmid was performed with a restriction enzyme in 50µl reaction. The mix was incubated for 2 hours at 37°C and purified by chloroform/phenol extraction. After EtOH precipitation the DNA was resuspended in TE, analyzed on a 1% agarose gel and stored at -20°C until further use.

The plasmids and the enzymes used are listed (Table 2.1).

2.3 Cell culture

2.3.1 Coverslip coating

Coverslips (VWR International) were treated in concentrated (65%) nitric acid in 50ml Falcon tube for 24-36 hours on a shaker, then washed extensively with water (2 days - 1 week), dried separately on Whatman filterpaper and backed at 175°C over night.

Coverslips were added to the culture wells and 500µl Poly-L-Lysin (10µg/ml, Sigma) in sterile water was added to coat the coverslips and dishes were incubated 1 hour at 37°C in the incubator (Hera). Poly-L-Lysin was then removed and dishes were let to dry for at least 30 minutes.

500µl laminin (3µg/ml, Invitrogen) in Hanks' Balanced Salt Solution (HBSS) were added to each well and the dishes were incubated for approximately 3 hours at 37°C in the incubator, washed and always kept moist. The coating of the coverslips was performed under a sterile hood (Hera).

2.3.2 Dissociated primary motor neuron culture

E10.5 and E11.5 *Hb9-GFP* mouse embryos were prepared as described in section 2.1.3 and the GFP positive embryos identified under a fluorescent stereomicroscope. Spinal cords were removed, cut in pieces of similar dimensions in Leibovitz's L-15 medium (Gibco) and transferred to a 15ml Falcon tube using a blue tip. In a sterile hood, L15 medium was carefully removed and 1ml HAM-F10 medium (Gibco) was added. After spinal cord pieces settled, HAM-F10 medium was removed and 1ml of fresh medium added. 10µl trypsin (2.5% w/v, final conc. 0.025%) were added and the sample was incubated for 9 minutes at 37°C, agitating every 2 minutes by tipping the tube. Medium was removed and 1ml complete medium [800µl L-15 complete medium (90% L-15 medium, 5% glucose [Sigma], 1% penicillin-streptomycin [Sigma], 1% N2 Supplement [Gibco], 1% conalbumin [Sigma], 2% horse serum [Invitrogen]), 100µl BSA (4% w/v in L-15 medium, Sigma) and 100µl DNAse (1mg/ml in L-15 medium, Sigma)] were added. The tissue pieces were disaggregated by tipping the tube and triturated twice with a blue tip. Fragments were let settling for 2 minutes and the supernatant was then transferred to a Falcon tube (tube B). To each tube containing the fragments 900µl L15 complete medium, 100µl BSA and 20µl DNAse were added. After 8 times trituration with a blue tip, fragments were let settling for 2 minutes and then supernatant was transferred to tube B. The same procedure was repeated once again and, before centrifuging for 5 minutes at 1500rpm, a ~1.5-2ml 4% BSA cushion was prepared onto the bottom of tube B using a Pasteur pipette.

Cells were resuspended in 1ml NB complete medium (NeuroBasal medium [Gibco], glutamine [200mM, Gibco], glutamate [25mM, Sigma], 0.1% β-mercaptoethanol [Sigma], 2% horse serum [Invitrogen], 2% B27 supplement [Gibco], 1% penicillin-streptomycin [Sigma]), counted and diluted to obtain 10^5 cells/ml. Growth factors (CNTF [10ng/ml], BDNF [1ng/ml],

GDNF [1ng/ml], Sigma) were added (1:1000) and cells were plated on coated coverslips (see 1.3.1) in 4-well culture dishes (Nunc).

2.3.3 Collapse assay in primary cultured motor neurons

Cells were allowed to grow for 5 or 11 hours for E11.5 and E10.5 embryos, respectively. Proteins (Table 2.4) were dialyzed against HBSS for 1 hour using the small Millipore filter (Millipore) with gentle agitation at 4°C. Protein was added at different concentrations, depending on the experiment (En1: 5ng/ml, 10ng/ml, 50ng/ml, 100ng/ml, 400ng/ml; En1SR: 100ng/ml, En2: 100ng/ml; ephrinA2/A5: 0.1µg/ml, 0.5µg/ml, 1µg/ml; Shh: 0.5µg/ml, 2.5µg/ml, 4µg/ml) by collecting 250µl of medium from each well, mixing it with the protein in an Eppendorf tube and re-adding the mixture in droplets scattered in the entire well. Culture dishes were incubated again for 30 minutes to 2 hours and then cells were fixed with 4% PFA for 30 minutes. After washing for 10 minutes with PBS, fluorescent immunocytochemistry was performed. Primary antibodies (chick anti-GFP and Rabbit anti-Lim-1 [Table 2.2]) in PBS-T containing 10% serum were incubated at 4°C over night and the following day, after three washing steps with PBS for 5 minutes, cells were incubated with secondary antibodies for one hour at room temperature in the dark. After three washing steps for 5 minutes each in PBS in the dark, coverslips were transferred on microscope glass slides and mounted with Mowiol mounting medium and kept in the dark until further analysis.

When indicated (see section 3.2.4), cells were pre-treated with inhibitors of translation (anisomycin, 10µM [Sigma]) or transcription (α-amanitin, 10µg/ml [Sigma]) for 15 minutes prior to addition of En1 and then handled as described.

Microscopy was performed on a Zeiss LSM 510 Meta confocal microscope with the N PLAN 40x oil objective.

Protein	**Source**
Engrailed 1	A. Prochiantz
Engrailed 1 SR	A. Prochiantz
Engrailed 2	A. Prochiantz
ephrinA2 (603-A2)	R&D Systems
ephrinA5 (374-EA)	R&D Systems
Shh (461-SH)	R&D Systems

Table 2.4. Proteins used for functional assays.

For E11.5 embryos, lateral LMC neurons were identified by co-expression of GFP and Lim1 and thereby distinguished from medial LMC neurons, which only express GFP. 50 neurons of each cell population per well were analyzed for the presence of collapsed or non-collapsed growth cones by an observer blind to the experimental conditions. Significance of differences between the two cell populations was determined using the Student's t-test.

2.3.4 Motor and DRG neuron explants

E11.5 and E12.5 embryos were dissociated as described in section 2.1.3 and spinal cords or DRGs were dissected and cut in pieces of similar dimensions. Matrigel (BD Bioscience) was kept on ice and briefly centrifuged at 4°C as soon as thawed. A Matrigel cushion (approximately 30µl) was prepared with a pipette onto the bottom of a culture plate and let gel for approx. 15 minutes. 4-5 explants were applied on the cushion and covered with approx. 80µl Matrigel. Dishes were incubated at 37°C for 50-60 minutes. DRG medium (NeuroBasal and Optimem medium [Gibco], glutamine [200mM], glucose [1M], heat inhibited FCS [Invitrogen], penicillin-streptomycin and NGF [20ng/ml, Sigma]) and MN medium (see section 2.3.2) were pre-warmed at 37°C and carefully (slowly and from the side) added to the plates. Explants were then incubated for 24-48 hours, until the presence of axons was visible. They were then fixed in 4% PFA for 30 minutes and after three wash steps for 10 minutes in PBS, immunocytochemistry was performed. The Chick anti-GFP and Rabbit anti-Lim1 (Table 2.2) primary antibodies in PBS-T containing 10% horse serum were incubated over night at 4°C. On the second day, explants were washed 3 times for 5 minutes in PBS-T before incubation with the secondary antibodies (Table 2.3) for one hour at room temperature in the dark. After 3 finally washing steps for 5 minutes in PBS, coverslips were mounted with Mowiol mounting medium and kept in the dark until microscopy investigation, as described for in situ hybridization.

3 Results

3.1 Screening for novel factors governing the dorsal-ventral choice of motor and sensory axons at the base of the limb

3.1.1 Enrichment of motor and sensory neurons

To identify novel genes that control the dorsal-ventral choice of motor and sensory neurons at the base of the limb, we compared gene expression profiles of motor and sensory neurons projecting dorsally or ventrally towards the limb in the developing mouse at E12.5.

Motor and sensory neuronal cell bodies were retrogradely labeled by injecting dextran bound to two different fluorescent dyes, Alexa488 into the dorsal mesenchyme of the limb and Alexa680 into the ventral part of the limb (Figure 3.1). This strategy specifically labels motor and sensory neurons based on their axonal projections: we obtained green neurons that project dorsally and red neurons that project ventrally towards the limb musculature. Dissociated green- and red-labeled motor and sensory neurons were purified by fluorescence activated cell sorting (FACS) (Figure 3.1).

For the preparation of motor neurons, spinal cords were extracted, the dorsal compartments removed and the ventral parts, containing the motor neurons, cut in 5 to 6 pieces of the same dimension. After trypsination and trituration, the cells were kept on ice until sorting. For the preparation of sensory neurons, DRGs were collected and pelleted by centrifugation and then treated with the same procedure used for motor neurons (see section 2.1.5).

For each biological replicate (in total 6 biological replicates for brachial motor neurons, 5 for brachial DRG neurons, 3 for lumbar DRG neurons and 5 for lumbar motor neurons), we used between 20 and 30 embryos of different litters and the total number of cells obtained was approximately 10^6.

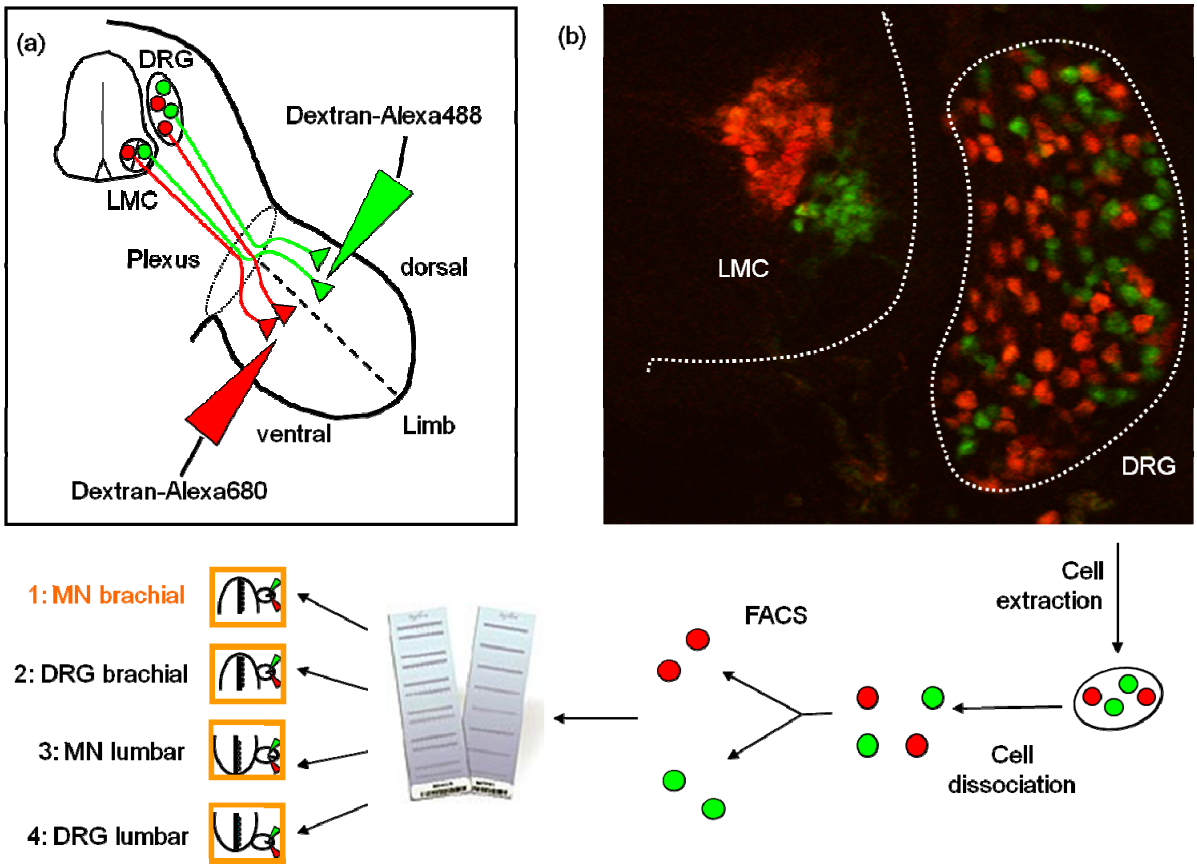

Figure 3.1. Schematic of the experimental procedure to identify differentially expressed genes in dorsally and ventrally projecting motor and sensory neurons. Sensory and motor neurons are differentially labeled according to their projection patterns by injection of two fluorescently labeled dextrans into the dorsal (dextran-alexa488, green) and ventral (dextran-alexa680, red) limb musculature of an E12.5 wild type mouse embryo. The fluorescent dyes are retrogradely transported to the cell bodies (A). A subset of dorsally (green) and ventrally (red) projecting sensory and motor neurons are retrogradely labeled. Differentially labeled neuronal populations were extracted, separated by FACS and RNA was used for microarray analysis. Four lists of candidate genes were obtained, corresponding to brachial and lumbar motor and sensory neurons (B).

After FACS the number of purified neurons was approximately 3000 positive for Alexa488 (Figure 3.2, highlighted in green) and 3000 for Alexa680 (Figure 3.2, highlighted in red). The small percentage of fluorescent positive cells obtained after sorting indicates that the retrogradely labeling of the neuronal cell bodies is not quantitative and that other cell types

are present in the samples, as shown in the FACS plot, were most of the cells are situated in the area correspondent to no-fluorescence (Figure 3.2, highlighted in black).

The total number of FACS-purified neurons (approximately 3000 cells) was similar in all the sortings we performed, thus demonstrating the reproducibility of the purification of retrogradely labeled motor and sensory neurons by FACS.

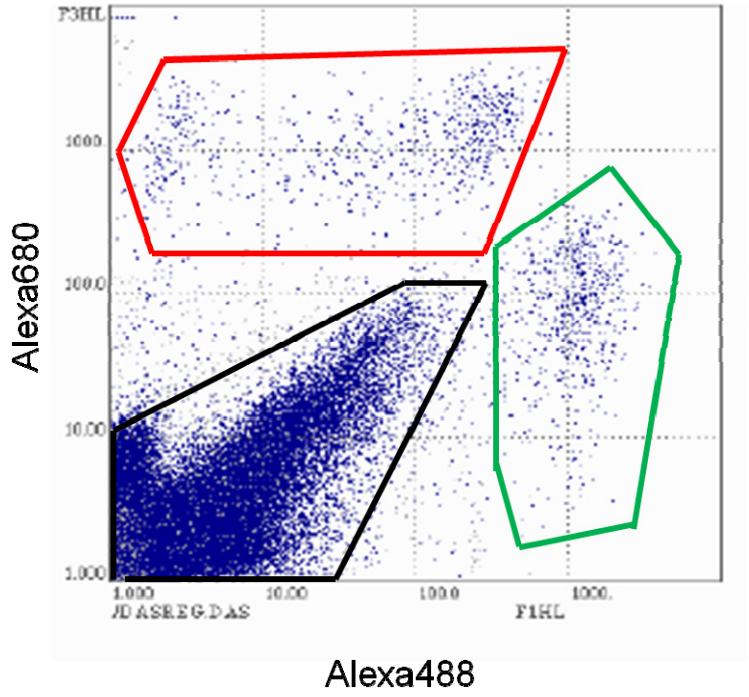

Figure 3.2. Enrichment of motor and sensory neurons by FACS. Dorsally and ventrally projecting motor and sensory neurons are separated by FACS on the base of their fluorescence. Approximately 3000 sorted Alexa488- and Alexa680-positive neurons are highlighted by green and red contour, respectively. The black contour highlights non-fluorescent cells.

3.1.2 RNA isolation from motor and sensory neurons

To ensure biological significance, purified motor and sensory neuronal populations projecting dorsally and ventrally towards the limb were collected from independent FACS purifications (biological replicates) and further used for RNA preparation**.**

RNA isolation from motor neurons projecting to the forelimb was performed immediately after FACS, using an RNAeasy Micro Kit (Qiagen). Briefly, samples were lysed and homogenized in presence of the supplemental reagents (N- and P- carriers, Artus) to ensure optimal RNA quality and yields from a small cell number. Before loading the lysate

onto the spin column, ethanol was added to provide ideal RNA binding conditions to the silica membrane and RNA was eluted (see section 2.1.7.1).

Purity of brachial motor neuron RNA samples was assessed with a Pico Bioanalyzer chip using the Agilent Bioanalyzer 2100 (Agilent Technologies). Only the samples with satisfactory quality, determined by the presence of one marker peak and two ribosomal peaks (18S and 28S) in the electropherogram, and a RNA integrity number (RIN) higher than 7, were selected to be amplified. These two criteria allowed comparing the quality of the samples, ensuring experimental reproducibility.

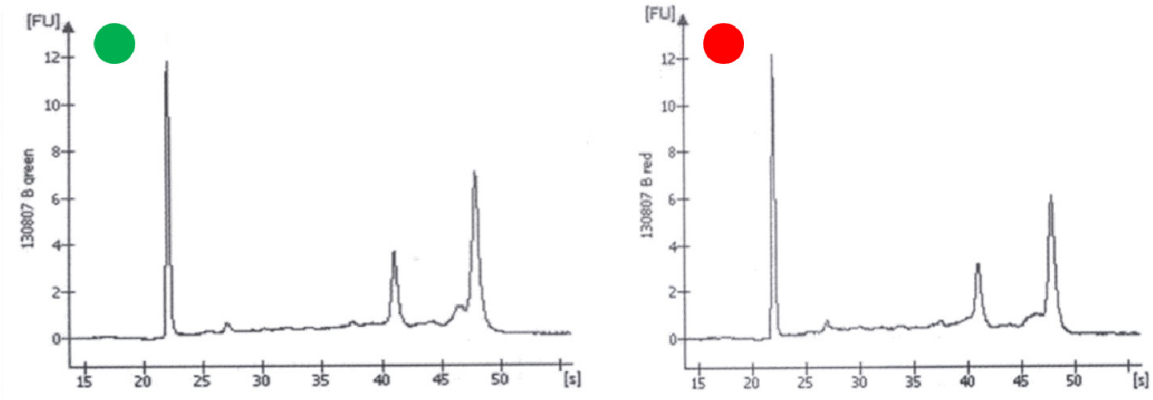

Figure 3.2. RNA electropherograms of dorsally and ventrally projecting brachial motor neurons. RNA was extracted from LMCl and LMCm neuronal populations and the quality control of the RNA samples was determined using the Agilent Bioanalyzer 2100. The presence of a marker peak and of two ribosomal peaks, 18S and 28S, respectively, in the electropherogram reveal the good quality of the extracted RNA. Only high-quality samples were selected for further experiments. RNA electropherograms of samples extracted from dorsally and ventrally projecting neurons are indicated with a green and a red point, respectively.

Highly pure RNA samples for both dorsally and ventrally projecting brachial motor neuron populations were submitted to a first amplification round with the MessageAmp II aRNA amplification kit (Ambion) and then the Illumina TotalPrep RNA amplification kit (Ambion) was used for a second cRNA amplification round that incorporates biotin-labeled nucleotides (see section 2.1.7.1).

Quality control of the amplified cRNA was assessed as described above and high quality cRNA samples were selected for hybridization with Illumina arrays (see section 3.1.3).

RNA isolation and microarray hybridization from brachial DRG neurons and for motor and DRG neurons projecting to the hindlimb was performed by the Miltenyi Biotec Company, using the SuperAmp service. Samples were handled according to Miltenyi's protocol: neurons were directly sorted into the SuperAmp Tubes (provided by the company) during FACS and pelleted by centrifugation. After lysis, cells were frozen at -20°C and sent to Miltenyi on dry ice (see section 2.1.7.2), where RNA amplification, quality control analysis and microarray hybridization on Agilent platform were performed.

Thus, we isolated highly pure RNA samples from differentially projecting motor and sensory neurons that we further used for microarray hybridization.

3.1.3 Genome-wide expression profiling of motor and sensory neurons either projecting dorsally or ventrally to the fore- or hindlimb

3.1.3.1 Microarray analysis of motor and sensory neurons

Gene expression analysis of the sorted neuronal subsets was performed separately for brachial and lumbar motor and sensory neurons, resulting in transcriptome profiling of four neuronal populations projecting dorsally or ventrally towards the limbs (Figure 3.1).

To examine gene expression differences between motor neurons elongating their projections dorsally or ventrally towards the forelimb, we employed Illumina microarrays. To control for sample variability, we used 6 biological replicates, isolated from between 20 and 30 embryos of different litters independently enriched by FACS.

Microarray experiments for brachial motor neurons were performed by Dyvia Mehta and Dr. Holger Prokisch at the Institute of Human Genetics at the Helmholtz Zentrum München.

Biotin-labeled cRNA samples were hybridized to a single Sentrix Mouse-6 BeadChip (Illumina), containing six whole-genome gene expression arrays. This experimental design allowed a direct comparison among samples, thus minimizing variability between experiments. After hybridization, the array was washed to remove unspecific bindings and then stained with streptavidin-Cy3. Lastly, the entire array was scanned and fluorescence emission by Cy3 was quantitatively detected to determine differential gene expression (see section 2.1.7.1).

For sensory neurons projecting to the forelimb and for motor and sensory neurons innervating the hindlimb we examined the gene expression of the sorted neurons using Agilent microarrays, using at least three biological replicates for each neuronal population, extracted from between 20 and 30 embryos of different litters.

The experiments were performed by the Miltenyi Biotec Company using the Agilent Whole Mouse Genome Microarrays 4 x 44K.

RNA was isolated via magnetic bead technology and the quality of the amplified samples was checked using the Agilent 2100 Bioanalyzer. Cy3-labeling was performed using the one-color method, where the individual sample was labeled and hybridized on one microarray, allowing for gene expression comparison among microarrays. After washing, Cy3-fluorescence intensity was detected using the Agilent's Microarray Scanner System (Agilent Technologies).

Microarray predictions provided information about the genes differentially expressed in motor and sensory neurons that may play a role in the guidance of their axons at the base of the limb.

3.1.3.2 Analysis of raw data from microarray experiments

Analysis of raw data from microarray experiments was performed by Dr. Gerhard Welzl and Theresa Faus-Kessler at the Institute of Developmental Genetics at the Helmholtz Zentrum München.

Statistical analysis at transcriptome level of the two RNA subsets of neuronal cells projecting dorsally and ventrally towards the limb was performed separately for Illumina and Agilent data, because of the difference in the design and structure of raw data between the two microarray platforms.

3.1.3.2.1 Illumina data

Illumina raw data were available for 12 arrays (6 biological replicates) and 34492 genes. Data pre-processing for the raw Illumina microarray data was subdivided in unspecific filtering, array normalization and quality assessment of normalized data.

In a first step unspecific filtering – that means excluding expression values with low technical quality – was used. For Illumina microarrays additionally to the intensity values, a p-value for the difference to the background was provided, that was used for unspecific filtering. Based on p-values less than 0.01, the number of genes passing this filtering

procedure was varying between 3554 and 9512 with respect to the 12 arrays. Afterwards, another filtering process based on the raw intensities solely was performed. Considering that for each gene there should be only a small number of arrays having very low raw intensity values, the function pOverA (Library Genefilter) with the parameters p=0.75 and A=300 was utilized and, thereby, only genes with at most three arrays with intensity values below 300 were accepted. With this filtering procedure the initial number of genes was reduced to 4801. The effect of this method is visualized in Figure 3.3.

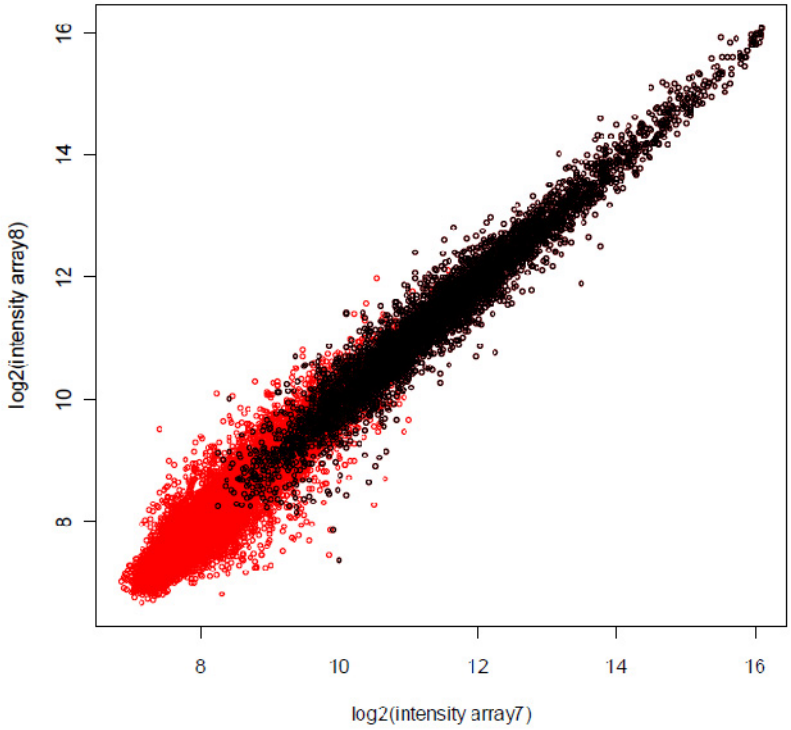

Figure 3.3. Pre-processing of Illumina microarray raw data. The effect of unspecific filtering is visualized in the scatterplot. Genes accepted or excluded (because of low technical quality) by Genefilter-procedure are indicated in black and red, respectively.

A second step in the preprocessing procedure was array normalization. Because for each of totally 6 biological replicates two arrays were available (projecting dorsally and ventrally), a direct normalization procedure was used based on MA-plots where

M = log2(intensity of red=dorsal) - log2(intensity of green=ventral) and

A = log2(intensity of red=dorsal) + log2(intensity of green=ventral).

To choose this procedure, we reasoned that most of the genes were not differentially expressed in dorsally and ventrally projecting neurons.

The last step of the preprocessing procedure was the quality assessment of normalized data. Besides MA-plots, inter-array correlations were calculated and a principal component

analysis with the normalized data was run. The results of this quality assessment led to the identification and exclusion of possible outlier samples (bad quality arrays).

With this normalized data the detection and selection of differentially expressed genes was performed. The test-procedure was related to a one-sample t-test. However, instead of using a separate estimator of the variances for each gene, an empirical Bayes method was used to shrink the probe-wise sample variances toward a common value (R function ebayes in limma-package). To resolve the issue of multiple tests, the false discovery rate (fdr) – the expected proportion of false discoveries amongst the rejected hypotheses – was controlled. For this purpose the method of Benjamini, Hochberg was used (Benjamini and Hochberg, 1995). Based on the function topTable (limma-package) with the parameter adjust="fdr" a table of the top-ranked genes from a linear model fit (with ebayes) was extracted. Only genes with a fold change (f.c.) higher than 2 or lower than -2 and a fdr-value lower than 0.9 were allowed for the top ranked gene list (Table 3.2). This list revealed a total number of 113 genes. 90 genes were higher expressed in the dorsally projecting neurons (fold change lower than -2) and 23 genes were expressed in the neurons elongating ventrally towards the limb (fold change higher than 2).

3.1.3.2.2 Agilent data

Raw data derived from Agilent microarray were analyzed separately for brachial DRG neurons and for sensory and motor neurons projecting to the hindlimb.

Pre-processing of raw data was also subdivided in unspecific filtering, array normalization and quality assessment of normalized data. Raw data were available for 41174 genes.

For Agilent data, intensity values were provided with an additional label 0 and 1, where 1 means "is positive and significantly different from background". In this way, a gene could pass the unspecific filtering procedure only if its intensity was significantly different from the background for all arrays (Figure 3.4).

The number of genes that was accepted by the unspecific filtering procedure is shown in Table 3.1.

Sample	Number of arrays	Number of genes passing the filtering procedure
Brachial DRG neurons	10	27090
Lumbar DRG neurons	6	23298
Lumbar motor neurons	10	26892

Table 3.1. Analysis of Agilent microarray data. Sample neural type with the correspondent array numbers and the number of genes selected after filtering are listed.

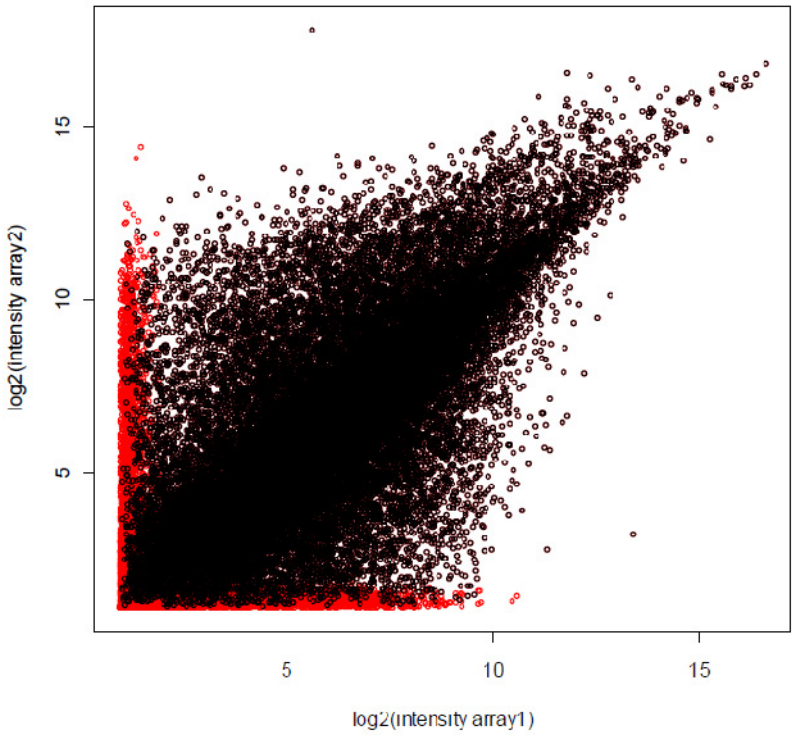

Figure 3.4. Pre-processing of Agilent microarray raw data. The effect of unspecific filtering is visualized in the scatterplot. Genes accepted or excluded (because of low technical quality) by Genefilter-procedure are indicated in black and red, respectively.

As a second step in the pre-processing a quantile normalization was performed (function normalize.quantiles in preprocessCore-library).

For the quality assessment of normalized data the same procedure used for Illumina data was applied.

With the normalized data, the detection of differentially expressed genes is related to a two-sample t-test, comparing the intensities of dorsally versus ventrally projecting neuronal populations. In the same manner as for the Illumina data, an empirical Bayes method was used for estimating variances and the false discovery rate was controlled (with a limit by 0.8). Then, only genes with a log fold change higher than 2 or lower than -2 and a fdr-value lower than 0.8 were allowed for the top ranked gene list (see Table 3.3 - Table 3.5).

The number of genes predicted by the microarray analysis to be differentially expressed in brachial DRG neurons was 13 (3 in dorsally and 10 in ventrally projecting neurons), in lumbar motor neurons was 19 (13 in dorsally and 6 in ventrally projecting neurons) and in lumbar DRG neurons was 97 (6 in dorsally and 91 in ventrally projecting neurons).

Together, the statistical analysis revealed genes differentially expressed in dorsally versus ventrally projecting motor and sensory neurons, thereby providing valuable information for further biological investigation.

3.1.3.3 Novel candidate genes differentially expressed in motor and sensory neurons projecting dorsally or ventrally towards the fore- and hindlimb

Genes differentially expressed in motor and sensory neurons elongating their projections dorsally or ventrally to the fore- and the hindlimb predicted by microarray analysis with the correspondent fold changes are listed in the Table 3.5, respectively. Candidate genes with a fold change higher than 2 were predicted to be higher expressed in the neurons elongating their axons to the ventral limb, while a fold change lower than -2 reveals genes enriched in dorsally projecting neurons.

Name	Fold Change	Name	Fold Change	Name	Fold Change
COL5A1	6,13	RHBDF1	2,86	EDNRB	2,15
COL4A1	6,01	D130017D19RIK	2,84	PTTG1IP	2,14
SULF1	5,38	D1ERTD471E	2,83	TPM4	2,13
GJA1	5,27	SYDE1	2,79	MMP14	2,12
COL4A2	5,14	ISL1	2,77	ODZ4	2,12
VTN	4,97	NFATC4	2,75	LOC100046586	2,10
RCSD1	4,89	MMP2	2,73	IL11RA1	2,09
COL18A1	4,65	FBLN1	2,72	VCAM1	2,09
DOCK6	4,42	EG637273	2,63	4833424O12RIK	2,08
IGF2	4,41	ITPR1	2,62	SGK	2,07
CCDC3	4,31	RBMS2	2,60	XPNPEP3	2,05
FKBP9	4,17	SLC1A3	2,55	KCNK2	2,05
ARHGAP29	4,05	IGFBP5	2,52	ITGB1	2,03
DCN	4,04	ANXA2	2,50	Msih2	2,00
H19	4,04	PRC1	2,49	HOXB4	-2,02
SERPINH1	3,99	ANXA5	2,49	CIRBP	-2,13
SCARF2	3,98	LOC224163	2,45	RUNX1T1	-2,15
1200009O22RIK	3,77	ZFP36L1	2,45	POU6F1	-2,15
AXL	3,68	PROM1	2,40	ACCN2	-2,17
CXCL12	3,65	EDG5	2,38	NN3	-2,20
2310033F14RIK	3,48	MCM5	2,38	EN1	-2,20
LHFPL2	3,47	MTAP7	2,37	GNG3	-2,23
RHOJ	3,45	EPHA8	2,35	PHF21B	-2,28
COL4A5	3,44	LOC234882	2,35	LOC100045019	-2,33
PON2	3,41	WWTR1	2,31	LOC547380	-2,53

GRB10	3,33	ELK3	2,31	REM2	-2,55
ANKRD25	3,33	PLS3	2,29	CRABP1	-2,57
LAMC1	3,28	X99384	2,28	OLIG1	-2,60
UACA	3,17	ZFYVE21	2,25	LOC100043919	-2,61
ANXA3	3,16	MEGF10	2,25	GBX2	-2,62
2310047A01RIK	3,15	MDK	2,23	6430547I21RIK	-2,71
SCL0002507.1_236	3,15	LOC100047167	2,22	A930011O12RIK	-2,73
EMID2	3,13	MCM4	2,22	ZBTB12	-3,08
MEST	3,12	SMAD3	2,19	GAD1	-3,35
LGALS1	3,03	FGFR2	2,18	IGFBPL1	-3,79
6720458D17RIK	2,90	CD8B	2,17	SLC32A1	-4,08
PLEKHA2	2,89	FOS	2,17	SLC30A3	-4,34
TIMP3	2,88	CTNNA1	2,15		

Table 3.2. Genes differentially expressed in brachial motor neurons. Candidate genes and the correspondent fold changes predicted by the microarray analysis to be differentially expressed in brachial motor neurons projecting to the dorsal (f.c. lower than -2) or the ventral part of the limb (f.c. higher than 2) are listed.

Name	Fold Change
Fyco1	47,90
Proz	16,48
Aurka	11,97
Ccdc55	-16,57
Nek1	-18,24
Dnajb4	-18,85
Olfr672	-19,27
Myc	-20,00
Cutl2	-28,86
Gnb4	-31,35
Plcd4	-40,79
Timm9	-42,02
Ift172	-64,33

Table 3.3. Genes differentially expressed in brachial DRG neurons. Candidate genes and the correspondent fold changes predicted by the microarray analysis to be differentially expressed in brachial motor neurons projecting to the dorsal (f.c. lower than -2) or the ventral part of the limb (f.c. higher than 2) are listed.

Name	Fold Change
Slfn10	51,58
AK043872	45,72
2700008B19Rik	40,01
4930431L04Rik	21,15
Phf20l1	13,68
C3ar1	5,33
Pxk	-6,78
8430410A17Rik	-7,55
Tmem138	-8,61

Ttc14	-8,62
Tnks1bp1	-11,49
Lancl1	-17,14
Orc2l	-20,14
Fyttd1	-20,50
Ift122	-23,45
Thap11	-24,85
Lig3	-39,79
Gtf2ird2	-45,47
Lrrc57	-108,33

Table 3.4. Genes differentially expressed in lumbar motor neurons. Candidate genes and the correspondent fold changes predicted by the microarray analysis to be differentially expressed in brachial motor neurons projecting to the dorsal (f.c. lower than -2) or the ventral part of the limb (f.c. higher than 2) are listed.

Name	Fold Change	Name	Fold Change	Name	Fold Change
Rbmx	176,66	Malat1	50,99	Clk1	23,47
Prnpip1	162,22	Ahcyl1	50,04	Capn7	23,29
Hmox2	126,17	2410016F19Rik	49,07	Mrpl32	22,76
1500012F01Rik	109,20	Irf2bp1	48,59	Pfkl	22,48
Ppgb	97,91	Rpl31	48,53	Adipor1	20,73
Cct8	95,16	Hipk3	48,43	AV036172	20,59
Asrgl1	94,98	Copa	47,67	D3Ucla1	19,60
Rbms1	93,64	1810008A18Rik	44,74	Ranbp1	19,55
Cct2	91,98	Ccpg1	42,70	Smyd2	18,90
Ccnh	91,50	Son	42,19	Dnajb10	18,86
Cpsf6	83,22	Msh6	40,96	Snx5	17,57
A930037G23Rik	79,27	Prdx4	39,35	AI427529	16,89
Mak10	78,15	A_52_P772584	38,68	Dctn1	16,73
Atg12	76,57	9630058J23Rik	38,64	NAP060490-1	16,67
NAP092627-001	74,96	4932416N17Rik	36,19	Exoc1	14,70
Lsm14b	74,82	Zc3h7b	35,72	Gnb1	14,14
Mrpl13	74,00	Rtf1	35,49	Csf1r	14,13
Psme2b-ps	71,58	Rnaseh2a	34,65	Zfp259	14,12
2600009E05Rik	67,64	Reep5	32,85	Eml5	13,56
Crabp2	61,73	Ppgb	32,10	Picalm	13,13
9430025N12	61,28	Btg2	31,84	Tmem66	12,10
Rpl10a	59,31	Pop4	31,49	C030046I01Rik	12,01
Hoxa5	57,40	Ivns1abp	30,76	Stmn2	10,84
Pprc1	56,72	X83328	30,38	Otub1	10,61
Atxn10	56,53	Atp5s	29,39	Zcchc17	10,14
Adipor1	55,34	1810006K21Rik	29,00	Fahd2a	-15,68
Ches1	54,58	Arl3	27,30	B430203M17Rik	-21,41
Wdr43	53,75	Sep09	26,14	6430573F11Rik	-27,86
Ext1	52,50	Gpiap1	24,77	Tslp	-34,04
Morf4l2	52,24	Ube2b	24,10	Mrpl37	-74,77
Rps3	52,12	1500011H22Rik	23,92	Ctbp2	-101,51

Dok4	52,08	Tmem88	23,56		
Trak1	52,05	Mest	23,56		

Table 3.5. Genes differentially expressed in lumbar DRG neurons. Candidate genes and the correspondent fold changes predicted by the microarray analysis to be differentially expressed in brachial motor neurons projecting to the dorsal (f.c. lower than -2) or the ventral part of the limb (f.c. higher than 2) are listed.

The number of genes predicted by the microarrays to be differentially expressed varied notably among motor or sensory neuronal populations elongating to the dorsal or ventral fore- or hindlimb (113 and 13 for brachial motor and sensory neurons, respectively, and 19 and 97 for lumbar motor and sensory neurons, respectively; compare Table 3.2 - Table 3.5), although several functional categories, such as extracellular and membrane proteins, signal transduction and transcription factors were enriched in these groups, according to Gene Ontology annotation (Figure 3.5). Furthermore, the microarray analysis did not predict any gene to be expressed by two or more neuronal populations, revealing that axon guidance mechanisms are different for brachial and lumbar motor and sensory innervations.

We further focused our investigation on candidate genes expressed in motor neurons innervating the forelimb musculature. Our choice was determined by the possibility to verify and confirm the reliability of the microarray analysis, because of the existence of markers for this neuronal population already known to be differentially expressed in dorsally (*Lim1*) and ventrally (*Isl1*, *Npn-2*) projecting neurons. Microarray analysis, indeed, correctly predicted the differential expression of these markers, thereby demonstrating that the screen worked successfully.

Furthermore, we reasoned that during the process of validation of novel motor neuron candidate genes, together with the use of in situ hybridization, to determine the mRNA expression patterns, we could have taken advantage of immunostaining with Lim1 and Isl1 antibodies, to distinguish LMCl and LMCm neurons, respectively. On the contrary, the analysis of candidates predicted to be differentially expressed in the DRG neuronal populations, would have been more laborious. Indeed, the validation process, because of the lack of markers to distinguish the dorsally and ventrally projecting DRG neurons, would have required the use of the retrograde labeling technique, to determine the specific dorsal or ventral expression of the candidate genes, in combination with in situ hybridization. The backfill technique, in comparison to immunohystochemistry, has the disadvantages to be not quantitative, as demonstrated in the FACS experiments (Figure 3.2) and more time-consuming.

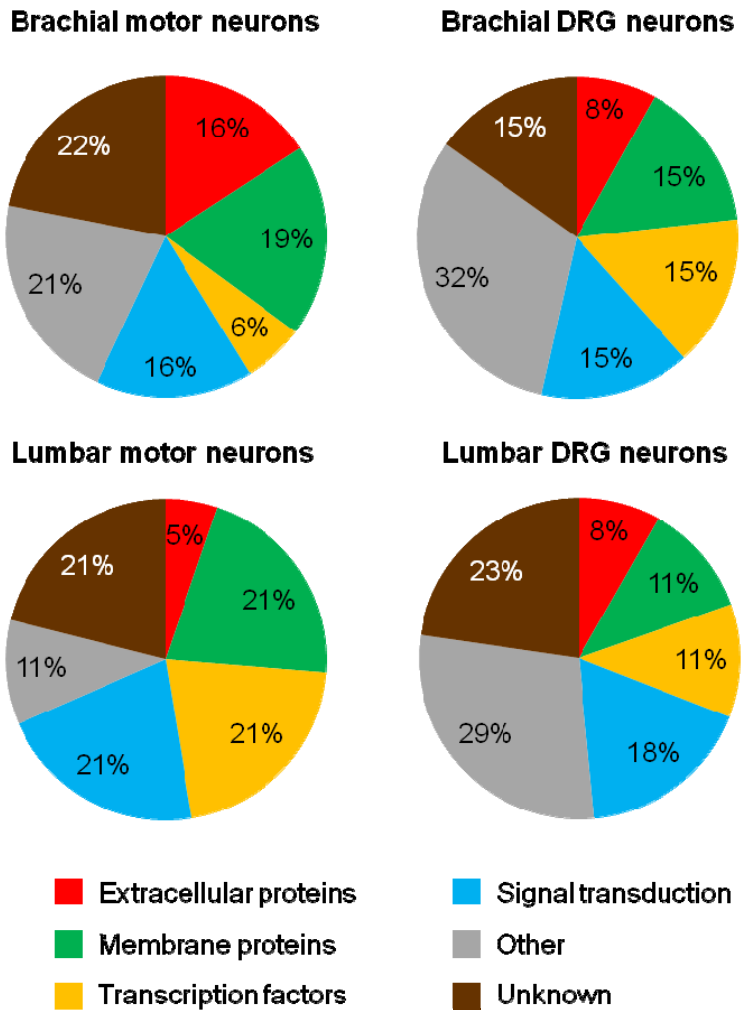

Figure 3.5. Functional categories enriched in the differentially projecting neuronal populations. The pie charts represent the main functions of the genes differentially expressed in brachial motor and DRG neurons and in lumbar motor and DRG neurons projecting to the dorsal or ventral part of the limb, according to gene ontology analysis.

3.1.3.4 The reliability of the the screening performed to identify novel cues governing the dorsal-ventral choice of motor and sensory axons at the base of the limb

To understand the molecular mechanism governing axon guidance at the base of the limb, we separated dorsal and ventral projecting motor and sensory neurons in order to examine their molecular specification. To this end, we performed an enrichment of motor and sensory neuronal populations by FACS, according to their different projection patterns. FACS analysis revealed comparable level of labeled motor and sensory neurons purified (approximately 3000) from a matchable number of embryos (between 20 and 30) for every biological replicate, demonstrating the reliability and reproducibility of the method we

employed. For microarray hybridization, only RNA samples with a satisfactory quality were selected, in order to ensure a reproducible dataset. To assess the consistency of microarray analysis, furthermore, we compared gene expression between independent samples derived from different litters and independently FACS purified and chip hybridized.

The differential expression of markers already known to be differentially enriched in the LMCl and LMCm divisions, such as *Lim1* and *EphA4*, *Isl1* and *Npn-2*, respectively, was predicted by the microarray analysis, thereby further confirming the reliability of the approach we used to assess differentially regulated genes within the motor and sensory neuronal populations.

Also the microarray prediction that many genes were expressed in common by differentially projecting neurons, as expected for neuronal populations that differ only by their dorsal-ventral axonal trajectory at the base of the limb, supported the reliability of the screening.

Together, these considerations provide evidence that it was possible to identify differentially expressed genes in dorsally and ventrally projecting motor and sensory neurons enriched by FACS.

3.1.4 Expression profiling of motor neurons projecting dorsally or ventrally towards the forelimb

Microarray analysis of motor neurons innervating the forelimb revealed 113 genes, which have a difference of 2 or higher in their fold change, predicted to be differentially expressed in dorsally versus ventrally projecting neurons (Table 3.2). These genes were grouped into six categories according to their main function to get a general overview (Table 3.6).

The identified candidates included extracellular proteins (e.g., *Igfbp5*, *Vtn*, *Igf2*), membrane proteins (e.g., *Ednrb*), genes involved in signal transduction (e.g., *ETO*, *G-protein γ3*, *Rhoj*) and transcription factors (e.g., *En1*, *Elk3*). The reliability of the microarray data was demonstrated by the finding of markers already known to be differentially expressed in dorsally projecting LMCl, such as *Lim1* and *EphA4*, and in ventrally projecting LMCm motor neurons, such as *Isl1* and *Npn-2* (Tsuchida et al., 1994; Kania and Jessell, 2003; Huber et al., 2005).

15 candidate genes (highlighted in Table 3.6) were selected on the basis of literature search that suggested a potential role in axon guidance. Embryonic mRNA expression

patterns in the spinal cord assembled in the GenePaint database (www.genepaint.org) provided additional information for the selection process. We chose *Igfbp5*, *Vtn*, *Dcn*, *Mdk*, *Igf2*, *Ednrb*, *En1*, *Elk3*, *ETO*, *G-protein γ3*, *Rhoj, Dock6, EphA8, Msih2 and Gad1* (for references see Table 2.1).

To validate the differential expression patterns of these candidate genes and thereby confirm the microarray predictions, we performed in situ hybridization with digoxigenin-labeled antisense cRNA-probes of the selected genes on E12.5 embryo sections in combination with immunohistochemistry for Isl1 and Lim1 antibodies, to discriminate between the medial and lateral columnar divisions, respectively.

The mRNA patterns of 50% of the analyzed candidate genes corresponded to the microarray prediction (highlighted in red and green in Table 3.6), while the validation of other candidates did not confirm the presence of the transcripts in the LMC (highlighted in grey in Table 3.6).

Extracellular proteins	Membrane proteins	Transcription factors	Signal transduction	Other	Unknown
IGFBP5	Cnx43	En1	ETO	GAD1	Rcsd1
Col4a1	SCARF2	Elk3	G-protein γ3	Anxa5	Ccdc3
Sulf1	Axl	Isl1	RhoJ	UACA	1200009O22RIK
Col4a2	LHFPL2	Gbx2	ARHGAP29	Emid2	2310033F14RIK
Col18a1	Pon2	HoxB4	Grb10	Rhbdf1	2310047A01RIK
FKBP9	Mest	NFATc4	ANKRD25	Prdx1	SCL0002507.1_236
SERPINH1	Timp3	Fos	PlekhA2	Itpr1	6720458D17RIK
Cxcl12	MMP2		Syde1	H19	D130017D19RIK
Col4a5	GLAST		Edg5	PRC1	D1ERTD471E
LAM1	Prom1		TAZ	CRABP1	RBMS2
LGALS1	Prxi-ps2		SMAD3	ZFP36L1	X99384
FBLN1	FGFR2		PTTG1IP	MCM5	ZFYVE21
Col5a1	CTNNA1		Treck1	MTAP7	MEGF10
IGFBPL1	MMP14		Pou6F1	Pls3	LOC100047167
Vtn	ODZ4		Rem2	MCM4	LOC100046586
DCN	IL11RA1		Olig1	CD8B	4833424O12RIK
MDK	Vcam1		Dock6	TPM4	PHDfingerprotein21B
IGF2	ITGB1		EphA8	Sgk1	LOC100045019
	Nn3			XPNPEP3	LOC547380
	SLC32A1			CIRBP	LOC100043919
	SLC30A3			ACCN2	6430547I21RIK
	EDNRB			Anxa2	ZBTB12
				Msih2	EG637273
				Anxa3	LOC234882
					A930011O12RIK

Table 3.6. Candidate genes differentially expressed in brachial motor neurons projecting to the dorsal or ventral limb are grouped according to their function. In situ hybridization

of 15 selected genes and immunohistochemistry for marker proteins were performed to validate their predicted RNA expression pattern in the LMC. Genes whose mRNA expression was confirmed to be higher expressed in LMCl or LMCm are highlighted in red and green, respectively. Genes whose differential expression in the LMC was not confirmed are highlighted in grey.

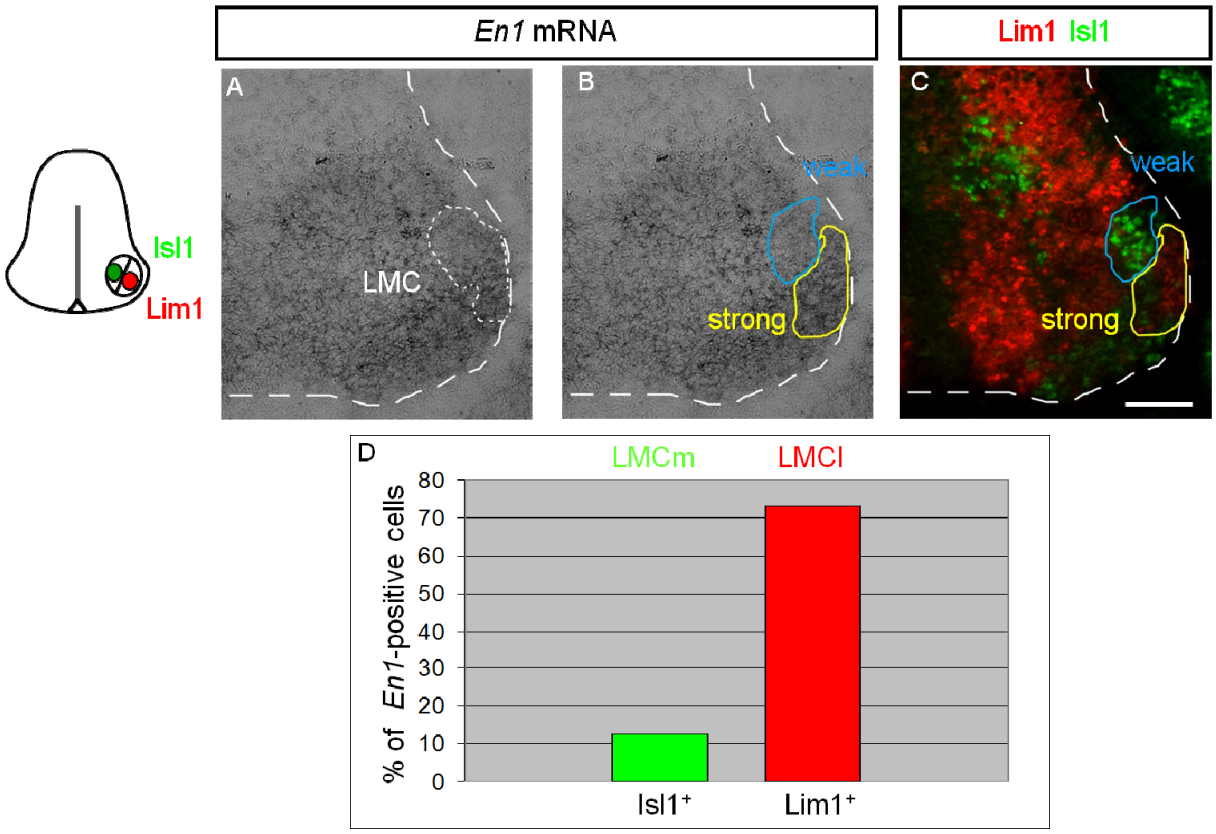

Figure 3.6. Validation of Engrailed 1 as differentially expressed in the LMC. Whole genome analysis predicted En1 to be higher expressed in dorsally projecting brachial motor neurons (fold change -2.2). In situ hybridization with digoxigenin-labeled *En1* RNA-probe shows a stronger expression of *En1* mRNA (yellow line in B and C) which correlates with Lim1-positive LMCl motor neurons. In Isl1-positive LMCm neurons only a very weak expression of *En1* was observed (blue line in B and C). Quantitative analysis (D) revealed that *En1* is expressed in more than 70% of Lim1-positive dorsally projecting neurons compared to only in 11% of Isl1-positive ventrally projecting neurons. Spinal cord is outlined with a dashed white line. Scale bar: 25µm (A,B,C).

Among the confirmed genes, we identified En1 as a particularly interesting candidate based on its functions as a transcription factor (Wurst et al., 1994) and on recent data from other systems showing its direct role in axon guidance (Brunet et al., 2005; Wizenmann et al., 2009). The whole genome analysis predicted a 2.2 fold higher expression of En1 mRNA in the lateral LMC neurons. In situ hybridization and Lim1 and Isl1 immunohistochemistry indeed confirmed that the expression of En1 mRNA in the LMCl was stronger than in the

medial LMC compartment (Figure 3.6A-C). To evaluate En1 mRNA signal on embryo sections, we firstly identified and outlined the LMC by overlaying the in situ hybridization and the immunohystochemistry pictures. Then the nuclei of the cells within the LMC region that showed the transcript signal in the cytoplasm were highlighted in yellow and neurons positive for both mRNA and immunohistochemical signals were identified by overlaying the two pictures. To determine whether the in situ hybridization signal was present either in the LMCl or in the LMCm, we used the Lim1 and Isl1 staining to discriminate motor neurons either projecting dorsally or ventrally towards the limb, respectively. Finally, we counted the neurons positive for the *En1* mRNA and for either the Lim1 or Isl1 signals to compare the percentage of cells expressing *En1* mRNA in the two motor column divisions. Quantitative analysis revealed the expression of *En1* transcripts in more than 70% of LMCl motor neurons and only in 11% of LMCm neurons (Figure 3.6D).

Thus, we confirmed by in situ hybridization the differential expression of Engrailed 1 in brachial motor neurons predicted by microarray analysis, thereby providing hints for its potential role in the guidance of motor neurons at the base of the limb.

3.2 Engrailed 1 is a repulsive cue for LMCl motor axons

3.2.1 Engrailed 1 expression in the spinal cord

To further investigate the role of Engrailed 1 in the guidance of motor axons at the base of the limb, we analyzed its expression in the spinal cord at developmental timepoints, when the dorsal-ventral guidance decision still has to occur, and the expression of Engrailed 1 in the neuronal cell bodies may therefore suggest its potential role in axon guidance. Indeed, the microarray screening and the validation process of the candidates mRNA patterns were conducted on E12.5 embryos, when the dorsal-ventral choice of motor and sensory axons at the base of the limb has already occurred. Thus, we analyzed the expression of *En1* in the spinal cord, performing in situ hybridization and immunohistochemistry at E10.5, when the axons convey at the plexus region and at E11.5, when spinal projections enter the forelimb. At E10.5, transcripts of our candidate are present in interneurons and in motor neurons which were identified by Lim1 and Isl1 staining, respectively (Figure 3.7A). Immunohistochemistry against En1 protein shows a nuclear staining in interneurons, as expected for a transcription

factor (Matise and Joyner, 1997). However, En1 is not detected in motor neurons (Figure 3.7D, G, L). The expression of *En1* mRNA in interneurons at E11.5 is still strong, while it becomes weaker in the motor neuron area (Figure 3.7B). At the same developmental stage, En1 protein is detected in motor neuron area, where it does not show a nuclear staining (Figure 3.7E, H, M). As already shown (Figure 3.6B), at E12.5, the time when the screening was performed, *En1* mRNA expression is stronger in the dorsally projecting neurons and weaker in the neurons elongating ventrally (Figure 3.7C), while the En1 protein is not detected in the motor neuron area (Figure 3.7F, I, N).

At E10.5 Lim1 is expressed by interneurons (Matise and Joyner, 1997) but is not present in motor neurons. At E11.5 it is still difficult to accurately distinguish the separation in the lateral and medial aspects of the LMC, because the subcolumnar markers Isl1 and Lim1 can properly identified the two motor neurons LMC divisions starting only around E12 (Tsuchida et al., 1994; Riddle et al., 1995; Vogel et al., 1995). It is therefore difficult at E11.5 to determine whether the En1 protein is expressed in the dorsally or ventrally projecting neurons.

Together the data show the presence of Engrailed 1 in motor neurons at a transcriptional, but not at a protein level, leaving the question open how it can guide motor axons without being expressed in their neuronal cell bodies.

3.2.2 Engrailed 1 protein is expressed on LMCl axons

The observation that the En1 protein is not expressed in motor neurons raised the question how an axon guidance cue could exert its function without being expressed by the neuronal cell bodies and prompted us to verify whether its presence was detectable on elongating motor axons.

We therefore performed immunohystochemical analysis on E11.5 embryo sections using the Growth associated protein 43 (Gap43) as a marker to identify all axons. En1 protein was detected on motor axons exiting the spinal cord (Figure 3.8A-C), but not on sensory projections emerging from the DRG (arrowhead in Figure 3.8C). A higher magnification at the plexus region, the area of dorsal-ventral bifurcation, allowed to determine that the En1 protein signal is preferentially detectable on the axons projecting to the dorsal limb (arrows in Figure 3.8F) compared to the ventrally projecting fibers (Figure 3.8E-F).

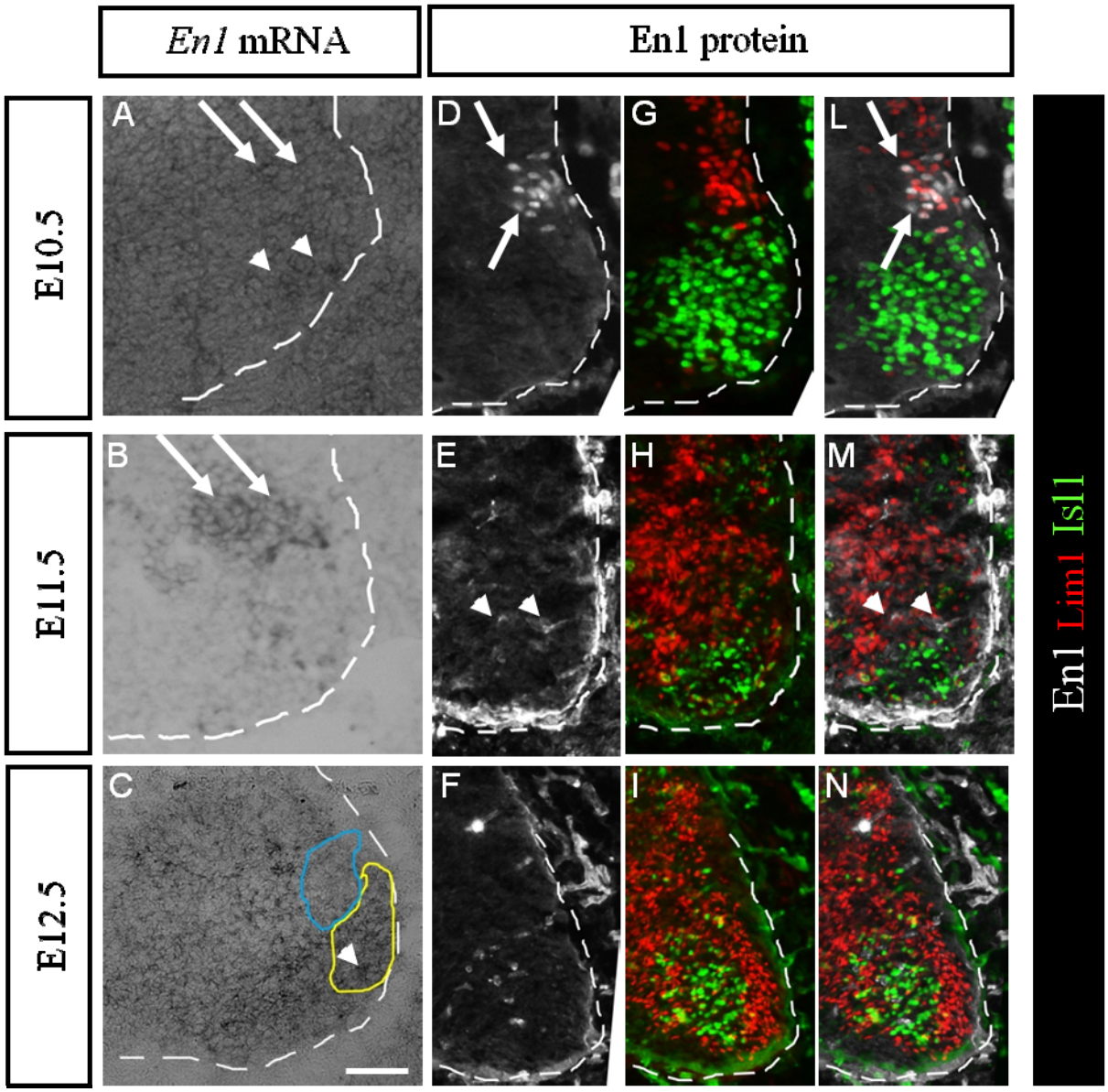

Figure 3.7. Engrailed 1 expression in the spinal cord. *En1* mRNA is present at E10.5 and E11.5 in interneurons (arrows in A,B) and in the LMC at E10.5 (arrowheads in A) and at E12.5 (arrowhead in C). Nuclear expression of En1 protein is detectable in Lim1-positive interneurons at E10.5 (arrows in D,L). At E11.5 a non nuclear expression is observed at LMC levels (arrowheads in E,M). Spinal cord is outlined with a dashed white line. Scale bar: 15µm (A), 20µm (B), 25µm (C), 27µm (D,G,L), 36µm (E,H,M), 45µm (F,I,N).

Thus we demonstrated the presence of En1 protein on motor axons elongating to the dorsal limb compartment, revealing that it may elicit the guidance of LMCl neuronal projections directly from their axons.

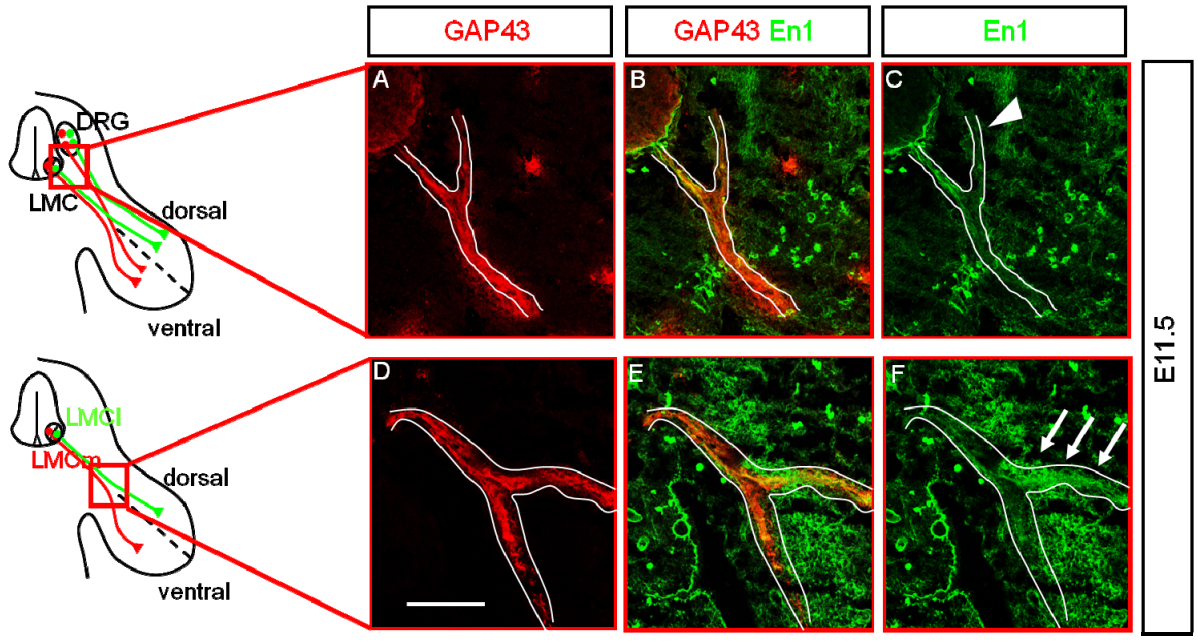

Figure 3.8. Engrailed 1 is expressed on LMCl axons. En1 protein was found on motor axons (B,C) but not on sensory axons exiting the DRG (arrowhead in C). Gap43 (red) reveals all axons. At the dorsal-ventral choice point, En1 protein is preferentially detectable on dorsally projecting motor axons (arrows in F). Motor and sensory axons projecting towards the limb are outlined with a white line. Scale bar: 200µm (A-C), 130µm (D-F).

3.2.3 Engrailed 1 expressed in the ventral limb ectoderm controls limb patterning

We next analyzed the expression of En1 in the limb and its function in limb patterning. The En1 protein is reported to be expressed in the limb starting at E9.5 (Davis et al., 1991). Our expression analysis showed that at E10.5 En1 is present in the ventral limb ectoderm, with a stronger expression at the level of the plexus region (Figure 3.9A-C). At E11.5 the protein is detected in the limb mesenchyme, particularly just ventrally of the region where the dorsal-ventral axonal bifurcation choice takes place (Figure 3.9D-F). The role of En1 in the limb was previously studied. It was shown that En1 expressed in the ventral ectoderm of the developing limb bud plays a crucial role in the ventral patterning of the limb, repressing the dorsalizing action of Wnt7a, a secreted factor expressed in the dorsal ectoderm (Wurst et al., 1994; Loomis et al., 1996). Indeed, the absence of En1 causes dorsal structural transformations of the paws, such as the presence of nail plates on both ventral and dorsal digit surface, the absence of distal-most ventral paw pads and the abnormal dorsal palmar flexion of the paw (Loomis et al., 1996). A detailed analysis of the effect of the loss of En1 function at a molecular level, however, was missing so far.

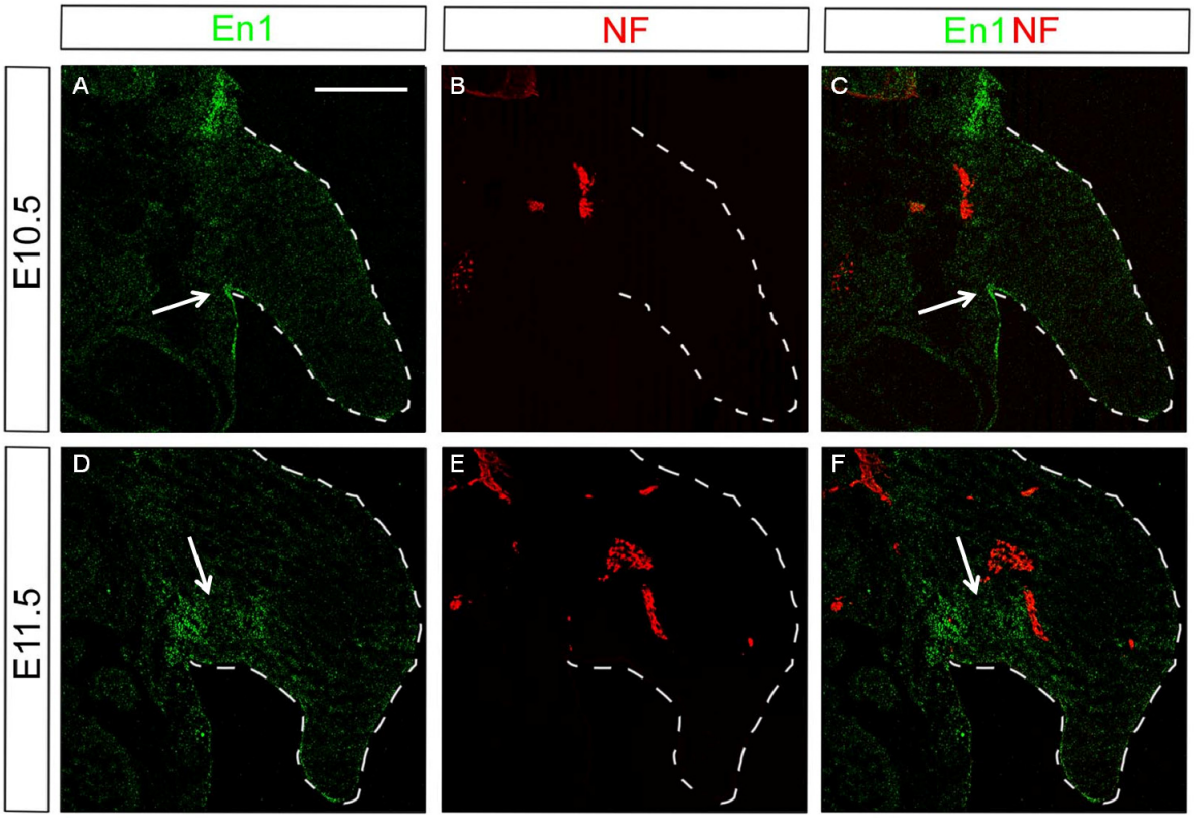

Figure 3.9. Engrailed 1 expression in the limb. En1 protein at E10.5 was detected in the ventral ectoderm of the forelimb (arrow in A,C). At E11.5 En1 is present in the region of the limb were spinal axons bifurcate to reach their dorsal or ventral targets (arrow in D,F). Gap43 (red) reveals all axons. The limb buds are outlined with a dotted white line. Scale bar: 400µm (A-C), 150µm (D-F).

We studied the role of En1 in the patterning of the forelimb analyzing the mRNA expression pattern of dorsal (e.g., LIM homeobox transcription factor beta (*Lmx1b*) and *Npn-2*) and ventral (e.g., Early B-cell factor 2 (*Ebf-2*)) limb markers in $En1^{Lki}$ mice (Hanks et al., 1995), where the *En1* coding sequence was replaced with the *LacZ* sequence, generating *En1* loss-of-function alleles and compared the results with the expression patterns of these markers in wild type embryos. In *En1* mutant mice, *En2* expression is reduced to a dorsal domain in the mid-hindbrain region and it was not ectopically expressed outside the central nervous system (Wurst et al., 1994). We reasoned that genes expressed dorsally in wild type mice would have been also found ventrally in case of limb dorsalization caused by the absence of *En1*, and, vice-versa, the expression of genes confined to the ventral part of the limb in wild type embryos would be diminished or disappeared in $En1^{-/-}$ embryos, where the ventral half of the limb has dorsal characteristics.

The transcription factor *Lmx1b* is expressed in the dorsal mesenchyme of the developing limb where it determines dorsal cell fates (Riddle et al., 1995; Vogel et al., 1995).

In addition it is also required for the appropriate dorsal-ventral spinal motor trajectories at the base of the limb (Kania et al., 2000; Kania and Jessell, 2003). Our in situ hybridization analysis showed that at E10.5 and E11.5 *Lmx1b* is expressed in the dorsal part of the limb in wild type mice (Figure 3.10A,C) and that in *En1*$^{-/-}$ mice an additional ectopic *Lmx1b* expression domain is found ventral (Figure 3.10B,D). These data corroborate the results obtained by whole-mount in situ hybridization analyzing *Lmx1b* expression in wild type and *En1* mutants at later developmental stages (Cygan et al., 1997; Loomis et al., 1998).

We also analyzed the expression pattern of another dorsal limb marker, *Npn-2*, a receptor expressed on LMCm axons and also present in the dorsal limb bud (Huber et al., 2005). At E10.5 *Npn-2* mRNA is expressed only in the dorsal compartment of the limb bud in wild type embryos (Figure 3.10E), while in *En1* mutants *Npn-2* is also ectopically expressed in the ventral part of the limb (Figure 3.10F). One day later, the situation changes somewhat: in wild type embryos *Npn-2* is still expressed in the dorsal limb division but is also weakly present in the ventral part of the limb (Figure 3.10G). In *En1*$^{-/-}$ mice, the expression of *Npn-2* diminishes in the dorsal part of the limb, while it remains strongly expressed ventrally (Figure 3.10H).

The transcription factor *Ebf-2* is important for the development of the nervous system. Indeed, *Ebf-2*$^{-/-}$ mice show slight uncoordination, presumably because of peripheral axon sorting defects and hypomyelination of the adult sciatic nerve (Corradi et al., 2003). Previous work showed that at E11.5 *Ebf-2* is expressed in the ventral limb bud next to the dorsal-ventral bifurcation point of motor and sensory axons projecting towards the limb (Krawchuk and Kania, 2008). Our in situ hybridization expression profiling showed that *Ebf-2* is expressed in the proximal ventral area of the developing limb in wild type mice at E10.5 and E11.5 (Figure 3.10I,M) and that its expression is strongly downregulated in *En1*$^{-/-}$ embryos at the same developmental stages (Figure 3.10L,N).

These results show that loss of En1 function causes ectopic ventral expression of dorsal markers and a decrease of ventral marker expression, thereby demonstrating that *En1* is required at a molecular level for the dorsal-ventral forelimb patterning.

Interestingly, the ectopic expression of both dorsal markers in the ventral part of the limb in *En1*$^{-/-}$ embryos does not represent a mirror image duplication of the dorsal wild type expression, but rather a partial dorsalization of the forelimb.

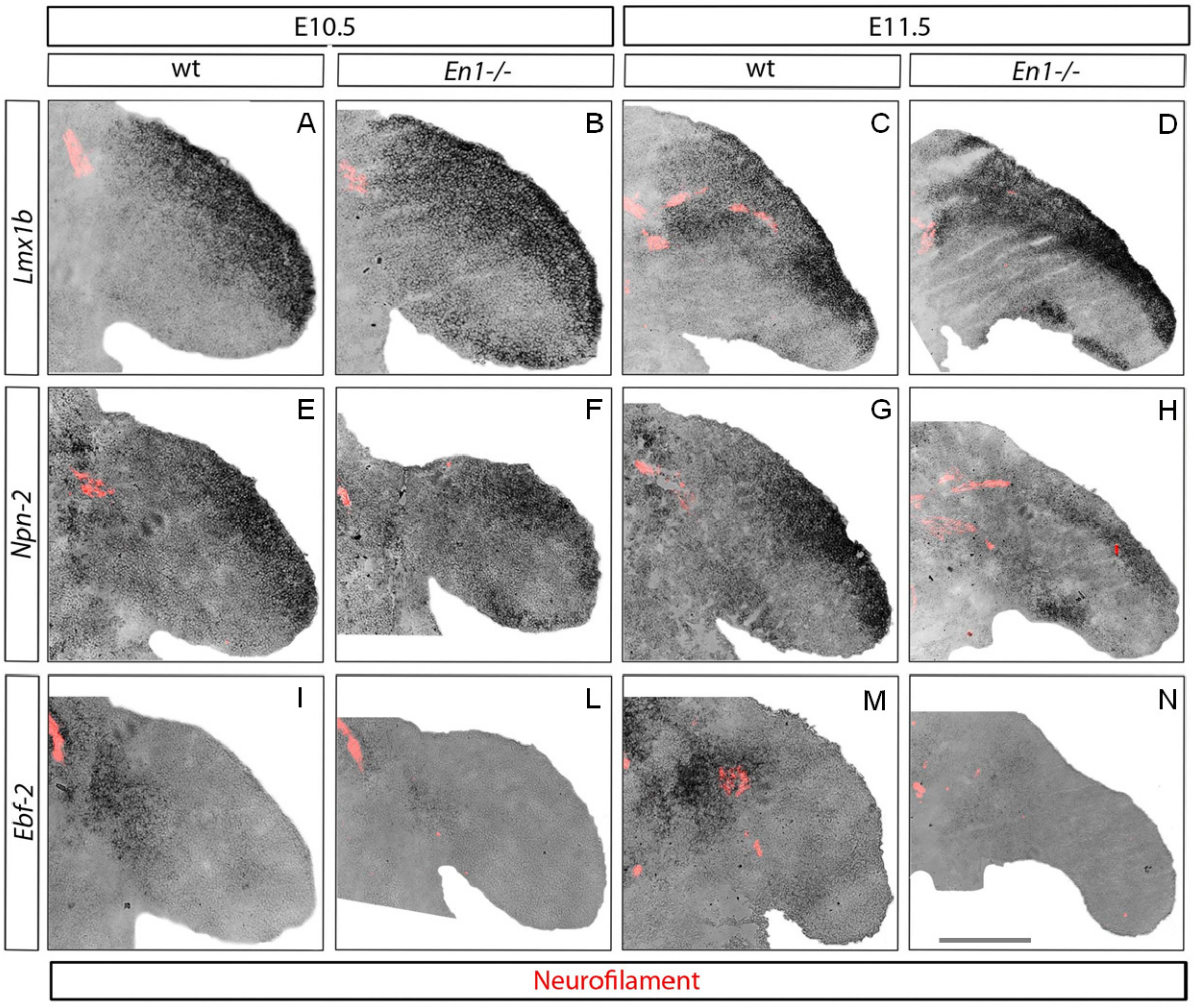

Figure 3.10. Engrailed 1 controls the dorsal-ventral patterning of the forelimb at a molecular level. In situ hybridization of dorsal and ventral limb markers on transverse sections of E10.5 (A,B,E,F,I,L) and E11.5 (C,D,G,H,M,N) wild type or *En1*$^{-/-}$ embryos. *Lmx1b* and *Npn-2* are expressed in the dorsal part of the limb in wild type embryos (A,C,E,G), while their expression is also ectopically detected in the ventral limb in *En1* mutant mice (B,D,F,H). The expression of the ventral marker *Ebf-2* is strongly downregulated in *En1* mutants (L,N) when compared to wild type embryos (I,M). Neurofilament staining identifies motor and sensory projections (red). Scale bar: 200µm (for E10.5) and 75µm (for E11.5).

3.2.4 Engrailed 1 has direct repulsive effect on LMCl axons

Besides *En1*'s well known role as transcription factor controlling the development of the mid-hindbrain junction region and limb patterning (Wurst et al., 1994; Loomis et al., 1996; Hanks et al., 1998), recent works showed that *En* can also act as a direct axon guidance cue in the *Xenopus* (Brunet et al., 2005) and in the chick visual system (Wizenmann et al., 2009).

Studies in *Xenopus* revealed that En expressed in a caudal-to-rostral gradient in the developing midbrain plays a role in patterning the optic tectum (Brunet et al., 2005). Indeed, it was shown that an external gradient of soluble Engrailed attracts growth cone temporal retinal axons and repels nasal axons. *In vitro* experiments demonstrated that En is internalized in the *Xenopus* retinal growth cones through its internalization sequence (Joliot et al., 1998) and it elicits the phosphorylation of proteins involved in translation initiation and activates the synthesis of new proteins that trigger axonal turning (Brunet et al., 2005). Very recent studies show that extracellular En plays a role also in the organization of the chick tectum, where it is expressed in an anterior-posterior gradient (Wizenmann et al., 2009). *In vivo* experiments revealed that temporal retinal axons map aberrantly to the posterior tectum when the activity of secreted En protein is disrupted. Furthermore, it was demonstrated that posterior wild type tecta membranes incubated with neutralizing extracellular En antibodies or posterior membranes of *En1*$^{-/-}$ mice exhibit diminished repulsive activity for temporal axons *in vitro*.

These findings together with the En1 expression data that we obtained prompted us to perform *in vitro* and *in vivo* functional studies, in order to investigate whether the En1 protein could act as an axon guidance cue for spinal cord motor axons and to identify its mechanism of action in the guidance of LMCl neurons towards the dorsal compartment of the limb.

To better understand the functional role of En1, we performed a growth cone collapse assay. Briefly, we cultured motor neurons of both LMC divisions dissected from *Hb9:GFP* embryos, where the green fluorescent protein is expressed under the control of the *Hb9* promoter, allowing for the specific identification of motor neurons. E11.5 motor neurons were cultured for four hours and exposed to different experimental conditions and then a total number of 100 growth cones (50 for LMCl and 50 for LMCm motor neurons) per well were counted and identified as "elaborated" (Figure 3.11A) and "collapsed" growth cones (Figure 3.11B); the percentage of collapsed growth cones was calculated and significance was determined as described in section 2.3.3. LMCl motor neurons were detected by the co-

expression of the GFP and the Lim1 staining and were therefore distinguishable from motor neurons belonging to the LMCm, which were only GFP positive.

Different concentrations of the En1 protein (5, 10, 50, 100 and 400ng/ml) were added to the cultured motor neurons (section 2.3.3). To test that the growth cone collapse effect was not caused by experimental proceeding, we used mock treatments where medium was collected from each well and re-added to the cultured motor neurons. Under this control condition around 20% to 30% of growth cones are collapsed for both neuronal populations, while a significant increase in the number of collapsed growth cones in the LMCl neuronal division was observed starting with 10ng/ml of En1 protein (Figure 3.11C). We performed a dose-response curve and found that increases in the concentration of the En1 protein corresponded to increases in the number of collapsed growth cones of LMCl neurons. This effect was detectable until a concentration of 100ng/ml, while at higher concentrations (e.g., 400ng/ml) the En1-collapsing effect became non-specific, causing the collapse of a significant percentage of LMCm growth cones.

To test whether the effect of the En1 protein was specific, we added different proteins as controls to the cultured motor neurons. En2, the other vertebrate Engrailed protein which has similar functions to En1 in the development of the midbrain and cerebellum (Joyner et al., 1991; Wurst et al., 1994) but is not expressed in the spinal cord (Hanks et al., 1995; Hanks et al., 1998). We considered En2 an essential control for our experiments, because previous studies showed that it directly participates as a soluble factor in topographic map formation of the *Xenopus* and chick visual system (Brunet et al., 2005; Wizenmann et al., 2009) and *in vitro* assays in *Xenopus* showed that it is internalized by temporal and nasal growth cones, eliciting their axonal turning response (Brunet et al., 2005).

We also used as control the En1SR protein, a form of the En1 which can not be internalized because of the presence of a mutation in the coding sequence of the Penetratin domain, necessary for En internalization, changing the tryptophan (W) and phenylalanine (F) residues at the positions 48 and 49 in the homeodomain to serine (S) and arginine (R) residues, respectively (Joliot et al., 1998). A further control consisted in the preincubation of En1 with an antibody (4G11) to block its function. As shown in the Figure 3.11D, under all these conditions, the percentage of collapsed growth cones was similar to the control conditions (between 20-30%), while adding 100ng/ml of En1 protein caused a significant increase in the percentage of collapsed growth cones of LMCl neurons (approximately 50%) compared to the LMCm ones (approximately 25%).

These data demonstrate that the En1 protein causes specific growth cone collapse of LMCl neurons and that this effect is dose-dependent.

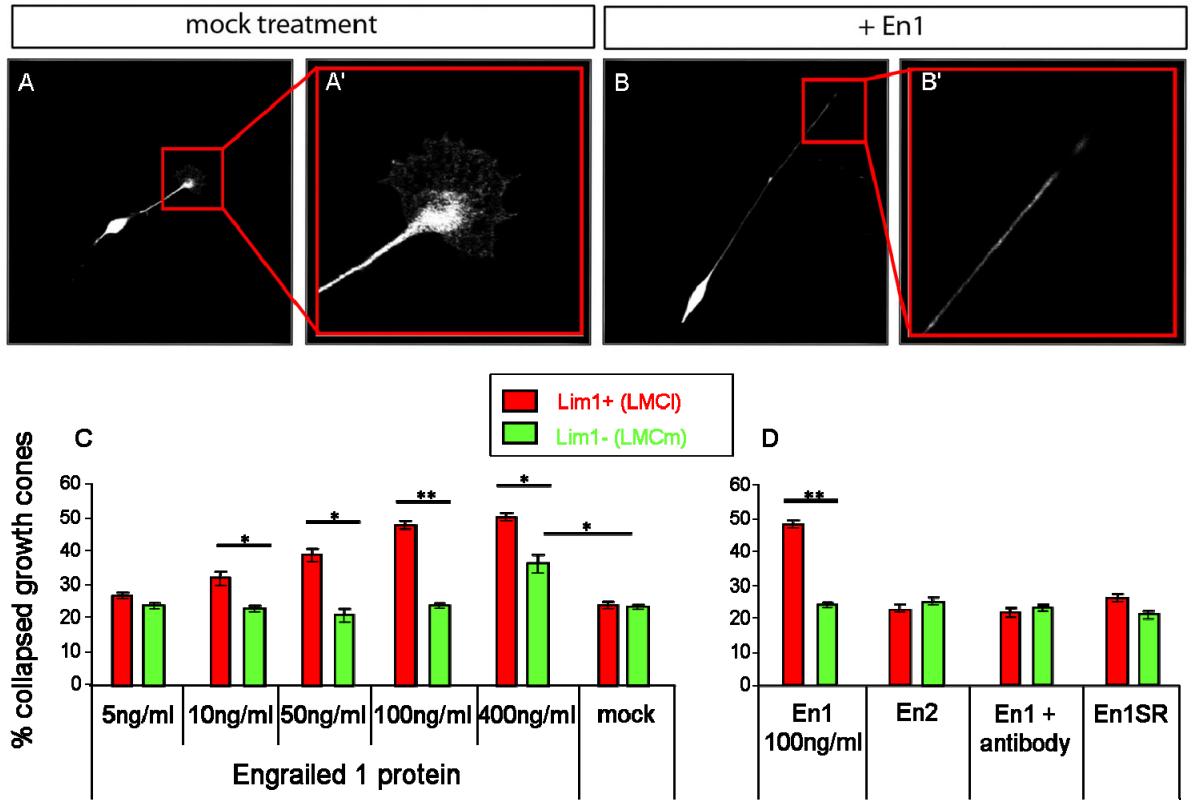

Figure 3.11. Engrailed 1 causes lateral LMC neuron growth cone collapse. "Elaborated" (A) and collapsed growth cones (B) from *Hb9:GFP* mice dissociated motor neurons were counted. The En1 protein specifically caused the collapse of lateral LMC growth cones (identified by Lim1 staining) in a dose dependent manner (C, n=3). Anti-En1 antibodies neutralized this effect, En2 and a non-internalizable mutant form of En1 (En1SR) had no effect (D, n=3). Significance was calculating using a Student's t-test and indicated by asterisks (*P<0.1; **P<0.0001). Error bars indicate SEM.

We then asked whether the specific growth cone collapse of LMCl neurons was caused by the action of the En1 protein at a transcriptional or translational level. Previous studies in *Xenopus* demonstrated that guidance molecules, such as Sema3A and Netrin-1, steer retinal axon elongation by activating the synthesis of new proteins in their growth cones (Campbell and Holt, 2001) and the same mechanism was shown to regulate the En-induced turning of temporal and nasal axons (Brunet et al., 2005). To test whether the growth cone collapse of LMCl neurons induced by En1 affected translation or transcription, we used pharmacological reagents that selectively interfere with one of these cellular mechanisms. As shown in Figure 3.12, adding 100ng/ml of En1 protein caused specific LMCl growth cones collapse. Previous incubation with anisomycin, a translation inhibitor, for 15 minutes before the addition of En1 protein did not abolish the growth cone collapse of motor neurons caused

by En1. Similarly to the effect of anisomycin, two transcriptional inhibitors, α-amanitin that blocks the RNA polymerase II, and actinomycin D that binds DNA at the transcription initiation complex preventing elongation by RNA polymerase, had no effect on En1 action. Lacking a control for proper functioning of the pharmacological inhibition of translation and transcription, we cannot unambiguously conclude that these two processes are not involved in En1-mediated collapse of LMCl growth cones.

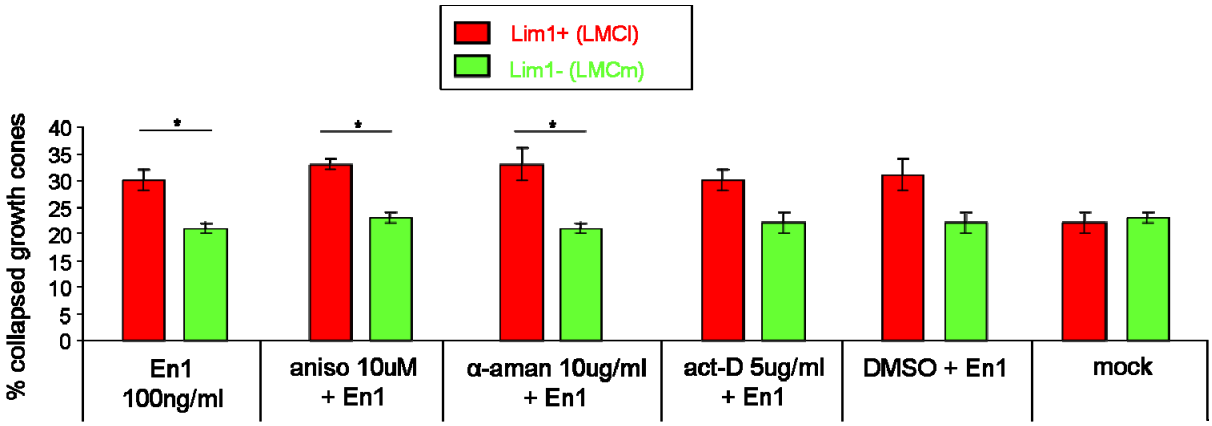

Figure 3.12. Translational and transcriptional inhibitors do not influence the response of motor neuron growth cones to En1. The incubation of translational (anisomycin) or transcriptional (α-amanitin and actinomycin D) inhibitors with LMC motor neurons for 15 minutes before the adding of the En1 protein did not have an effect on En1-induced motor neuron growth cone collapse (n=3). Significance was calculating using a Student's t-test and indicated by asterisks (*P<0.1). Error bars indicate SEM.

A recent study indicated that the En protein interacts with ephrinA5 and increases the sensitivity of chick temporal axons to this guidance factor (Wizenmann et al., 2009).

In the motor system, ephrin/Eph signaling regulates the dorsal-ventral choice of motor axons at the base of the limb. EphrinAs expressed in the ventral limb compartment interact with the EphA4 receptor, present on LMCl axons, repelling them to the dorsal part of the limb (Kania et al., 2000; Kania and Jessell, 2003; Eberhart et al., 2004). A symmetrical molecular mechanism regulated by the ephrinB2/EphB1 signaling directs the guidance of medial LMC axons towards the ventral limb compartment. The presence of ephrinB2 in the dorsal limb mesenchyme, indeed, provides repulsive signals for LMCm axons expressing the EphB1 receptors, guiding them to innervate the dorsal limb musculature (Eberhart et al., 2002; Kania and Jessell, 2003; Luria et al., 2008).

These findings prompted us to investigate whether En1 acts cooperatively with the LMCl axons repellents ephrinAs, expressed in the ventral limb, to cause motor neurons growth cone collapse. To test this hypothesis, we used an *in vitro* assay, incubating LMC

neurons with En1 and ephrinA2/A5 and asked whether En1 increases the sensitivity of LMCl motor axons to the growth cone collapse-inducing ephrinAs. We first determined the subthreshold ephrinAs concentration that resulted in baseline level collapse (0.1µg/ml). When En1 at a subthreshold concentration of 10ng/ml was added for 30 or 120 minutes together with 0.1µg/ml of ephrinAs to the medium, growth cone collapse occurred at levels similar to controls (Figure 3.13). Furthermore, the percentage of collapsed LMCl growth cones did not change significantly when motor neurons were incubated for 120 minutes with En1 and then ephrinAs were then added for 30 minutes (Figure 3.13). Our results show that there is no increase in the percentage of LMCl growth cone collapse and thus the En1 protein does not cooperate with ephrinAs *in vitro* to cause growth cone collapse of motor neurons.

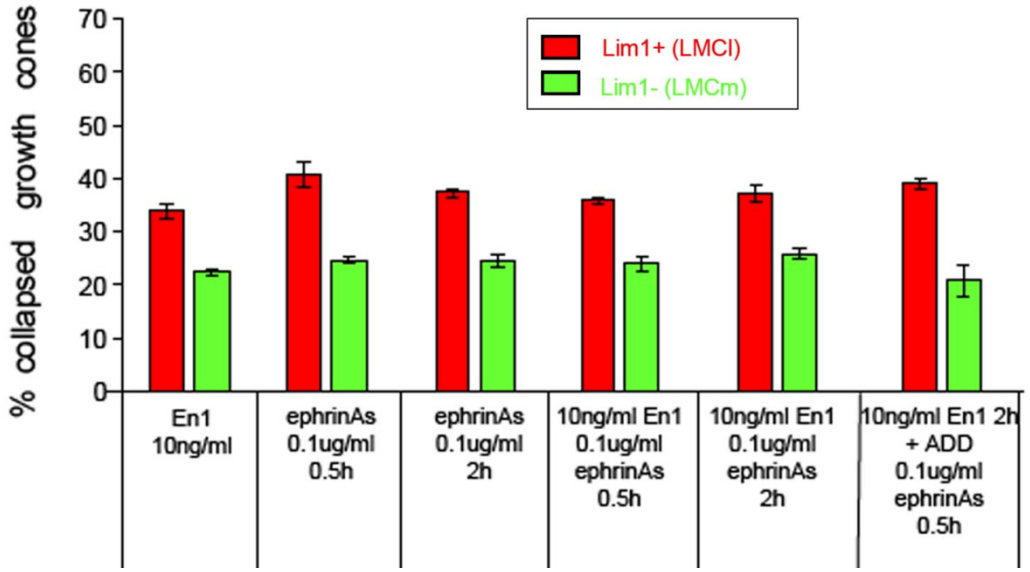

Figure 3.13. Engrailed 1 and ephrinA2/A5 do not cooperate *in vitro* for motor neuron growth cone collapse. EphrinA ligands expressed in the ventral limb selectively collapsed LMCl growth cones. We tested whether En1 and ephrinAs act cooperatively by adding subthreshold levels of both proteins together, however, no increased collapse was observed (n=3).

Together, the *in vitro* assays we performed show that Engrailed 1 specifically causes growth cones collapse of lateral LMC neurons. The cellular mechanism used by Engrailed 1 to elicit growth cone collapse is currently unclear. Furthermore, our results reveal that in the spinal motor system, differently from the visual system, Engrailed 1 does not cooperate with ephrinAs in the establishment of neuronal circuits.

3.2.5 Dorsal-ventral choice of brachial LMC axons is impaired in *En1*$^{-/-}$ mice

To assess whether the absence of *En1* could affect the dorsal-ventral choice of motor axons at the base of the limb *in vivo* we analyzed the development of motor axonal projections targeting the forelimb in *En1*$^{-/-}$ mice (Hanks et al., 1995). Motor neurons of E12.5 wild type and *En1* mutant mouse embryos were retrogradely labeled by injection of dextran-conjugated Rhodamine into the dorsal or ventral limb musculature (Figure 3.14A,E), allowing analyzing the effects of *En1* ablation on the dorsal-ventral motor axon projection towards the limb.

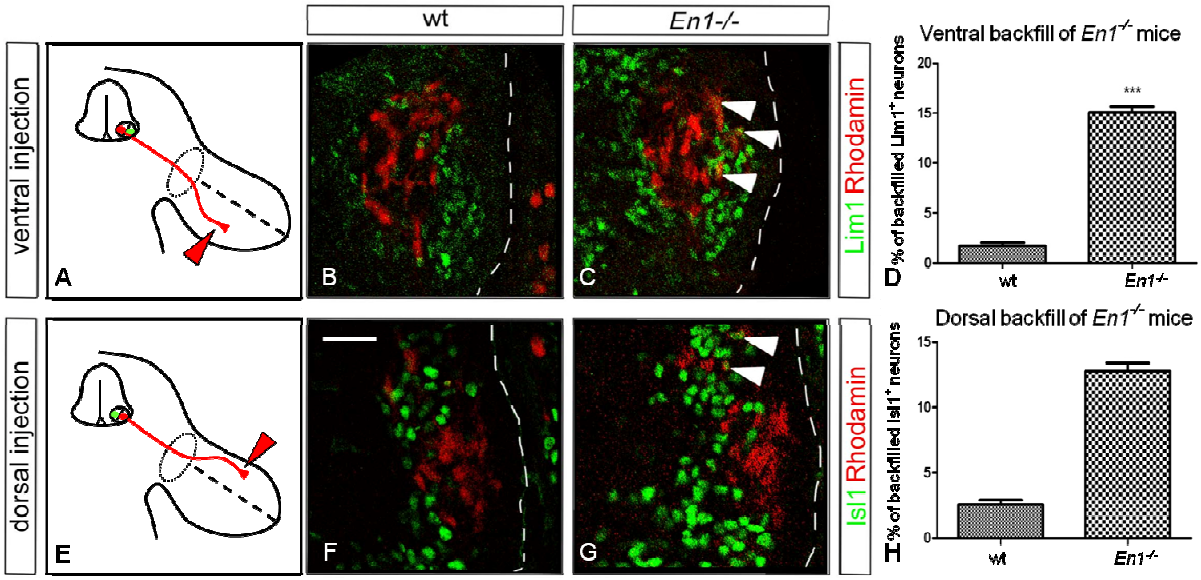

Figure 3.14. The dorsal-ventral choice of LMC axons is impaired in the absence of Engrailed 1. To analyse the effect of the loss of En1 on the dorsal-ventral guidance decision of motor neurons, Rhodamine-labeled dextran was injected in the dorsal (A) and ventral (E) limb musculature of E12.5 *En1*$^{-/-}$ embryos at brachial level. Counterstaining with the LMCl Lim1 marker (B,C) reveals that 15.1% ± 1.1 SEM of LMCl axons project aberrantly to the ventral limb compartment (C,D, n=3), compared to only 1.7% ± 0.5 SEM in wild type embryos (B,D, n=3). Isl1 staining, used to identify the LMCm division (F,G), shows that 12.8% ± 0.6 SEM of LMCm neurons misproject to the dorsal limb (G,H, n=2), compared to wild type controls, where only 2.5% ± 0.5 SEM of Isl1-positive neurons showed guidance errors (F,H, n=2). The spinal cord is outlined with a dashed white line. Misprojecting neurons are indicated with arrowheads (C,G). Significance was calculated using a Student's t-test and indicated by asterisks (***P<0.00005). Error bars indicate SEM. Scale bar 25µm (B,C,F,G).

To investigate whether dorsal-ventral patterning of lateral LMC neurons occurred correctly in *En1*$^{-/-}$ mice, we injecting dextran-conjugated Rhodamine in the ventral part of the

limb. Staining with Lim1 antibody, which identifies neurons belonging to the lateral division of the LMC, allowed for the detection of LMCl neurons projecting aberrantly to the ventral limb compartment (Figure 3.14C). Counting of the Rhodamine-Lim1-double positive LMCl neurons revealed that in *En1*$^{-/-}$ embryos (n=3), 15.1% ± 1.1 SEM of the LMCl neurons aberrantly project towards the ventral part of the limb (Figure 3.14D), compared to control mice (Figure 3.14B) where only 1.7% ± 0.5 SEM of LMCl axons choose a false trajectory to ventral limb musculature (Figure 3.14D). We used the same procedure to analyze dorsal-ventral pathfinding of LMCm neurons by injecting dextran-conjugated Rhodamine into the dorsal limb. Counterstaineing with Isl1 antibody allowed identifying LMCm neurons. Preliminary data (n=2) show that approximately 12.8% ± 0.6 SEM of the LMCm neurons project aberrantly to the dorsal limb (Figure 3.14G,H), compared to wild type embryos, where only 2.5% ± 0.5 SEM of the LMCm axons elongated into the dorsal limb (Figure 3.14F,H). These data show that the dorsal-ventral choice of brachial LMC axons is impaired in *En1*$^{-/-}$ mice. This phenotype could be caused by the absence of *En1* in the motor neurons or in the ventral limb ectoderm, or by the mispatterned forelimb.

3.2.6 Dorsal-ventral axon pathfinding does not depend on Engrailed 1 in LMC neurons

To determine the source of En1 responsible for LMC axon guidance errors at the dorsal-ventral decision point at the base of the limb, we took advantage of tissue specific ablation of *En1* in motor neurons. *En1*^{cond} mice, where loxP sites were inserted in the intron and in the second exon of *En1* to generate a conditional allele (Sgaier et al., 2007), were crossed with the *Hb9-Cre* mouse line (Arber et al., 1999), where *Cre* is specifically expressed under the control of the *Hb9* promoter and therefore active only in motor neurons. We used retrograde tracing again to reveal any dorsal-ventral guidance defects at E12.5. The injection of Rhodamin-dextran in the ventral part of the limb (Figure 3.15A) together with the Lim1 immunostaining did not reveal a dorsal-ventral miswiring of LMCm axons (Figure 3.15B,C). The percentage of axons choosing an aberrant direction towards the dorsal limb compartment was only 1.7% ± 0.2 SEM in *En1*^{cond}*:Hb9-Cre* mice (n=3, Figure 3.15D) compared to 1.4% ± 0.1 SEM in control embryos (Figure 3.15D).

These findings indicate that *En1* expressed in the limb is responsible for the aberrantly projections of both LMCl and LMCm axons revealed by retrograde labeling of motor neuron cell bodies of *En1*$^{-/-}$ mouse embryos.

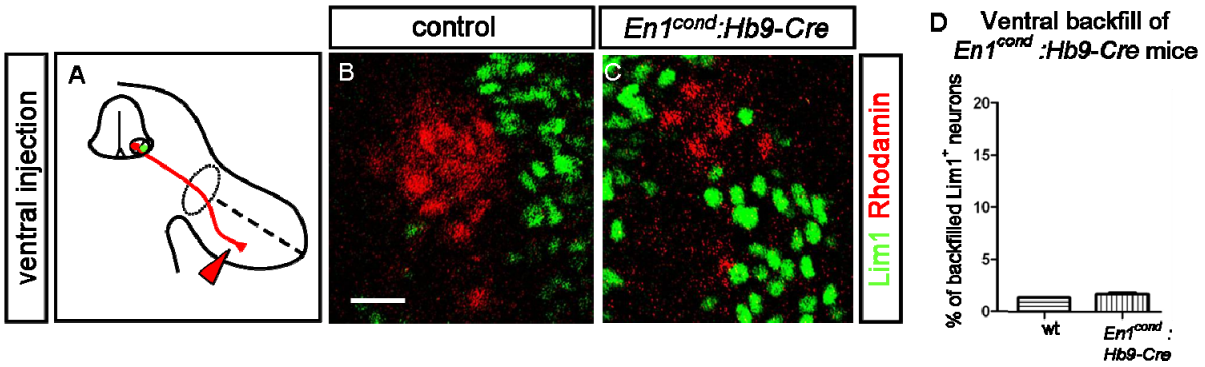

Figure 3.15. LMC axons project correctly to the limb when Engrailed 1 is specifically ablated in motor neurons. The ventral musculature of *En1*^{cond}*:Hb9-Cre* embryos was injected with dextran-conjugated Rhodamine to analyze the projections of LMCm neurons towards the limb (A). The retrograde labeling of motor neuron cell bodies of the mutant embryos did not reveal a phenotype in the dorsal-ventral choice of motor axons at the base of the limb (C, n=3). In fact, the percentage of LMCm axons projecting aberrantly to the dorsal limb was only 1.7% ± 0.2 SEM in *En1*^{cond}*:Hb9-Cre* mutants (C,D) which was not statistically significantly different from control embryos (1.4% ± 0.1 SEM, B,D, n=3). Scale bar: 50µm (B,C).

4 Discussion

My PhD project contributes to a better understanding of the cues and mechanisms that govern axon guidance in the establishment of neuronal circuitry during development. Spinal motor and sensory axons are guided towards their targets located in the dorsal or ventral limb by guidance cues that enable them to find the correct trajectory. Axon guidance molecules regulating the dorsal-ventral pathfinding of motor axons at the base of the limb have been previously identified, whereas so far no such cues for sensory neurons have been discovered. This work identifies novel potential cues that govern the dorsal-ventral guidance decision of motor and sensory axons at the base of the limb, thereby revealing the first potential markers to distinguish sensory neurons with regard to the limb compartment they innervate.

Furthermore, this thesis characterizes Engrailed 1, a candidate gene identified in the brachial motor neuron screen, as a repulsive cue for motor axons projecting to the dorsal limb and demonstrates that En1 is essential to establish the correct dorsal-ventral pathfinding of motor axons into the limb. This data, therefore, shed light on the mechanisms governing the establishment of neuronal connectivity in the spinal sensory-motor system.

In the following, I will discuss the data obtained and give perspectives on future directions for the analysis of different aspects of neuronal circuit formation.

4.1 Genome-wide screening for novel axon guidance cues governing the dorsal-ventral choice of motor and sensory axons to the limb

4.1.1 Spinal sensory and motor axon guidance

The wiring of the nervous system during development requires axonal elongation, pathfinding, and the establishment of synapses with the correct target. Neuronal projections elongate throughout the developing body along sometime very long distances to innervate the periphery, as it is demonstrated for the human sciatic nerve that extends for more than 50 cm from the lumbar spinal cord to its muscular targets in the leg and the foot. To get the right direction in an almost infinitive possibility of trajectories, axonal growth is patterned by guidance cues expressed in the surrounding tissues and on other axons that project along the same trajectories. Guidance factors, which can act as repellents or attractants over long or short distances, interact with receptors expressed by the axons or their growth cones (Tessier-Lavigne and Goodman, 1996; Dickson, 2002).

In the spinal sensory-motor system, motor and sensory neurons are settled in two separated body areas, the lateral motor column (LMC) in the ventral horn of the spinal cord and the dorsal root ganglia (DRG), respectively. However, immediately after having left their site of origins, motor and sensory axons join together and elongate tightly fasciculated along the same trajectories to innervate target areas, which are located close to each other in the limb. Their outgrowth is therefore spatially and temporally highly regulated, so that they proceed together until the plexus region, where they defasciculate and sort into new target-specific bundles to innervate their peripheral targets.

Motor neurons projecting dorsally and ventrally towards the limb musculature express two different transcription factors, *Lim1* and *Isl1* respectively, which can be used as markers to distinguish the two neural populations. These markers allow identifying the position of LMCl and LMCm neurons in the spinal cord, which topographically corresponds to the location of their targets in the periphery (Figure 1.2). Furthermore, some signaling pathways that regulate the dorsal-ventral decision of motor axons at the base of the limb have been identified. They include the class 3 Semaphorin-Neuropilin (Huber et al., 2005), the

ephrinAs/EphA4 (Helmbacher et al., 2000; Kania and Jessell, 2003) and the ephrinB2/EphB1 (Luria et al., 2008) signaling pathways.

On the contrary, retrograde tracing experiments revealed that sensory neuron cell bodies are located in the DRG in a salt-pepper manner and, until now, no markers able to identify sensory neurons projecting to the dorsal or the ventral limb have been discovered (Figure 4.1). The lack of knowledge about sensory axon guidance cues could be partially explained by work done in the 1980ies by Landmesser and Honig: in the chick embryo sensory axons follow motor axons to reach the limb. Indeed, Landmesser and Honig demonstrated that after surgical removal of motor neurons, sensory axons were not able to find their targets in the periphery (Landmesser and Honig, 1986). Recent work in mouse, however, demonstrated that even if motor axons are severely defasciculated, patterning of sensory projections is still normal, suggesting that the establishment of sensory trajectories in the distal limb is independent of motor axons (Huettl et al., submitted).

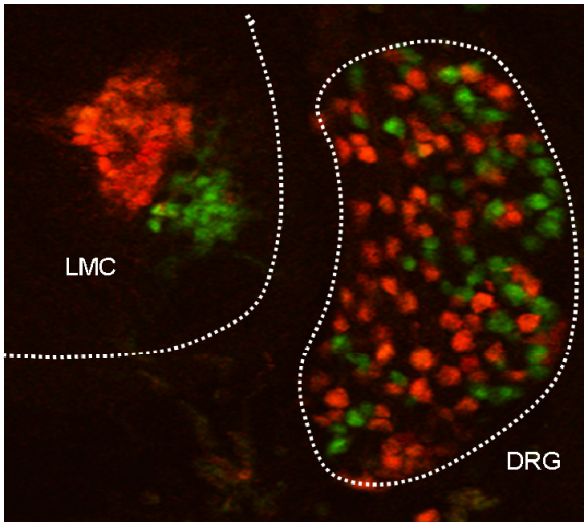

Figure 4.1. Distribution of sensory neurons in the DRG. Retrograde tracing of sensory neurons reveals that they are not organized in a topographic manner reflecting their projection trajectories towards the dorsal or ventral limb in the DRG.

4.1.2 Novel candidate cues for motor and sensory axon guidance

During the development of the spinal sensory-motor system, motor and sensory neurons elongate their axons towards the base of the limb, where they choose a dorsal or ventral trajectory. Some guidance cues regulating the dorsal-ventral binary decision of motor

axon have been identified, such as ephrinAs, ephrinBs and Sema3F, but further investigation is required to extend our limited knowledge.

To this goal, for the first time, we performed a genome-wide screening to identify novel cues that govern axonal pathfinding at the base of the limb in the spinal sensory-motor system. Previous studies reported the employment of microarray screening in other systems, aimed to identify genes that control the specification and development of corticospinal motor neurons (Arlotta et al., 2005) or to discover molecular cues governing the differential expression of receptors in the olfactory epithelium (Tietjen et al., 2005), but a global transcriptome analysis was not employed in the spinal system, yet.

To identify novel guidance cues that govern the dorsal-ventral choice of motor and sensory axons at the base of the fore- and hindlimb, we distinguished the two neuronal populations on the basis of their peripheral projection patterns by injecting two differentially fluorescently labeled dextrans into the dorsal and ventral limb musculature. The subsequent uptake and retrograde transport of the fluorescent dyes into the neuronal cell bodies allowed for distinguishing motor and sensory neuronal populations projecting dorsally or ventrally (Figure 1.3). Differentially labeled neurons were sorted by FACS and the two RNA pools subjected to microarray analysis to identify differentially expressed genes.

We demonstrated the reliability of the screening, verifying that microarray predictions correctly assessed the differential expression of already known motor neuron markers in the dorsally (*Lim1*) and ventrally (*Isl1* and *Npn-2*) projecting neuronal populations.

Comparative analysis of the differentially expressed genes, motor and sensory neurons projecting to the fore- or to the hindlimb and brachial and lumbar motor or sensory neurons, did not reveal any gene specifically expressed in more than one of these neuronal subpopulations, suggesting that motor and sensory axonal growth towards the fore- and hindlimb is regulated by the expression of different molecules. These data are supported by previous studies revealing that different cues regulate axonal innervation of the fore- or hindlimb, such as the LMCl receptor EphA4. Indeed, *EphA4* mutant mice analysis revealed the complete absence of the dorsal peroneal nerve, projecting to the hindlimb, and only a mild reduction of the dorsal nerve in the forelimb, therefore suggesting a less critical role for EphA4 in the pathfinding of motor axons towards the forelimb (Helmbacher et al., 2000).

The fact that the screening did not reveal any genes to be expressed by more than one neuronal population, however, does not exclude that similar regulatory networks could be involved in the dorsal-ventral guidance decision at the base of the limb of the four neuronal populations. The candidates we obtained from the screening, indeed, could regulate pathways

that modulate the same factors to steer and properly guide the axons toward their targets. Further analysis may discover whether neuronal projections directed to the same musculature (e.g. motor and sensory axons towards the dorsal forelimb) or the same neuronal populations (e.g. motor axons projecting to the dorsal fore- and hindlimb) are guided by common regulatory networks that govern their axonal elongation towards the periphery.

Candidate genes that we expected to be predicted by microarray analysis included adhesion molecules, receptors, signal transduction regulators and transcription factors that, by controlling different molecular mechanisms of axonal pathfinding regulation, would have suggested their potential role in axon guidance. The screenings performed, indeed, revealed the expression of extracellular proteins (e.g. *Igfbp5*), molecules involved in signal transduction (e.g. *G-protein γ3*), and transcription factors (e.g. *En1*), which, on one side, offered a wide variety of interesting potential candidates and, on the other side, confirmed once more the success of our transcriptome analysis, demonstrating the reasonableness of the microarray predictions.

The screening, furthermore, opens interesting opportunities to further investigate the regulation of axon guidance, exploring a possible role of microRNAs (miRNA) in the formation of neuronal connectivity. Indeed, very recent data (G. Luxenhofer, personal communication) revealed that *miR-9*, a miRNA that was predicted to target Engrailed 1 is present in lateral LMC neurons, at the same developmental timepoints when this motor neuron population expresses *En1* mRNA. The observation that En1 protein was not detected in the cell bodies of motor neurons may suggest a potential role for *miR-9* in the degradation and/or repression of En1 translation in motor neuron cell bodies, but not in their axons, for reasons that are still unknown, but that may imply its role in the guidance of motor axons. Axon guidance regulation mediated by miRNAs is not surprising, even if it would be the first demonstration for their contribution in the formation of the spinal motor system, since previous studies revealed that miRNAs are involved in zebrafish axon pathfinding (Giraldez et al., 2005) and in retinal axon outgrowth in the mouse visual system (Pinter and Hindges, 2010).

4.2 Engrailed 1: a novel brachial motor axon guidance cue

One intriguing candidate identified by the brachial motor screening was the transcription factor Engrailed 1. In situ hybridization together with immunohystochemical analysis performed to validate microarray predictions confirmed that *En1* transcripts were found to be enriched in the LMCl neurons that extend their axons towards the dorsal limb. *En1* belongs to the homeodomain transcription factor family and is known as a potent determinant of the mid/hindbrain junction formation starting around E8 (Wurst et al., 1994). From E9.5 it is also expressed in the ventral limb ectoderm, where it regulates the patterning of the limb (Davis et al., 1991). Within the central nervous system, it was shown that En1 is also expressed by interneurons extending their projections ventrally towards somatic motor neurons, even if it was not possible to determine in mouse whether the En1-positive interneurons synapse with motor neurons (Saueressig et al., 1999). However, in other model systems, such as chick and zebrafish, their direct synaptic connection with motor neurons was demonstrated (Wenner et al., 2000; Higashijima et al., 2004).

In addition to its well-known role as transcription factor, more recently it has been shown in *Xenopus* that Engrailed has a direct repulsive and attractive effect on temporal and nasal axons, respectively (Brunet et al., 2005). It was also demonstrated that extracellular Engrailed plays a direct role in axon guidance in the chick, where it contributes to the anterior-posterior mapping of the visual system (Wizenmann et al., 2009). These recent results prompted us to investigate whether En1 plays a similar role in the spinal sensory-motor system.

En is not the only example of a homeodomain protein that can be internalized. It was previously shown that other homeodomain transcription factors, such as *Otx2* in the visual cortex (Sugiyama et al., 2008) and *Pax6* in the retina (Lesaffre et al., 2007), possess the secretion and internalization sequences that enable an intercellular passage and potentially allow for a direct non-cell-autonomous activity in the development of the visual system.

4.2.1 Engrailed 1 is expressed in motor neurons and axons

Our En1 expression analysis was performed at relevant developmental time points: at E10.5 when the axons converge at the plexus region, at E11.5 when they enter the limb bud and at E12.5 when the dorsal-ventral axonal bifurcation decision at the base of the limb has already occurred. The presence of the En1 protein in spinal motor neurons was observed in the nuclei of E10.5 interneurons, as expected for a transcription factor (Matise and Joyner, 1997), but only a non-nuclear expression was observed at LMC level at E11.5, suggesting that En1 could derive from external sources, such as the interneurons. The absence of En1 expression in the motor neuron cell bodies raised the question whether En1 protein was present on LMC axons. Our immunohistochemical analysis showed that at E11.5 En1 is preferentially detectable on LMCl axons projecting dorsally, while is not found on sensory axons emerging from the dorsal root ganglia. These observations suggest two possible scenarios: the En1 protein present in LMCl cell bodies is immediately transported into axons and growth cones, or motor neurons do express *En1* both at mRNA and protein levels, but internal cellular mechanisms downregulate En1 transduction, resulting in detectable quantities only on axons (see section 4.1.2).

Another possible explanation for our observations of the presence of En1 only on axons could be that it is not expressed in motor neurons, but it stems from other sources. To determine whether the *En1* locus is active in motor neurons, the expression of *LacZ* in the $En1^{Lki}$ (Hanks et al., 1995) mice could be analyzed. This analysis would reveal whether the En1 protein is derived from the motor neurons themselves or from other sources, such as the interneurons or the ventral limb ectorderm.

An alternative possible En1 origin could be, indeed, the En1-positive interneurons that project to motor neurons, which might also explain the presence of non-nuclear En1 at LMC level at E11.5. Another potential source for En1 is the ventral limb bud, from where the En1 protein could be takenup and retrogradely transported in the LMCl axons.

This last hypothesis arises the question how En1 is specifically uptaken only by dorsally projecting motor axons, since it has also to be considered that En1 derives from the ventral limb. One possible explanation could be given by the specific expression of receptors on LMCl axons that recognize and elicit En1 internalization. To verify this hypothesis it will be fundamental to identify the receptor, to show that it is selectively expressed on the surface of LMCl neurons and to perform *in vitro* antagonist experiments that will reveal whether the

growth cone collapsing effect of En1 on LMCl axons diminishes or is impaired in the presence of a receptor-specific antagonist.

Another possibility that would explain En1 detection only in LMCl axons could be that En1 is internalized by both LMC axons, and then LMCm axonal mechanisms downregulate its expression.

To provide answers to the question concerning En1 specificity, it will be worth to use fluorescently labeled En1 protein (see Table 2.1) and observe whether it can be specifically captured and retrogradely transported into LMCl axons. Live imaging of cultured LMCl and LMCm neurons exposed to media containing fluorescently labeled En1 will enable to visualize whether the fluorescent En1 is uptaken by neuronal growth cones. Subsequent immunostaining with Lim1 antibody, to distinguish LMCl from LMCm neurons, will reveal whether the En1 signal is specifically present in LMCl axons and cell bodies.

Previous studies in *Xenopus*, indeed, demonstrated that fluorescently labeled En accumulated in the body of the growth cones and along the neurite shaft of retinal axons (Brunet et al., 2005).

4.2.2 Engrailed 1 expressed in the ventral limb ectoderm controls limb patterning

Previous studies revealed that En1 plays a role in the patterning of the limb. Starting at E9.5 En1 is expressed in the ventral limb ectoderm, where it suppresses the dorsalizing action of Wnt7a, conferring the limb its proper ventral characteristics (Loomis et al., 1996). However, the analysis of *En1*$^{-/-}$ mice so far focused on limb patterning only at structural and morphological levels (Wurst et al., 1994; Loomis et al., 1996). In the present work we showed that *En1* ablation causes the ectopic expression of dorsal limb markers in the ventral limb compartment and the downregulation of the expression of ventral limb markers. Therefore, our data revealed that limb patterning of *En1*$^{-/-}$ embryos is compromised also at a molecular level, resulting in a partial dorsalization of the limb.

A possible explanation for the partial limb dorsalization that we observed at E10.5 and E11.5 at a molecular level could be the presence of other cues that regulate the patterning of the ventral limb at early stages, whose effect diminishes progressively during development. Indeed, anatomical studies conducted in newborn *En1* mutant embryos did not reveal alterations in the dorsal-ventral patterning of the limb (Wurst et al., 1994). These observations

may suggest that the dorsal-ventral patterning of the limb is controlled by different regulatory systems during the continuation of limb development.

4.3 Novel insights into the role of Engrailed 1 in axon guidance

4.3.1 Engrailed 1 has direct repulsive effect on LMCl axons

The collapsing effect caused by the En1 protein on LMCl axons reveals that it acts on specific neuronal population, as it was demonstrated also in the visual system (Brunet et al., 2005; Wizenmann et al., 2009). En presented as an external gradient of soluble En is internalized by *Xenopus* retinal axons where it regulates translational mechanisms present in the growth cone, triggering the rapid phosphorylation of proteins involved in translation initiation and the local synthesis of novel proteins that elicit axonal turning (Brunet et al., 2005). More recent data in chick, demonstrated that extracellular En and ephrinA5, expressed in a posterior to anterior gradient in the tectum, cooperate to regulate the pathfinding of temporal retina axons, contributing to the formation of the retinotectal map (Wizenmann et al., 2009).

Our data show that En1 acts in a dose-dependent manner and requires at least 60 minutes to collapse LMCl growth cones. The long time required for the collapsing response prompted us to investigate whether the mechanism of action of En1 affected transcription or translation. Experiments conducted in the presence of two transcription inhibitors, α-amanitin and actinomycin D, had no effect on En1 capacity to cause growth cone collapse. We showed that also the translation inhibitor anisomycin did not influence the response of LMCl neurons growth cones to En1, showing that En1 does not affect transcription or translation to cause growth cones collapse. The results obtained from these experiments, however, are not conclusive, since a positive control, which would demonstrate that the pharmacological reagents worked, is missing. As positive control, for example, it would be possible to include in the experiments other neuronal types, such as the *Xenopus* retinal neurons. Indeed, in this neuronal population, it was already shown that the translation inhibitor anisomycin is able to affect growth cone turning in response to Engrailed, whereas α-amanitin, which interferes with transcription, had no effect (Brunet et al., 2005).

The fact that En1 protein requires 60 minutes to collapse growth cones, let us hypothesize that it requires co-factors to exert its collapsing function. We therefore asked whether En1 cooperates with guidance cues present in the ventral limb to cause the specific collapse of LMCl growth cones and we performed a set of experiments adding the En1 protein together with different factors. Indeed, in the recent publication of Wizenmann et al., (Wizenmann et al., 2009) it was shown that En1 increases the sensitivity of retinal axons to ephrinA5. We tested whether En1 acts together with the LMCl axonal repellent ephrinAs (A2/A5) also in the motor system (Figure 4.2). However, in our system, the addition of En1 protein in combination with ephrinAs did not increase the percentage of collapsed growth cones, showing that En1 does not collaborate with ephrinA2/A5 to cause growth cone collapse of LMCl neurons, at least *in vitro*.

These data indicate that different molecular mechanisms regulate the establishment of neuronal connectivity within the motor and the visual system. Indeed, in the visual system, ephrinAs and extracellular Engrailed gradients are present in the tectum along the anterior-posterior axis and they cooperate to repel temporal axons, thereby contributing to the formation of the retinotectal map. In the spinal motor system, axon pathfinding towards the limb is regulated by attractive and repulsive signals present in the dorsal and ventral target area that guide the elongating projections. Axonal dorsal-ventral trajectory selection, indeed, is regulated by different guidance molecules expressed in the dorsal (Sema3F, ephrinBs) and ventral (ephrinAs) limb compartment that specifically interact with the receptors expressed on axonal surface. Therefore, it is important to consider that ephrinAs are not the only players that could cooperate with Engrailed 1 to govern axon guidance in the motor system and other potential co-factors, such as Sema3A, Sema3F, and ephrinB2, have to be taken into account. To test whether the sensitivity of LMCl increases in the presence of the co-factors, it will be possible to perform growth cone collapse assay in the presence of potential interacting cues.

Another possible explanation for the long incubation time required for En1 to cause LMCl growth cone collapse may be found on a technical experimental level. Our experiments were conducted with dissociated motor neurons, where the cells could be immature or where some key factors may be missing. We therefore tested another culture paradigm. We used motor neuron explants, cultured in presence or absence of interneurons, which might present a possible source of important factors absent in dissociated motor neuron cultures. Unfortunately, due to a much slower axonal elongation in motor neuron explants compared to dissociated cultures - a difference bigger than two days – it was not possible to compare the percentage of collapsed growth cones between the two culture paradigms.

To quantify the effect of En1 *in vitro*, growth cones were classified as "collapsed" or "elaborated", and "axonal traces" of previously present axons were defined as "collapsed" based on the assumption that under the influence of En1 those axons collapsed and retracted. However, other aspects might also be responsible for their presence, for example En1 might play a role in motor axon branching and fasciculation. These "axonal traces" would therefore be the consequence of different mechanisms of action of En1. Live imaging of primary motor neuron cultures after addition of En1 protein will allow for visualization of the En1-induced effect on growth cones and small axonal protrusions.

To test whether En1 has an effect on axonal branching, axonal branching points could be counted and their number compared between LMCl and LMCm axons within the same sample, but also between control samples and samples where the En1 protein was added. If En1 exerts a specific role in axonal branching, we would expect to see less branching points in LMCl axons exposed to En1. The effect of En1 on axonal branching could also be tested *in vivo* in *En1*$^{-/-}$ mice using neurofilament immunohistochemistry. The analysis of mutant embryos at E13.5-14.5, when the axons branch to find there muscular targets in the limb, will reveal whether the muscles of the mutants are less innervated than those of control embryos.

Our immunohistochemical analysis showed the presence of En1 at E10.5 and E11.5 in the limb mesenchyme, just ventrally of the region where the dorsal-ventral axonal bifurcation takes place. The expression pattern of En1 and the presence of "axonal traces" in our *in vitro* experiments let also hypothesize whether the En1 protein plays a role in the formation of motor axons tracts towards the limb, too. Immunohistochemical techniques in whole-mount embryo preparations at crucial developmental time points (E10.5-E12.5) will reveal whether En1 plays a role in the timing of motor axonal elongation and fasciculation towards the periphery. This will be particularly interesting to clarify, since previous studies showed gross limb deformations in *En1*$^{-/-}$ embryos, including supernumerary digits fusion and truncation of the digits and delete digit ossification (Wurst et al., 1994). In this respect, these limb defects suggest alterations of axonal projections, such as retard in limb ingrowth or defasciculation.

Our *in vitro* assays, therefore, might show novel potential rules for En1, beside its direct LMCl axonal repulsion, revealing its possible effect on different and multiple aspects of the formation of neuronal circuits, such as axonal branching and fasciculation.

A further open question that the growth cone collapse assays we employed did not allow to answer consists in determining whether the effect of the En1 protein was exerted on growth cones or on neuronal cell bodies. Possible assays to address this question would be the addition of the En1 protein, alone or in combination with other factors, into different

compartments of the Campenot chamber and the observation of the consequent effect produced on motor neuron growth cones.

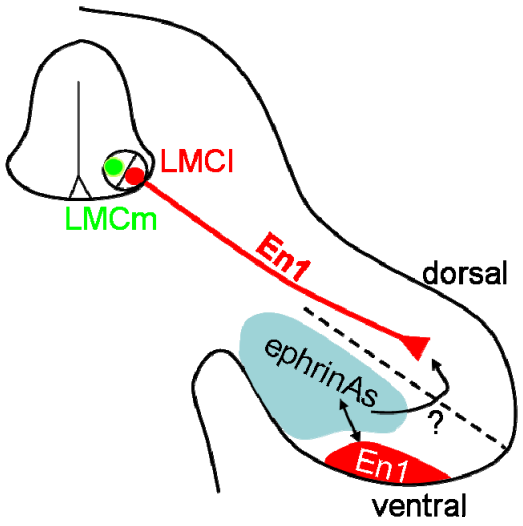

Figure 4.2. Model for a potential cooperation between En1 and ephrinAs in the ventral limb compartment. En1 present in the ventral limb ectoderm could cooperate with other factors expressed in the ventral limb (e.g., ephrinAs) to direct LMCl neurons to the dorsal limb musculature.

Previous studies showed that En can be internalized by the mediation of a 16 amino acids sequence, called Penetratin, and have direct access to the cells, thus eleciting non-cell-autonomous signaling (Derossi et al., 1994; Chatelin et al., 1996). In the *Xenopus* visual system, a soluble gradient of Engrailed attracts nasal and repels temporal axons, respectively. It was demonstrated that the engrailed-induced axonal turning involves internalization by growth cone and induction of local synthesis of proteins that trigger axonal response. These results suggest a similar En1-internalization mechanism to elicit growth cone collapse in the motor system. Indeed a source of soluble En1 could be uptaken in motor axons and trigger growth cone collapse response.

We showed that the growth cone collapse exerted by En1 is specific for LMCl motor neurons. An intriguing question that our data raise is why En1 does not cause the collapse of LMCm neurons. One possible explication is that En1 protein is specifically uptaken and transported only by LMCl neurons. One way to confirm or confute our hypothesis would be add fluorescently labeled En1 protein to dissociated motor neurons and thereby visualize the existence of a specific uptake and retrograde transport mechanism into the axons or cell bodies of LMCl neurons.

Another possibility to explain En1 specific growth cone collapse consists in the fact that En1 could utilize the binding to specific sugars expressed on LMCl neuronal surface to facilitate its internalization. Data arising from the developing visual cortex show that cellular internalization of homeoprotein family members such as *Otx2* is facilitated by the binding to specific sugar epitopes expressed on the cell surface (Sugiyama et al., 2008). En1 might use similar internalization mechanisms binding to sugar epitopes specifically expressed on the surface of LMCl neurons that may facilitate its uptake. It will be therefore helpful to know if and which sugar epitopes are differentially expressed on the surface of LMC neurons and to analyze whether putative En1 binding sites are found in their sequences.

4.3.2 The dorsal-ventral choice of brachial LMC axons is impaired in *En1*$^{-/-}$ mice

Retrograde tracing techniques were used to analyze the fidelity of the dorsal-ventral choice of motor axonal trajectory to the limb. Backfilled brachial motor neuron cell bodies revealed dorsal-ventral guidance defects in *En1* mutant mice. The relatively small percentage of axons that take aberrant decisions at the dorsal-ventral choice point could be explained by the existence of other guidance cues still present at the limb bifurcation point that are able to partially correct the trajectory of motor axons impaired in the absence of *En1*, such as ephrinAs for dorsally projecting neurons, and ephrinBs and Sema3F for neurons projecting in the ventral limb. Another possible explanation can be found in the fact that *En1*$^{-/-}$ embryos show only a partial dorsalization of the limb bud. Indeed, the expression of the dorsal limb markers *Lmx1b* and *Npn-2* does not represent a mirror image of the presence of these markers in the dorsal limb compartment. The uncomplete limb dorsalization is also revealed by the expression of the ventral limb marker *Ebf-2* greatly reduced though not completely absent in mutant mice. Therefore, motor axons at the bifurcation point are only partially misled because of the presence of an only partially dorsalized ventral limb that in part maintains its ventral characteristics that still enable motor neurons to recognize the correct trajectory to innervate the appropriate limb compartment.

The partial limb patterning defect could also explain the fact that not only motor neurons located in the lateral division of the LMC, but also LMCm neuron axonal pathfinding is impaired. LMCm axons are prevented to project ventrally into the limb by the ectopic expression of dorsal limb markers and by the decreased expression of ventral limb markers that enable them to aberrantly invade the dorsal limb musculature. A similar axonal guidance

phenotype, although more severe, was shown in the absence of *Lmx1b*, a transcription factor responsible for the dorsal-ventral patterning in the developing limb (Vogel et al., 1995; Chen et al., 1998). In *Lmx1b*$^{-/-}$ mice, that show complete loss of dorsal limb structures, LMC medial and lateral axons choose a random dorsal-ventral axonal trajectory (Kania et al., 2000; Kania and Jessell, 2003).

4.3.3 Engrailed 1 source responsible for brachial motor neurons projection

The brachial axon misrouting we observed in the *En1*$^{-/-}$ embryos can be caused by the absence of *En1* in different parts of the developing mouse body. To define whether the En1 source responsible for the phenotype is derived from the motor neurons or from the ventral limb ectoderm (Figure 4.3), we took advantage of the tissue-specific ablation of *En1*. We used a mouse-line that expresses Cre-recombinase under the control of the *Hb9* promoter (Arber et al., 1999). This promoter, being active starting at E9.5, allows the ablation of *En1* in all motor neurons, some days before their axons take the dorsal-ventral decision. The analysis of the backfilled LMC cell bodies revealed that the percentage of aberrantly projecting neurons in *En1*^{cond}*:Hb9-Cre* embryos was not statistically significant different from wild type mice.

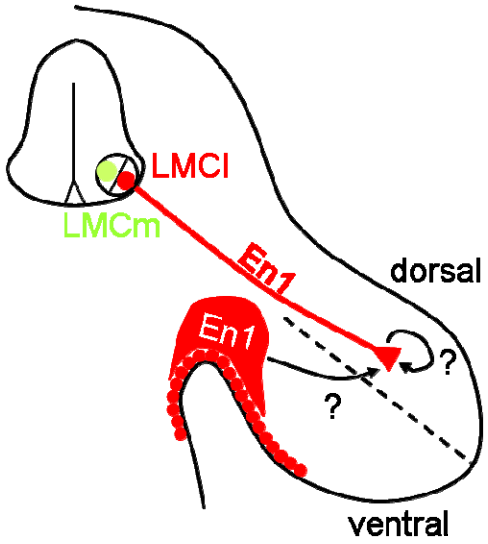

Figure 4.3. Model for potential En1 sources responsible for dorsal-ventral motor axonal pathfinding at the base of the limb. Brachial motor axon wiring can be guided by two different En1 sources acting on motor neuron growth cones: En1 present in the motor axons or En1 expressed in the ventral limb ectoderm.

These experiments demonstrated that the source of En1 responsible for the correct guidance of motor axons is to be found in the ventral limb ectoderm. However, it still needs to be determined whether *En1* is effectively completely ablated in motor neurons, because Cre might be active only in a subset of LMC neurons. In situ hybridization with *En1* RNA-probe on E11.5 *En1*^{cond}*:Hb9-Cre* mutant embryo brachial sections will reveal if *En1* is really ablated in motor neurons. Alternatively, in case of a negative answer, it would be possible to use another mouse-line, where the promoter regulating *Cre*-expression is *Olig-2*. This promoter is expressed already in motor neuron precursors and acts upstream of *Hb9* to determine motor neuron cell fate (Wichterle et al., 2002), giving a further possibility to achieve *En1* ablation in a higher percentage of motor neurons.

Previous data (Loomis et al., 1996) and our own results showing that the limb is dorsalized in *En1*$^{-/-}$ mice both at morphological and molecular levels, respectively, together with the expression pattern of En1 protein in the plexus region (E10.5, Figure 3.9A) and just ventrally of the dorsal-ventral bifurcation point (E11.5, Figure 3.9D), raised another interesting issue for discussion. We reasoned that the dorsal-ventral axonal trajectory errors observed in *En1*$^{-/-}$ embryos could be caused either by limb mispatterning or by the absence of a direct axonal repulsion effect exerted by En1 expressed in the ventral limb ectoderm. To be enable to distinguish between these two potential mechanisms of En1 action further investigation is required. Experiments in the chick consisting in the injection of En1 protein or in the implantation of En1-soaked beads into the dorsal part of the limb will show whether the ectopic presence of En1 in the dorsal limb compartment acts directly on the projection of motor axons. Furthermore, it will be possible to neutralize the effect of extracellular En1 by electroporating single-chain antibodies in the ventral limb compartment (Wizenmann et al., 2009). Electroporating the plasmid for single-chain antibodies into motor neurons will allow for addressing the impact of En1 uptake into motor growth cones.

Immunostaining with EphA4 antibody will allow comparing whether there is a difference in the distribution of the EphA4 receptor on motor axons of manipulated and wild type embryos, thereby determining whether either the ectopic expression of En1 or its neutralization in the dorsal or ventral limb, respectively, caused an effect on the dorsal-ventral choice of motor axon. In case the analysis would reveal motor axon dorsal-ventral choice errors, it will be necessary to determine whether the En1 ectopic expression or neutralization provoked a defect in the patterning of the limb, thereby causing a dorsal-ventral miswiring of motor projections, by performing in situ hybridization with dorsal (e.g., *Lmx1b* and *Npn-2*) and ventral (*Ebf2*) limb markers.

4.4 Outlook

The genome-wide microarray screening for novel guidance cues governing the dorsal-ventral choice of motor and sensory axons at the base of the limb identified potential guidance molecules that mediate the formation of the spinal sensory-motor system, thereby expanding our knowledge of the establishment of neuronal circuitries during development. Investigating the molecular mechanisms regulating these factors and the downstream pathways implicated in axonal guidance are essential to understand how extracellular environmental stimuli are internalized and integrated in neuronal signaling transduction pathways that control cytoskeletal modifications.

The screening we performed revealed the differential expression of molecules implicated in the regulation of different cellular aspects, including extracellular molecules (e.g. *Igfbp5*), receptors (e.g. *Ednrb*) molecules involved in signal transduction (e.g. *G-protein γ3*) and transcription factors (e.g. *En1*). Indeed, the relatively small number of guidance cues identified so far implicates the existence of common regulators that integrate extracellular axon guidance signals and elicit cytoskeletal modification, thereby generating axonal responses. Previuos studies revealed that members of the Rho family GTPases constitute a key link between guidance signals and actin-associated proteins, thereby regulating the assembly and disassembly of actin filaments and regulating axon patterning (Luo and Rho, 2000; Newsome et al., 2000). To this goal, functional characterization of the candidate genes will reveal whether the cues identified here share regulatory networks and use similar molecular mechanisms to govern the guidance of motor and sensory projections towards the limb. For example, it would be interesting to verify whether among the candidates identified by the different screenings there are molecules that regulate the same transduction pathways, whether they interact and whether their interaction is direct or mediated by other factors.

Furthermore, our screening might reveal the first markers to distinguish sensory neurons projecting dorsally and ventrally towards the limb. This discovery, besides revealing for the first time which molecules determine the dorsal-ventral choice of sensory neurons, will also provide a big advantage for future studies, since it will allow to discriminate DRG neurons with regard to their peripheral pathway without the necessity to use retrograde labeling techniques.

The genome-wide screen for cues guiding brachial motor neurons revealed a novel role for Engrailed 1: besides an early role as a transcription factor patterning the forelimb, En1 also acts directly as a repulsive guidance cue for lateral LMCl axons.

The growth cone collapse effect exerted by En1 *in vitro* on LMCl motor axons and its expression in the ventral limb compartment reveal a repulsive role on LMCl axons and, at the same time, let us hypothesize an attractive role on LMCm axons. Possible further experiments to gain more insight into En1 action could be the coculture of COS or HEK cells expressing En1 and backfilled motor neuron explants. This assay will permit to investigate whether wild type LMCl and LMCm axons are repelled and attracted, respectively, from the En1 source and will also allow for analysis of the effect of En1 on *En1*$^{-/-}$ axons. However, on a technical level, it still remains to assess whether it will be possible to obtain enough retrograde labeled axons for the analysis.

Another issue that still needs to be clarified is whether En1 has an indirect action as transcription factor. One possibility to confirm or confute this hypothesis will be to investigate the presence of axon guidance receptors expressed on LMCl axons, such as *EphA4*, comparing its expression in *En1*$^{-/-}$ and wild type embryos. If *En1* acts as a transcription factor regulating this receptor, immunohistochemical analysis will reveal a downregulation of EphA4 expression on *En1*$^{-/-}$ motor axons projecting to the dorsal limb compartment.

4.5 Conclusion

Taken together, this work concurred to extend basic knowledge governing connectivity in the nervous system, contributing to identify molecular factors that regulate the pathfinding of motor and sensory neurons towards their peripheral targets in the dorsal or ventral limb musculature in the vertebrate sensory-motor system.

I showed the feasibility of enriching populations of motor and sensory neurons based on their projection patterns and of assessing differentially expressed genes that govern the dorsal-ventral choice of motor and sensory axons at the base of the limb. To functionally characterize Engrailed 1, a candidate gene in dorsally projecting motor neurons, I combined various cell culture paradigms and analysis of axon pathfinding in *En1* mutant mice. The data obtained reveal that Engrailed 1 repels motor axons that innervate the dorsal limb and is involved in the selection of motor axonal dorsal-ventral trajectories, thus contributing to the topographic organisation of motor projections.

Together, this work extended our understanding of the molecular basis of sensory-motor circuit formation and has the potential to provide valuable information for the

development of treatments useful to re-build the function of the motor-spinal system in case of trauma or neurological diseases.

List of Figures

List of Tables

List of Abbreviations

BCIP	5-bromo-4-chloro-3-indolylphosphate
BDNF	brain-derived neurotrophic factor
BMP	bone morphogenetic protein
bp	base pairs
C. elegans	*Caenorhabditis elegans*
CAM	cell adhesion molecule
Cy2	cyanine-2 (green)
Cy3	cyanine-3 (red)
DCC	deleted in colorectal carcinoma
DIG	digoxigenin
DMSO	dimethylsulfoxide
DNA	deoxyribonucleic acid
dNTP	desoxy-nucleotide-tri-phosphate
DRG	dorsal root ganglion
Drosophila	*Drosophila melanogaster*
E	embryonic day
Edn	endothelin
EH	en homology regions
En	engrailed
f.c.	fold change
FACS	fluorescent activated cell sorting
FITC	fluorescein isothiocyanate (green)
GAP43	growth associated protein 43
GDNF	glial-cell-derived neurotrophic factor
GFP	green fluorescent protein
GO	gene ontology
Hb9	homeobox gene Hb9
HD	homeodomain
IHC	immunohistochemestry
ISH	in situ hybridization
Isl1	LIM homeodomain protein Islet-1
Lim1	LIM homeobox protein 1
LMC	lateral motor column
LMCl	lateral motor column lateral
LMCm	lateral motor column medial
MMC	medial motor column
MMCl	medial motor column lateral
MMCm	medial motor column medial
MN	motor neuron

NES	nuclear export signal
NLS	nuclear localization signal
NGF	nerve growth factor
Npn	neuropilin
NT-3	neurotrophin-3
Plx	plexin
PSA	polysialic acid
PMC	preganglionic motor column
RNA	ribonucleic acid
Robo	roundabout
Sema	semaphorin
Shh	sonic hedgehog
TF	transcription factor
TrK	tyrosine receptor kinase
VEGF	vascular endothelial growth factor
Xenopus	*Xenopus laevis*

Bibliography

Adams, R. H., M. Lohrum, A. Klostermann, H. Betz and A. W. Puschel (1997). "The chemorepulsive activity of secreted semaphorins is regulated by furin-dependent proteolytic processing." EMBO J **16**(20): 6077-6086.

Arber, S., B. Han, M. Mendelsohn, M. Smith, T. M. Jessell and S. Sockanathan (1999). "Requirement for the homeobox gene Hb9 in the consolidation of motor neuron identity." Neuron **23**(4): 659-674.

Arber, S., D. R. Ladle, J. H. Lin, E. Frank and T. M. Jessell (2000). "ETS gene Er81 controls the formation of functional connections between group Ia sensory afferents and motor neurons." Cell **101**(5): 485-498.

Arlotta, P., B. J. Molyneaux, J. Chen, J. Inoue, R. Kominami and J. D. Macklis (2005). "Neuronal subtype-specific genes that control corticospinal motor neuron development in vivo." Neuron **45**(2): 207-221.

Bagnard, D., M. Lohrum, D. Uziel, A. W. Puschel and J. Bolz (1998). "Semaphorins act as attractive and repulsive guidance signals during the development of cortical projections." Development **125**(24): 5043-5053.

Battye, R., A. Stevens and J. R. Jacobs (1999). "Axon repulsion from the midline of the Drosophila CNS requires slit function." Development **126**(11): 2475-2481.

Benjamini, Y. and Y. Hochberg (1995). "Controlling the false discovery rate: a practical and powerful approach to multiple testing." Journal of the Royal Statistical Society Series B **57**: 289-300.

Bibel, M. and Y. A. Barde (2000). "Neurotrophins: key regulators of cell fate and cell shape in the vertebrate nervous system." Genes Dev **14**(23): 2919-2937.

Bourikas, D., V. Pekarik, T. Baeriswyl, A. Grunditz, R. Sadhu, M. Nardo and E. T. Stoeckli (2005). "Sonic hedgehog guides commissural axons along the longitudinal axis of the spinal cord." Nat Neurosci **8**(3): 297-304.

Brunet, I., A. A. Di Nardo, L. Sonnier, M. Beurdeley and A. Prochiantz (2007). "The topological role of homeoproteins in the developing central nervous system." Trends Neurosci **30**(6): 260-267.

Brunet, I., C. Weinl, M. Piper, A. Trembleau, M. Volovitch, W. Harris, A. Prochiantz and C. Holt (2005). "The transcription factor Engrailed-2 guides retinal axons." Nature **438**(7064): 94-98.

Burrill, J. D., L. Moran, M. D. Goulding and H. Saueressig (1997). "PAX2 is expressed in multiple spinal cord interneurons, including a population of EN1+ interneurons that require PAX6 for their development." Development **124**(22): 4493-4503.

Campbell, D. S. and C. E. Holt (2001). "Chemotropic responses of retinal growth cones mediated by rapid local protein synthesis and degradation." Neuron **32**(6): 1013-1026.

Charron, F., E. Stein, J. Jeong, A. P. McMahon and M. Tessier-Lavigne (2003). "The morphogen sonic hedgehog is an axonal chemoattractant that collaborates with netrin-1 in midline axon guidance." Cell **113**(1): 11-23.

Chatelin, L., M. Volovitch, A. H. Joliot, F. Perez and A. Prochiantz (1996). "Transcription factor hoxa-5 is taken up by cells in culture and conveyed to their nuclei." Mech Dev **55**(2): 111-117.

Chedotal, A., J. A. Del Rio, M. Ruiz, Z. He, V. Borrell, F. de Castro, F. Ezan, C. S. Goodman, M. Tessier-Lavigne, C. Sotelo and E. Soriano (1998). "Semaphorins III and IV repel hippocampal axons via two distinct receptors." Development **125**(21): 4313-4323.

Chen, H., Y. Lun, D. Ovchinnikov, H. Kokubo, K. C. Oberg, C. V. Pepicelli, L. Gan, B. Lee and R. L. Johnson (1998). "Limb and kidney defects in Lmx1b mutant mice suggest an involvement of LMX1B in human nail patella syndrome." Nat Genet **19**(1): 51-55.

Cheng, H. J., A. Bagri, A. Yaron, E. Stein, S. J. Pleasure and M. Tessier-Lavigne (2001). "Plexin-A3 mediates semaphorin signaling and regulates the development of hippocampal axonal projections." Neuron **32**(2): 249-263.

Cheng, H. J., M. Nakamoto, A. D. Bergemann and J. G. Flanagan (1995). "Complementary gradients in expression and binding of ELF-1 and Mek4 in development of the topographic retinotectal projection map." Cell **82**(3): 371-381.

Chisholm, A. and M. Tessier-Lavigne (1999). "Conservation and divergence of axon guidance mechanisms." Curr Opin Neurobiol **9**(5): 603-615.

Colamarino, S. A. and M. Tessier-Lavigne (1995). "The axonal chemoattractant netrin-1 is also a chemorepellent for trochlear motor axons." Cell **81**(4): 621-629.

Corradi, A., L. Croci, V. Broccoli, S. Zecchini, S. Previtali, W. Wurst, S. Amadio, R. Maggi, A. Quattrini and G. G. Consalez (2003). "Hypogonadotropic hypogonadism and peripheral neuropathy in Ebf2-null mice." Development **130**(2): 401-410.

Cosgaya, J. M., A. Aranda, J. Cruces and E. Martin-Blanco (1998). "Neuronal differentiation of PC12 cells induced by engrailed homeodomain is DNA-binding specific and independent of MAP kinases." J Cell Sci **111 (Pt 16)**: 2377-2384.

Covault, J. and J. R. Sanes (1986). "Distribution of N-CAM in synaptic and extrasynaptic portions of developing and adult skeletal muscle." J Cell Biol **102**(3): 716-730.

Culotti, J. G. and A. L. Kolodkin (1996). "Functions of netrins and semaphorins in axon guidance." Curr Opin Neurobiol **6**(1): 81-88.

Cygan, J. A., R. L. Johnson and A. P. McMahon (1997). "Novel regulatory interactions revealed by studies of murine limb pattern in Wnt-7a and En-1 mutants." Development **124**(24): 5021-5032.

Dalla Torre di Sanguinetto, S. A., J. S. Dasen and S. Arber (2008). "Transcriptional mechanisms controlling motor neuron diversity and connectivity." Curr Opin Neurobiol **18**(1): 36-43.

Darnell, D. K. and G. C. Schoenwolf (1997). "Vertical induction of engrailed-2 and other region-specific markers in the early chick embryo." Dev Dyn **209**(1): 45-58.

Davidson, D., E. Graham, C. Sime and R. Hill (1988). "A gene with sequence similarity to Drosophila engrailed is expressed during the development of the neural tube and vertebrae in the mouse." Development **104**(2): 305-316.

Davis, C. A., D. P. Holmyard, K. J. Millen and A. L. Joyner (1991). "Examining pattern formation in mouse, chicken and frog embryos with an En-specific antiserum." Development **111**(2): 287-298.

Davis, C. A. and A. L. Joyner (1988). "Expression patterns of the homeo box-containing genes En-1 and En-2 and the proto-oncogene int-1 diverge during mouse development." Genes Dev **2**(12B): 1736-1744.

Deiner, M. S., T. E. Kennedy, A. Fazeli, T. Serafini, M. Tessier-Lavigne and D. W. Sretavan (1997). "Netrin-1 and DCC mediate axon guidance locally at the optic disc: loss of function leads to optic nerve hypoplasia." Neuron **19**(3): 575-589.

Derossi, D., A. H. Joliot, G. Chassaing and A. Prochiantz (1994). "The third helix of the Antennapedia homeodomain translocates through biological membranes." J Biol Chem **269**(14): 10444-10450.

Desplan, C., J. Theis and P. H. O'Farrell (1985). "The Drosophila developmental gene, engrailed, encodes a sequence-specific DNA binding activity." Nature **318**(6047): 630-635.

Dickson, B. J. (2002). "Molecular mechanisms of axon guidance." Science **298**(5600): 1959-1964.

Dickson, B. J. (2005). "Wnts send axons up and down the spinal cord." Nat Neurosci **8**(9): 1130-1132.

Dotti, C. G., R. G. Parton and K. Simons (1991). "Polarized sorting of glypiated proteins in hippocampal neurons." Nature **349**(6305): 158-161.

Dotti, C. G. and K. Simons (1990). "Polarized sorting of viral glycoproteins to the axon and dendrites of hippocampal neurons in culture." Cell **62**(1): 63-72.

Drescher, U., C. Kremoser, C. Handwerker, J. Loschinger, M. Noda and F. Bonhoeffer (1995). "In vitro guidance of retinal ganglion cell axons by RAGS, a 25 kDa tectal protein related to ligands for Eph receptor tyrosine kinases." Cell **82**(3): 359-370.

Eberhart, J., J. Barr, S. O'Connell, A. Flagg, M. E. Swartz, K. S. Cramer, K. W. Tosney, E. B. Pasquale and C. E. Krull (2004). "Ephrin-A5 exerts positive or inhibitory effects on distinct subsets of EphA4-positive motor neurons." J Neurosci **24**(5): 1070-1078.

Eberhart, J., M. E. Swartz, S. A. Koblar, E. B. Pasquale and C. E. Krull (2002). "EphA4 constitutes a population-specific guidance cue for motor neurons." Dev Biol **247**(1): 89-101.

Ericson, J., P. Rashbass, A. Schedl, S. Brenner-Morton, A. Kawakami, V. van Heyningen, T. M. Jessell and J. Briscoe (1997). "Pax6 controls progenitor cell identity and neuronal fate in response to graded Shh signaling." Cell **90**(1): 169-180.

Fitzgerald, M., G. C. Kwiat, J. Middleton and A. Pini (1993). "Ventral spinal cord inhibition of neurite outgrowth from embryonic rat dorsal root ganglia." Development **117**(4): 1377-1384.

Fricke, C., J. S. Lee, S. Geiger-Rudolph, F. Bonhoeffer and C. B. Chien (2001). "astray, a zebrafish roundabout homolog required for retinal axon guidance." Science **292**(5516): 507-510.

Gardner, C. A., D. K. Darnell, S. J. Poole, C. P. Ordahl and K. F. Barald (1988). "Expression of an engrailed-like gene during development of the early embryonic chick nervous system." J Neurosci Res **21**(2-4): 426-437.

Gehring, W. J. (1985). "The homeo box: a key to the understanding of development?" Cell **40**(1): 3-5.

Gehring, W. J., Y. Q. Qian, M. Billeter, K. Furukubo-Tokunaga, A. F. Schier, D. Resendez-Perez, M. Affolter, G. Otting and K. Wuthrich (1994). "Homeodomain-DNA recognition." Cell **78**(2): 211-223.

Giniger, E. (2002). "How do Rho family GTPases direct axon growth and guidance? A proposal relating signaling pathways to growth cone mechanics." Differentiation **70**(8): 385-396.

Giraldez, T., T. E. Hughes and F. J. Sigworth (2005). "Generation of functional fluorescent BK channels by random insertion of GFP variants." J Gen Physiol **126**(5): 429-438.

Gu, C., E. R. Rodriguez, D. V. Reimert, T. Shu, B. Fritzsch, L. J. Richards, A. L. Kolodkin and D. D. Ginty (2003). "Neuropilin-1 conveys semaphorin and VEGF signaling during neural and cardiovascular development." Dev Cell **5**(1): 45-57.

Guimera, J., D. V. Weisenhorn and W. Wurst (2006). "Megane/Heslike is required for normal GABAergic differentiation in the mouse superior colliculus." Development **133**(19): 3847-3857.

Hamburger, V. (1993). "The history of the discovery of the nerve growth factor." J Neurobiol **24**(7): 893-897.

Hanks, M., W. Wurst, L. Anson-Cartwright, A. B. Auerbach and A. L. Joyner (1995). "Rescue of the En-1 mutant phenotype by replacement of En-1 with En-2." Science **269**(5224): 679-682.

Hanks, M. C., C. A. Loomis, E. Harris, C. X. Tong, L. Anson-Cartwright, A. Auerbach and A. Joyner (1998). "Drosophila engrailed can substitute for mouse Engrailed1 function in mid-hindbrain, but not limb development." Development **125**(22): 4521-4530.

Harris, R., L. M. Sabatelli and M. A. Seeger (1996). "Guidance cues at the Drosophila CNS midline: identification and characterization of two Drosophila Netrin/UNC-6 homologs." Neuron **17**(2): 217-228.

He, Z. and M. Tessier-Lavigne (1997). "Neuropilin is a receptor for the axonal chemorepellent Semaphorin III." Cell **90**(4): 739-751.

Hedgecock, E. M., J. G. Culotti and D. H. Hall (1990). "The unc-5, unc-6, and unc-40 genes guide circumferential migrations of pioneer axons and mesodermal cells on the epidermis in C. elegans." Neuron **4**(1): 61-85.

Helmbacher, F., S. Schneider-Maunoury, P. Topilko, L. Tiret and P. Charnay (2000). "Targeting of the EphA4 tyrosine kinase receptor affects dorsal/ventral pathfinding of limb motor axons." Development **127**(15): 3313-3324.

Henkemeyer, M., D. Orioli, J. T. Henderson, T. M. Saxton, J. Roder, T. Pawson and R. Klein (1996). "Nuk controls pathfinding of commissural axons in the mammalian central nervous system." Cell **86**(1): 35-46.

Higashijima, S., M. A. Masino, G. Mandel and J. R. Fetcho (2004). "Engrailed-1 expression marks a primitive class of inhibitory spinal interneuron." J Neurosci **24**(25): 5827-5839.

Hindges, R., T. McLaughlin, N. Genoud, M. Henkemeyer and D. D. O'Leary (2002). "EphB forward signaling controls directional branch extension and arborization required for dorsal-ventral retinotopic mapping." Neuron **35**(3): 475-487.

Hobert, O., T. D'Alberti, Y. Liu and G. Ruvkun (1998). "Control of neural development and function in a thermoregulatory network by the LIM homeobox gene lin-11." J Neurosci **18**(6): 2084-2096.

Holland, L. Z., M. Kene, N. A. Williams and N. D. Holland (1997). "Sequence and embryonic expression of the amphioxus engrailed gene (AmphiEn): the metameric pattern of transcription resembles that of its segment-polarity homolog in Drosophila." Development **124**(9): 1723-1732.

Huang, E. J. and L. F. Reichardt (2001). "Neurotrophins: roles in neuronal development and function." Annu Rev Neurosci **24**: 677-736.

Huber, A. B., A. Kania, T. S. Tran, C. Gu, N. De Marco Garcia, I. Lieberam, D. Johnson, T. M. Jessell, D. D. Ginty and A. L. Kolodkin (2005). "Distinct roles for secreted semaphorin signaling in spinal motor axon guidance." Neuron **48**(6): 949-964.

Huber, A. B., A. L. Kolodkin, D. D. Ginty and J. F. Cloutier (2003). "Signaling at the growth cone: ligand-receptor complexes and the control of axon growth and guidance." Annu Rev Neurosci **26**: 509-563.

Huettl, R. E., H. Soellner, E. Bianchi, B. G. Novitch and A. B. Huber (submitted). "Npn-1-mediated axon-axon interactions differentially control sensory and motor innervation of the limb." PLoS Biology

Jessell, T. M. (2000). "Neuronal specification in the spinal cord: inductive signals and transcriptional codes." Nat Rev Genet **1**(1): 20-29.

Joliot, A., A. Maizel, D. Rosenberg, A. Trembleau, S. Dupas, M. Volovitch and A. Prochiantz (1998). "Identification of a signal sequence necessary for the unconventional secretion of Engrailed homeoprotein." Curr Biol **8**(15): 856-863.

Joliot, A., A. Trembleau, G. Raposo, S. Calvet, M. Volovitch and A. Prochiantz (1997). "Association of Engrailed homeoproteins with vesicles presenting caveolae-like properties." Development **124**(10): 1865-1875.

Joyner, A. L. (1996). "Engrailed, Wnt and Pax genes regulate midbrain--hindbrain development." Trends Genet **12**(1): 15-20.

Joyner, A. L., K. Herrup, B. A. Auerbach, C. A. Davis and J. Rossant (1991). "Subtle cerebellar phenotype in mice homozygous for a targeted deletion of the En-2 homeobox." Science **251**(4998): 1239-1243.

Joyner, A. L., T. Kornberg, K. G. Coleman, D. R. Cox and G. R. Martin (1985). "Expression during embryogenesis of a mouse gene with sequence homology to the Drosophila engrailed gene." Cell **43**(1): 29-37.

Joyner, A. L. and G. R. Martin (1987). "En-1 and En-2, two mouse genes with sequence homology to the Drosophila engrailed gene: expression during embryogenesis." Genes Dev **1**(1): 29-38.

Kania, A. and T. M. Jessell (2003). "Topographic motor projections in the limb imposed by LIM homeodomain protein regulation of ephrin-A:EphA interactions." Neuron **38**(4): 581-596.

Kania, A., R. L. Johnson and T. M. Jessell (2000). "Coordinate roles for LIM homeobox genes in directing the dorsoventral trajectory of motor axons in the vertebrate limb." Cell **102**(2): 161-173.

Kaplan, D. R., B. L. Hempstead, D. Martin-Zanca, M. V. Chao and L. F. Parada (1991). "The trk proto-oncogene product: a signal transducing receptor for nerve growth factor." Science **252**(5005): 554-558.

Kidd, T., K. S. Bland and C. S. Goodman (1999). "Slit is the midline repellent for the robo receptor in Drosophila." Cell **96**(6): 785-794.

Klein, R., S. Q. Jing, V. Nanduri, E. O'Rourke and M. Barbacid (1991). "The trk proto-oncogene encodes a receptor for nerve growth factor." Cell **65**(1): 189-197.

Knoll, B. and U. Drescher (2002). "Ephrin-As as receptors in topographic projections." Trends Neurosci **25**(3): 145-149.

Knoll, B., K. Zarbalis, W. Wurst and U. Drescher (2001). "A role for the EphA family in the topographic targeting of vomeronasal axons." Development **128**(6): 895-906.

Kobayashi, H., A. M. Koppel, Y. Luo and J. A. Raper (1997). "A role for collapsin-1 in olfactory and cranial sensory axon guidance." J Neurosci **17**(21): 8339-8352.

Kolodkin, A. L., D. V. Levengood, E. G. Rowe, Y. T. Tai, R. J. Giger and D. D. Ginty (1997). "Neuropilin is a semaphorin III receptor." Cell **90**(4): 753-762.

Kolodkin, A. L., D. J. Matthes, T. P. O'Connor, N. H. Patel, A. Admon, D. Bentley and C. S. Goodman (1992). "Fasciclin IV: sequence, expression, and function during growth cone guidance in the grasshopper embryo." Neuron **9**(5): 831-845.

Koppel, A. M., L. Feiner, H. Kobayashi and J. A. Raper (1997). "A 70 amino acid region within the semaphorin domain activates specific cellular response of semaphorin family members." Neuron **19**(3): 531-537.

Kornberg, T. (1981). "Engrailed: a gene controlling compartment and segment formation in Drosophila." Proc Natl Acad Sci U S A **78**(2): 1095-1099.

Kramer, E. R., L. Knott, F. Su, E. Dessaud, C. E. Krull, F. Helmbacher and R. Klein (2006). "Cooperation between GDNF/Ret and ephrinA/EphA4 signals for motor-axon pathway selection in the limb." Neuron **50**(1): 35-47.

Krawchuk, D. and A. Kania (2008). "Identification of genes controlled by LMX1B in the developing mouse limb bud." Dev Dyn **237**(4): 1183-1192.

Kullander, K. and R. Klein (2002). "Mechanisms and functions of Eph and ephrin signalling." Nat Rev Mol Cell Biol **3**(7): 475-486.

Kullander, K., N. K. Mather, F. Diella, M. Dottori, A. W. Boyd and R. Klein (2001). "Kinase-dependent and kinase-independent functions of EphA4 receptors in major axon tract formation in vivo." Neuron **29**(1): 73-84.

Lance-Jones, C., N. Omelchenko, A. Bailis, S. Lynch and K. Sharma (2001). "Hoxd10 induction and regionalization in the developing lumbosacral spinal cord." Development **128**(12): 2255-2268.

Landmesser, L., L. Dahm, K. Schultz and U. Rutishauser (1988). "Distinct roles for adhesion molecules during innervation of embryonic chick muscle." Dev Biol **130**(2): 645-670.

Landmesser, L. and M. G. Honig (1986). "Altered sensory projections in the chick hind limb following the early removal of motoneurons." Dev Biol **118**(2): 511-531.

Landmesser, L. T. (2001). "The acquisition of motoneuron subtype identity and motor circuit formation." Int J Dev Neurosci **19**(2): 175-182.

Lawrence, P. A. and G. Struhl (1982). "Further studies of the engrailed phenotype in Drosophila." EMBO J **1**(7): 827-833.

Lee, K. J. and T. M. Jessel (1999). "The specification of dorsal cell fates in the vertebrate central nervous system." Annu. Rev. Neurosci. **22**: 261-294.

Lesaffre, B., A. Joliot, A. Prochiantz and M. Volovitch (2007). "Direct non-cell autonomous Pax6 activity regulates eye development in the zebrafish." Neural Dev **2**: 2.

Liu, Y., J. Shi, C. C. Lu, Z. B. Wang, A. I. Lyuksyutova, X. J. Song and Y. Zou (2005). "Ryk-mediated Wnt repulsion regulates posterior-directed growth of corticospinal tract." Nat Neurosci **8**(9): 1151-1159.

Logan, C., M. C. Hanks, S. Noble-Topham, D. Nallainathan, N. J. Provart and A. L. Joyner (1992). "Cloning and sequence comparison of the mouse, human, and chicken engrailed genes reveal potential functional domains and regulatory regions." Dev Genet **13**(5): 345-358.

Loomis, C. A., E. Harris, J. Michaud, W. Wurst, M. Hanks and A. L. Joyner (1996). "The mouse Engrailed-1 gene and ventral limb patterning." Nature **382**(6589): 360-363.

Loomis, C. A., R. A. Kimmel, C. X. Tong, J. Michaud and A. L. Joyner (1998). "Analysis of the genetic pathway leading to formation of ectopic apical ectodermal ridges in mouse Engrailed-1 mutant limbs." Development **125**(6): 1137-1148.

Lowe, C. J. and G. A. Wray (1997). "Radical alterations in the roles of homeobox genes during echinoderm evolution." Nature **389**(6652): 718-721.

Luo and L. Rho (2000). "GTPases in neuronal morphogenesis." Nature Rev. Neuroscience **1**: 173-180.

Luo, Y., D. Raible and J. A. Raper (1993). "Collapsin: a protein in brain that induces the collapse and paralysis of neuronal growth cones." Cell **75**(2): 217-227.

Luria, V., D. Krawchuk, T. M. Jessell, E. Laufer and A. Kania (2008). "Specification of motor axon trajectory by ephrin-B:EphB signaling: symmetrical control of axonal patterning in the developing limb." Neuron **60**(6): 1039-1053.

Maizel, A., M. Tassetto, O. Filhol, C. Cochet, A. Prochiantz and A. Joliot (2002). "Engrailed homeoprotein secretion is a regulated process." Development **129**(15): 3545-3553.

Makita, T., H. M. Sucov, C. E. Gariepy, M. Yanagisawa and D. D. Ginty (2008). "Endothelins are vascular-derived axonal guidance cues for developing sympathetic neurons." Nature **452**(7188): 759-763.

Mann, F., S. Ray, W. Harris and C. Holt (2002). "Topographic mapping in dorsoventral axis of the Xenopus retinotectal system depends on signaling through ephrin-B ligands." Neuron **35**(3): 461-473.

Marti, E., D. A. Bumcrot, R. Takada and A. P. McMahon (1995). "Requirement of 19K form of Sonic hedgehog for induction of distinct ventral cell types in CNS explants." Nature **375**(6529): 322-325.

Matise, M. P. and A. L. Joyner (1997). "Expression patterns of developmental control genes in normal and Engrailed-1 mutant mouse spinal cord reveal early diversity in developing interneurons." J Neurosci **17**(20): 7805-7816.

Messersmith, E. K., E. D. Leonardo, C. J. Shatz, M. Tessier-Lavigne, C. S. Goodman and A. L. Kolodkin (1995). "Semaphorin III can function as a selective chemorepellent to pattern sensory projections in the spinal cord." Neuron **14**(5): 949-959.

Millen, K. J., W. Wurst, K. Herrup and A. L. Joyner (1994). "Abnormal embryonic cerebellar development and patterning of postnatal foliation in two mouse Engrailed-2 mutants." Development **120**(3): 695-706.

Mitchell, K. J., J. L. Doyle, T. Serafini, T. E. Kennedy, M. Tessier-Lavigne, C. S. Goodman and B. J. Dickson (1996). "Genetic analysis of Netrin genes in Drosophila: Netrins guide CNS commissural axons and peripheral motor axons." Neuron **17**(2): 203-215.

Moran-Rivard, L., T. Kagawa, H. Saueressig, M. K. Gross, J. Burrill and M. Goulding (2001). "Evx1 is a postmitotic determinant of v0 interneuron identity in the spinal cord." Neuron **29**(2): 385-399.

Morgan, R. (2006). "Engrailed: complexity and economy of a multi-functional transcription factor." FEBS Lett **580**(11): 2531-2533.

Nedelec, S., I. Foucher, I. Brunet, C. Bouillot, A. Prochiantz and A. Trembleau (2004). "Emx2 homeodomain transcription factor interacts with eukaryotic translation initiation factor 4E (eIF4E) in the axons of olfactory sensory neurons." Proc Natl Acad Sci U S A **101**(29): 10815-10820.

Newsome, T. P., S. Schmidt, G. Dietzl, K. Keleman, B. Asling, A. Debant and B. J. Dickson (2000). "Trio combines with dock to regulate Pak activity during photoreceptor axon pathfinding in Drosophila." Cell **101**(3): 283-294.

Nobes, C. D. and A. Hall (1995). "Rho, rac, and cdc42 GTPases regulate the assembly of multimolecular focal complexes associated with actin stress fibers, lamellipodia, and filopodia." Cell **81**(1): 53-62.

Okamoto, H. and J. Y. Kuwada (1991). "Outgrowth by fin motor axons in wildtype and a finless mutant of the Japanese medaka fish." Dev Biol **146**(1): 49-61.

Patel, N. H., B. Schafer, C. S. Goodman and R. Holmgren (1989). "The role of segment polarity genes during Drosophila neurogenesis." Genes Dev **3**(6): 890-904.

Patel, T. D., A. Jackman, F. L. Rice, J. Kucera and W. D. Snider (2000). "Development of sensory neurons in the absence of NGF/TrkA signaling in vivo." Neuron **25**(2): 345-357.

Peltenburg, L. T. and C. Murre (1997). "Specific residues in the Pbx homeodomain differentially modulate the DNA-binding activity of Hox and Engrailed proteins." Development **124**(5): 1089-1098.

Pierani, A., L. Moran-Rivard, M. J. Sunshine, D. R. Littman, M. Goulding and T. M. Jessell (2001). "Control of interneuron fate in the developing spinal cord by the progenitor homeodomain protein Dbx1." Neuron **29**(2): 367-384.

Pinter, R. and R. Hindges (2010). "Perturbations of microRNA function in mouse dicer mutants produce retinal defects and lead to aberrant axon pathfinding at the optic chiasm." PLoS One **5**(4): e10021.

Plump, A. S., L. Erskine, C. Sabatier, K. Brose, C. J. Epstein, C. S. Goodman, C. A. Mason and M. Tessier-Lavigne (2002). "Slit1 and Slit2 cooperate to prevent premature midline crossing of retinal axons in the mouse visual system." Neuron **33**(2): 219-232.

Prochiantz, A. and A. Joliot (2003). "Can transcription factors function as cell-cell signalling molecules?" Nat Rev Mol Cell Biol **4**(10): 814-819.

Przyborski, S. A., B. B. Knowles and S. L. Ackerman (1998). "Embryonic phenotype of Unc5h3 mutant mice suggests chemorepulsion during the formation of the rostral cerebellar boundary." Development **125**(1): 41-50.

Renzi, M. J., T. L. Wexler and J. A. Raper (2000). "Olfactory sensory axons expressing a dominant-negative semaphorin receptor enter the CNS early and overshoot their target." Neuron **28**(2): 437-447.

Riddle, R. D., M. Ensini, C. Nelson, T. Tsuchida, T. M. Jessell and C. Tabin (1995). "Induction of the LIM homeobox gene Lmx1 by WNT7a establishes dorsoventral pattern in the vertebrate limb." Cell **83**(4): 631-640.

Ringstedt, T., J. E. Braisted, K. Brose, T. Kidd, C. Goodman, M. Tessier-Lavigne and D. D. O'Leary (2000). "Slit inhibition of retinal axon growth and its role in retinal axon pathfinding and innervation patterns in the diencephalon." J Neurosci **20**(13): 4983-4991.

Roelink, H., J. A. Porter, C. Chiang, Y. Tanabe, D. T. Chang, P. A. Beachy and T. M. Jessell (1995). "Floor plate and motor neuron induction by different concentrations of the amino-terminal cleavage product of sonic hedgehog autoproteolysis." Cell **81**(3): 445-455.

Rutishauser, U. and T. M. Jessell (1988). "Cell adhesion molecules in vertebrate neural development." Physiol Rev **68**(3): 819-857.

Saueressig, H., J. Burrill and M. Goulding (1999). "Engrailed-1 and netrin-1 regulate axon pathfinding by association interneurons that project to motor neurons." Development **126**(19): 4201-4212.

Schmitt, A. M., J. Shi, A. M. Wolf, C. C. Lu, L. A. King and Y. Zou (2006). "Wnt-Ryk signalling mediates medial-lateral retinotectal topographic mapping." Nature **439**(7072): 31-37.

Serafini, T., S. A. Colamarino, E. D. Leonardo, H. Wang, R. Beddington, W. C. Skarnes and M. Tessier-Lavigne (1996). "Netrin-1 is required for commissural axon guidance in the developing vertebrate nervous system." Cell **87**(6): 1001-1014.

Sgaier, S. K., Z. Lao, M. P. Villanueva, F. Berenshteyn, D. Stephen, R. K. Turnbull and A. L. Joyner (2007). "Genetic subdivision of the tectum and cerebellum into functionally related regions based on differential sensitivity to engrailed proteins." Development **134**(12): 2325-2335.

Sharma, K. and J. C. Belmonte (2001). "Development of the limb neuromuscular system." Curr. Opin. Cell Biol. **13**: 204-210.

Shepherd, I., Y. Luo, J. A. Raper and S. Chang (1996). "The distribution of collapsin-1 mRNA in the developing chick nervous system." Dev Biol **173**(1): 185-199.

Shepherd, I. T., Y. Luo, F. Lefcort, L. F. Reichardt and J. A. Raper (1997). "A sensory axon repellent secreted from ventral spinal cord explants is neutralized by antibodies raised against collapsin-1." Development **124**(7): 1377-1385.

Shirasaki, R. and S. L. Pfaff (2002). "Transcriptional codes and the control of neuronal identity." Annu Rev Neurosci **25**: 251-281.

Smith, S. J. (1988). "Neuronal cytomechanics: the actin-based motility of growth cones." Science **242**(4879): 708-715.

Song, H. and M. Poo (2001). "The cell biology of neuronal navigation." Nat Cell Biol **3**(3): E81-88.

Sonnier, L., G. Le Pen, A. Hartmann, J. C. Bizot, F. Trovero, M. O. Krebs and A. Prochiantz (2007). "Progressive loss of dopaminergic neurons in the ventral midbrain of adult mice heterozygote for Engrailed1." J Neurosci **27**(5): 1063-1071.

Sugiyama, S., A. A. Di Nardo, S. Aizawa, I. Matsuo, M. Volovitch, A. Prochiantz and T. K. Hensch (2008). "Experience-dependent transfer of Otx2 homeoprotein into the visual cortex activates postnatal plasticity." Cell **134**(3): 508-520.

Tamagnone, L., S. Artigiani, H. Chen, Z. He, G. I. Ming, H. Song, A. Chedotal, M. L. Winberg, C. S. Goodman, M. Poo, M. Tessier-Lavigne and P. M. Comoglio (1999). "Plexins are a large family of receptors for transmembrane, secreted, and GPI-anchored semaphorins in vertebrates." Cell **99**(1): 71-80.

Tang, J., L. Landmesser and U. Rutishauser (1992). "Polysialic acid influences specific pathfinding by avian motoneurons." Neuron **8**(6): 1031-1044.

Tang, J., U. Rutishauser and L. Landmesser (1994). "Polysialic acid regulates growth cone behavior during sorting of motor axons in the plexus region." Neuron **13**(2): 405-414.

Taniguchi, M., S. Yuasa, H. Fujisawa, I. Naruse, S. Saga, M. Mishina and T. Yagi (1997). "Disruption of semaphorin III/D gene causes severe abnormality in peripheral nerve projection." Neuron **19**(3): 519-530.

Tapon, N. and A. Hall (1997). "Rho, Rac and Cdc42 GTPases regulate the organization of the actin cytoskeleton." Curr Opin Cell Biol **9**(1): 86-92.

Tessier-Lavigne, M. and C. S. Goodman (1996). "The molecular biology of axon guidance." Science **274**(5290): 1123-1133.

Tessier-Lavigne, M., M. Placzek, A. G. Lumsden, J. Dodd and T. M. Jessell (1988). "Chemotropic guidance of developing axons in the mammalian central nervous system." Nature **336**(6201): 775-778.

Thor, S., S. G. Andersson, A. Tomlinson and J. B. Thomas (1999). "A LIM-homeodomain combinatorial code for motor-neuron pathway selection." Nature **397**(6714): 76-80.

Tietjen, I., J. Rihel and C. G. Dulac (2005). "Single-cell transcriptional profiles and spatial patterning of the mammalian olfactory epithelium." Int J Dev Biol **49**(2-3): 201-207.

Tolkunova, E. N., M. Fujioka, M. Kobayashi, D. Deka and J. B. Jaynes (1998). "Two distinct types of repression domain in engrailed: one interacts with the groucho corepressor and is preferentially active on integrated target genes." Mol Cell Biol **18**(5): 2804-2814.

Tosney, K. W. and L. T. Landmesser (1985). "Development of the major pathways for neurite outgrowth in the chick hindlimb." Dev Biol **109**(1): 193-214.

Tosney, K. W., M. Watanabe, L. Landmesser and U. Rutishauser (1986). "The distribution of NCAM in the chick hindlimb during axon outgrowth and synaptogenesis." Dev Biol **114**(2): 437-452.

Tsuchida, T., M. Ensini, S. B. Morton, M. Baldassare, T. Edlund, T. M. Jessell and S. L. Pfaff (1994). "Topographic organization of embryonic motor neurons defined by expression of LIM homeobox genes." Cell **79**(6): 957-970.

van Dijk, M. A. and C. Murre (1994). "extradenticle raises the DNA binding specificity of homeotic selector gene products." Cell **78**(4): 617-624.

Varela-Echavarria, A., A. Tucker, A. W. Puschel and S. Guthrie (1997). "Motor axon subpopulations respond differentially to the chemorepellents netrin-1 and semaphorin D." Neuron **18**(2): 193-207.

Vignal, E., M. De Toledo, F. Comunale, A. Ladopoulou, C. Gauthier-Rouviere, A. Blangy and P. Fort (2000). "Characterization of TCL, a new GTPase of the rho family related to TC10 andCcdc42." J Biol Chem **275**(46): 36457-36464.

Vogel, A., C. Rodriguez, W. Warnken and J. C. Izpisua Belmonte (1995). "Dorsal cell fate specified by chick Lmx1 during vertebrate limb development." Nature **378**(6558): 716-720.

Wang, K. H., K. Brose, D. Arnott, T. Kidd, C. S. Goodman, W. Henzel and M. Tessier-Lavigne (1999). "Biochemical purification of a mammalian slit protein as a positive regulator of sensory axon elongation and branching." Cell **96**(6): 771-784.

Watanabe, K., N. Tamamaki, T. Furuta, S. L. Ackerman, K. Ikenaka and K. Ono (2006). "Dorsally derived netrin 1 provides an inhibitory cue and elaborates the 'waiting

period' for primary sensory axons in the developing spinal cord." Development **133**(7): 1379-1387.
Wedeen, C. J. and D. A. Weisblat (1991). "Segmental expression of an engrailed-class gene during early development and neurogenesis in an annelid." Development **113**(3): 805-814.
Wenner, P., M. J. O'Donovan and M. P. Matise (2000). "Topographical and physiological characterization of interneurons that express engrailed-1 in the embryonic chick spinal cord." J Neurophysiol **84**(5): 2651-2657.
Wichterle, H., I. Lieberam, J. A. Porter and T. M. Jessell (2002). "Directed differentiation of embryonic stem cells into motor neurons." Cell **110**(3): 385-397.
Wilkinson, D. G. (2001). "Multiple roles of EPH receptors and ephrins in neural development." Nat Rev Neurosci **2**(3): 155-164.
Wizenmann, A., I. Brunet, J. S. Lam, L. Sonnier, M. Beurdeley, K. Zarbalis, D. Weisenhorn-Vogt, C. Weinl, A. Dwivedy, A. Joliot, W. Wurst, C. Holt and A. Prochiantz (2009). "Extracellular Engrailed participates in the topographic guidance of retinal axons in vivo." Neuron **64**(3): 355-366.
Wurst, W., A. B. Auerbach and A. L. Joyner (1994). "Multiple developmental defects in Engrailed-1 mutant mice: an early mid-hindbrain deletion and patterning defects in forelimbs and sternum." Development **120**(7): 2065-2075.
Yazdani, U. and J. R. Terman (2006). "The semaphorins." Genome Biol **7**(3): 211.
Zhong, S. C., X. S. Chen, Q. Y. Cai, X. Luo, X. H. Chen, J. Liu and Z. X. Yao (2010). "Dynamic expression and heterogeneous intracellular location of En-1 during late mouse embryonic development." Cells Tissues Organs **191**(4): 289-300.
Zou, Y. and A. I. Lyuksyutova (2007). "Morphogens as conserved axon guidance cues." Curr Opin Neurobiol **17**(1): 22-28.

Acknowledgments

Finally, I want to thank all the people who contributed in different ways to the realization of this work and who also made my time at the Institute of Developmental Genetics enjoyable. In particular I want to mention:

***Prof. Dr. Wolfgang Wurst**, who gave me the opportunity to work in his Institute, and for his direct and indirect support and interest in my work;*

***Dr. Andrea Huber Brösamle**, for having accepted me at the beginning of the establishment of the Neuron circuit formation group and for having strongly contributed to my understanding in the field of developmental neurobiology. I want to thank Andrea for having given me a challenging and fascinating research topic and for her continuous support and motivation during my PhD;*

***Prof. Dr. Rüdiger Klein (MPI, Martinsried) and Dr. Reinhard Köster**, members of my Thesis committee, for scientific suggestions, discussions and questions that contributed to accomplish my doctoral work;*

***Dr. Wolfgang Beisker (TOXI)**, for his expert support and teaching with FACS experiments and for his always ready availability;*

***Dr. Holger Prokisch and Dyvia Mehta (IHG),** for the technical support in the realization of microarray experiments;*

***Dr. Gerhard Welzl and Theresa Faus-Kessler**, for the statistical analysis of microarray data and fruitful discussions;*

***Prof. Dr. Alain Prochiantz and Dr. Rajiv Joshi (CNRS, Paris)**, for providing me with Engrailed protein, indispensable for my experiments, and for fruitful ideas, discussions and collaborations;*

***Prof. Dr. Alexandra Joyner (MSKCC, New York)**, for sending me the $En1^{cond}$ mice;*

Dr. Laure Bally-Cuif, Prof. Dr. Jochen Graw, Dr. Reinhard Köster, Dr. Chichung Lie and Dr. Nilima Prakash*, for providing research material, for making available laboratory equipments and supporting me with excellent discussions;*

Frau Fieder, Clarinda and Manuela, *for their technical assistance and care in the mouse facilities;*

Our secretaries, Elisabeth, Karin and Angelika*, who took care and helped me with many bureaucratic tasks;*

Boehringer Hingelheim and DAAD fonds*, for having given me the opportunity to participate to EMBO course and international conferences, as well as for having in part financially supported my PhD work;*

all the members of the "AHB group", Georg, Corinna, Rosa, Heidi, Steffie, Jana, Sandra, Daniela, Katharina, Karina, Antonella, Emre, Jörn, Josè, Julia, Michaela, Nikola, Ruth, Steffie, Tobi *(and sorry if I forgot someone ...), because you helped me at different levels in several aspects of my daily research, but in particular because you made my lab-time "lighter" and enjoyable over the years: many and sincere THANKS!!!*

And last but not least ... ***my parents and family****, for having helped and supported me, even if you were more than 500km far away;* ***Lele****, for too many things and facts happened in these years, and the* ***new-coming baby****, who kept me company during the writing of this thesis!*